# SOLUTIONS OF THE HEAT-CONDUCTION EQUATION

# WITH PHASE CHANGE AND MOVING BOUNDARIES

by

Mohammad Ali REJAL

Thesis submitted for the degree of

Doctor of Philosophy

of

University of London

October 1983

Department of Mechanical Engineering
Imperial College of Science & Technology
London SW7 2BX

## ABSTRACT

A general potential field problem is cast into matrix form, using the finite element method. Heat conduction, as an especial case of the aforesaid problem, is solved for three-dimensional case with internal heat sources as well as all the various possible boundary conditions except for the radiation. A clarification is, herein this work, suggested for replacing any system of discrete and distributed loads (acting all over the solution-domain) by an equivalent system of distinct loads acting only at the nodes.

The formulations are rederived, in detail, for a general two-dimensional heat conduction problem with variable thermophysical properties. A computer program is developed in which functional variations for such properties are also incorporated. This is applied to a steady-state temperature field problem in an LMFBR fuel element with non-uniform boundary conditions and/or the cases with non-uniform gap between the eccentrically situated pellet and the cladding.

Transient problems are solved by a single numerical formulation, using a parameter which includes Galerkin and Crank-Nicholson methods but in a more general feature. Thus, this formulation for transient cases, for both heating-up and cooling-down systems, is included in a further developed computer code. Excellent agreement has already been reached with other well-established methods in this respect.

This method is also further developed to include Multi-phase problems with motionless as well as moving boundaries in both steady-state and transient cases, respectively.

Each interface is, numerically, located so much so that its movement and shape can be monitored at any given time. Each interface is separately used to refine the existing mesh so that each element will always be in a single phase. Consequently, no new modelling is needed.

This formulation, together with the relevant computer coding, as a major part of this work, can predict the change of phase in a reactor core which may influence the course of accidents.

## ACKNOWLEDGEMENTS

Most of all, I wish to express my utmost appreciation to my wife, Loabat, for her outstanding patiance and extreme tolerance towards my prolonged efforts in concluding this work.

I am grateful to my parents for paying the university fees and financing me during the first year of my studies by selling their home furniture. This attitude encouraged me,even further, to continue my studies abroad.

The assistance given by my supervisor, Dr.J.L.Head, in the preparation of this work was invaluable. Thanks are also due to Dr.N.Shah for his continuous help and co-operation.

My sincere gratuted to Mr.H.Afham who subsidised me out of sheer generosity throughtout the course.

## CONTENTS                                                    PAGE

## NOMENCLATURE

| | | |
|---|---|---|
| $A, B, C$ & $D$ | : | coefficients used in temperature modelling |
| $a$, $b$, & $c$ | : | element characteristics |
| $e$ | : | reference (No.) to the element in question |
| $C_p$ | : | specific heat at a constant pressure |
| $C_{i,j}$ | : | thermal energy capacity between nodes $i$ & $j$ |
| $\vec{F}$ | : | loads (heat loads) |
| $F$ , $G$ | : | functionals |
| $H$ | : | local sink |
| $h$ | : | heat transfer coefficient |
| $I$ | : | integral notations (see equation 2.15) |
| $i$, $j$, $k$,... | : | node numbers |
| $k$ | : | thermal conductivity |
| $L$ | : | latent heat |
| $\ell$ | : | length (of the element in question) |
| $\ell_{x, y, z}$ | : | cosine directions along $x$, $y,z$ axis, respectively |
| $N_{i,j,\cdots,k}$ | : | position functions (or area co-ordinates) of a point inside an element |
| $Q$ | : | local rate of thermal energy generation (source term) |
| $q$ | : | heat flux |
| $q_{cond}$ | : | conductive heat flux |
| $S$ | : | overall boundary surface of the solution-domain |
| $S_1$ | : | boundary surface with prescribed temperatures |
| $S_2$ | : | conductive boundary surface |
| $S_3$ | : | convective boundary surface |
| $S_4$ | : | radiative boundary surface |

$S^e$       :   elemental area for integration

$T$       :   temperature

$T_s$       :   solidus temperature

$T_\ell$       :   liquidus temperature

$t$       :   time

$V^e$       :   elemental volume for integration

$X$       :   functional


## Greek Symbols


$\epsilon$       :   emissivity

$\delta$       :   Dirac delta function

$\delta X$       :   change of functional $X$

$\Delta_e$       :   area of element $e$

$\Delta_{i, \, j \, \& \, k}$       :   areas of sub-elements opposite nodes $i$, $j$ & $k$, respectively, in triangle $i \, j \, k$

$\lambda$       :   a parameter used in the Matrix equation for transient heat conduction problem

$\rho$       :   density

$(\rho . C_p)$       :   thermal energy capacity

$(\rho \cdot C_p)_{eff}$       :   effective thermal energy capacity

$\sigma$       :   Stefan-Boltzmann constant

$\tau$       :   a given time over a time-step

$\theta$       :   temperature

$\theta_b$       :   prescribed temperatures on boundary surface $S_1$

$\theta_w$       :   prescribed temperatures on the wall facing radiative boundary surface $(S_4)$

$\theta_\infty$       :   prescribed temperatures of the environment adjacent to convective boundary surface $(S_3)$

$X$       :   functional

## Subscripts

1,2,3 & 4   :   refer to boundary surfaces $S_1$, $S_2$, $S_3$ & $S_4$, respectively

$i$, $j$, $k$, .. :   refer to nodes $i$, $j$, $k$, .. , respectively

$\ell$             :   liquidus

$h$            :   refers to convective terms

$Q$            :   internal heat sources

$q$            :   refers to heat flux

$s$            :   solidus

$x$, $y$, $z$    :   along x, y & $z$-directions, respectively

## Matrices

$[C]$          :   thermal energy capacity matrix

$[C_{eff}]$     :   effective thermal energy capacity matrix

$\{F\}$          :   load matrix

$[H]$          :   thermal convective matrix

$[K]$          :   thermal conductivity matrix

$\{\theta\}$          :   nodal temperatures matrix

12

## LIST OF FIGURES

CHAPTER 4

CHAPTER 5

## APPENDIX A

## APPENDIX B

## LIST OF TABLES

## CHAPTER 1

## INTRODUCTION TO THE CONDUCTION OF HEAT

## AND THE OBJECTIVES OF THIS WORK

### 1.1 INTRODUCTION

Heat is a vital element in nature, upon which life depends heavily, and it plays an important part in the cycle of evolution. Man has always been trying to control heat in order to put it to a better use.

In nature, the sun is the greatest source of energy, but enormous heat can also be produced by fission. For example, reproduction by the division of living cells into two parts, each of which becomes a complete organism. Also, the splitting of an atomic nucleus, as by bombardment with neutrons, especially into approximately equal parts, results in the release of enormous quantities of energy when certain heavy elements, such as uranium and plutonium, are split.

It was as long ago as 1720 when Hatif of Esfahan, an Iranian scientist as well as philosopher, stated that "... if you cleave an atom, you will find a sun inside". Only in the twentieth century did Einstein formulate his theories of relativity, suggesting that energy can be released by cleaving an atom.

In recent years, both successive governments and various environmental groups all over the world have applied enormous pressure on scientists, especially those related to nuclear engineering, to build safe and more fuel-efficient power plants. One of the most important factors in the design of new equipment is, of course, the conduction of heat through materials. The objective of this work is to propose a reliable numerical method with which to tackle the conduction of heat through materials in different states.

Some physical problems, such as heat conduction (steady and transient),

torsion of prismatic shafts, seepage through porous media (lubrication of pad bearings), electro-static fields, magneto-static fields, gravitation, hydro-static fields, diffusion, and steady electrical currents, are treated in the same way and they are termed the "potential field problems".

A potential field problem may be considered in two ways, namely, physically and mathematically. Generally, mathematically, it is governed by a second order partial differential equation, which may be classified as linear or non-linear, depending on whether the physical properties of the material are independent of or dependent on the potential, respectively. But from the physical point of view, a potential field might be classified as equilibrium, eigenvalue or propagation.

## 1.2 PHYSICAL CLASSIFICATIONS

Most problems in engineering and physics can be classified as either continuous or discrete. A discrete system consists of a finite number of inter-dependent sub-systems, whereas a continuous system involves a continuous domain. Continuous or discrete systems, which may be linear or non-linear, can each be further sub-divided into equilibrium, eigenvalue and propagation problems, as follows:

(a) Equilibrium problems are those in which the state of the system remains constant with time: the problem is fully time-independent, the system state is stationary and stable, and they are often known as "steady-state field problems".

(b) Eigenvalue problems can be considered as extensions of the equilibrium problems, in which, in addition to the corresponding steady-state configuration, specific critical values of certain other parameters must be determined as well. The system is sensitive to some critical conditions, and, although the system

state is stationary, it is unstable, such as in buckling or

electro-static discharge.  These are just like equilibrium

problems, while some critical conditions are not satisfied.

(c)  Propagation problems include transient and unsteady-state

phenomena, and are those in which the state of the system

depends on the system state at some previous time, usually known

as initial values.  Hence, they are called the "initial value

problems".  They are time-dependent and the region of interest

is open in time dimension [1].


The following table (Table 1.1) summarises some features of these

physical classifications [1].


## 1.3  MATHEMATICAL CLASSIFICATIONS

In theory, one-, two- and three-dimensional potential field problems

may be analysed in the same manner.  Here, we have chosen to analyse a

two-dimensional potential field problem in detail;  such a field may be

governed by a second order partial differential equation involving two

independent variables, such as $x$ and $y$, and one  dependent variable, such

as $\theta$.  The general form of such an equation may be written as:

$$A \cdot \frac{\partial^2 \theta}{\partial x^2} + B \cdot \frac{\partial^2 \theta}{\partial x \, \partial y} + C \cdot \frac{\partial^2 \theta}{\partial y^2} + D \cdot \frac{\partial \theta}{\partial x} + E \cdot \frac{\partial \theta}{\partial y} + F \cdot \theta + G = 0 \qquad (1.1)$$

If the coefficients $A$ to $G$ in equation (1.1) depend only on $x$ and $y$,

the equation is said to be linear.  Otherwise, if any of these also

depend on $\theta$ or its derivatives, the equation is called non-linear.  The

values of these coefficients may be used to determine the character of the

equation, and hence the best method of its solution.  For example, when

$G = 0$, the equation is called "homogeneous", otherwise it is said to be

TABLE 1.1

Physical Classification of a Problem [1]

| Feature of the Field | Physical Classification | | |
|---|---|---|---|
| | Equilibrium | Eigenvalue | Propagation |
| Status | Stable stationary (steady-state) | Unstable stationary (sensitive) | Transient (time-dependent régime) |
| Potentials | Time-independent | At the critical value (buckling) | Time-dependent |
| Initial Values | Not essential | | Necessary |
| Boundaries | Closed | | Open |
| Governing Equations | Ordinary or partial differential | | Partial differential |
| Type of Equations | Elliptic | | Parabolic or hyperbolic |
| Equations in the Field Domain | $[K] \cdot \{\theta\} = \{F\}$ | $[K] \cdot \{\theta\} = \lambda \cdot [M] \cdot \{\theta\}$ | $[K] \cdot \{\theta\} = \{F\}$ , when $t > t_o$ <br> $[B] \cdot \{\theta_o\} = \{F_o\}$ , when $t = t_o$ as initial values |
| Equations on the Boundaries, as Prescribed | $[A] \cdot \{\theta\} = \{g\}$ | $[A] \cdot \{\theta\} = \lambda \cdot [B] \cdot \{\theta\}$ | $[C] \cdot \{\theta\} = \{g\}$ , when $t \geqslant t_o$ |

Subscript $o$ refers to the initial values

"inhomogeneous".

Equation (1.1) can be classified by a classification parameter, defined as:

$$\Delta = B^2 - 4 . A . C \tag{1.2}$$

and is said to be elliptic, parabolic or hyperbolic according to whether the classification parameter, $\Delta$, is negative, zero or positive, respectively. While it is possible for the type of an equation to change inside the solution domain if $A$, $B$ or $C$ vary, this does not occur normally in practical problems. Classifications can also be applied to higher order equations, and to those involving more than two independent variables.

A very common and practical form of equation (1.1) is:

$$\frac{\partial^2 \theta}{\partial x^2} + \frac{\partial^2 \theta}{\partial y^2} = \psi_1 (x,y) \tag{1.3}$$

which is linear and is also elliptic, according to the above definition (since $\Delta = -4$); it is termed a "harmonic equation". This equation (1.3), in general, is inhomogeneous, and it is called Poisson's equation if $\psi_1 = C$, where $C$ is constant. Laplace's equation is obtained as a special case when $\psi_1 = 0$; in this case, it is homogeneous.

If any of the terms in equation (1.1) depend on time or its derivatives, the solution of the problem obviously changes with respect to time. These problems are time-dependent (unsteady) and of the propagation type (transient heat conduction, for example); otherwise, the problem is time-independent (steady) and is of the equilibrium or eigenvalue type (steady-state heat conduction, for example).

Elliptic equations normally occur in equilibrium problems, whereas the parabolic and hyperbolic types occur in propagation problems. A

difference between equilibrium and propagation problems is in terms of the type of conditions applied at the boundaries of the solution domain. The domain for a propagation problem is to be open, but for an equilibrium problem the domain has to be closed. Also, the boundary conditions (some values) are to be prescribed around the entire boundary. Therefore, such problems are also said to be of the boundary value type [2].

The physical conditions of the particular problem will impose certain boundary conditions, and a boundary value problem is said to be well-posed if it has a unique solution which is also stable. These problems are governed by partial differential equations which are solved in either closed or open regions [3].

The types of boundary conditions of particular interest are as follows:

(a) Dirichlet type of boundary conditions: the values of $\theta$ are specified on the boundary.

(b) Neumann type of boundary conditions: the derivative of $\theta$ with respect to the normal to the boundary is specified at the boundary.

(c) Cauchy type of boundary conditions: a linear combination of $\theta$ and its derivatives with respect to the normal to the boundary are specified at the boundary.

The following table (Table 1.2) summarises results which can be established for second-order partial differential equations and identifies which problems are well-posed.

## 1.4 GOVERNING EQUATIONS OF A POTENTIAL FIELD

In a cartesian coordinate system, in general, a potential field may

## TABLE 1.2

| Boundary Condition | Region | Type of Partial Differential Equation | | |
|---|---|---|---|---|
| | | Elliptic | Parabolic | Hyperbolic |
| Dirichlet | Open surface | Insufficient | Unique, stable in one direction | Insufficient |
| | Closed surface | Well-posed | Too restrictive | Too restrictive |
| Neumann | Open surface | Insufficient | Unique, stable in one direction | Insufficient |
| | Closed surface | Well-posed | Too restrictive | Too restrictive |
| Cauchy | Open surface | Unstable solution | Too restrictive | Well-posed |
| | Closed surface | Too restrictive | Too restrictive | Too restrictive |

be described mathematically by [2]:

$$\frac{\partial}{\partial x}\left(k_x \cdot \frac{\partial \theta}{\partial x}\right) + \frac{\partial}{\partial y}\left(k_y \cdot \frac{\partial \theta}{\partial y}\right) + \frac{\partial}{\partial z}\left(k_z \cdot \frac{\partial \theta}{\partial z}\right) + Q - H$$

$$= \rho \cdot C_p \cdot \frac{\partial \theta}{\partial t} + \rho \cdot C_v \cdot \left(u \cdot \frac{\partial \theta}{\partial x} + v \cdot \frac{\partial \theta}{\partial y} + w \cdot \frac{\partial \theta}{\partial z}\right) \qquad (1.4)$$

in which the unknown physical quantity, $\theta$, is assumed to be single valued and stands for the potential, and it is a function of $x$, $y$, $z$ and $t$ inside the region of interest; other variables are all known and specified functions of $x$, $y$, $z$, $\theta$ and $t$. The $x$, $y$ and $z$ coordinate axes must coincide with the principal axes of the material, and $k_x$, $k_y$ and $k_z$ are the potential conductivities along the $x$, $y$ and $z$ directions, respectively. It may be noted here that the orientation of the coordinate axes is not so important if the material is isotropic (where $k_x$, $k_y$ and $k_z$ are equal). $Q$ is the source (input) term, the local power source. $H$ is the local sink, $\rho$ is the density, and $C$ is the specific energy capacity, and $t$ stands for time. $u$, $v$ and $w$ are the relative velocity components along the $x$, $y$ and $z$ directions, respectively.

A solid region may be defined as a domain with all the points stationary relative to each other on the macroscopic scale. This also includes a moving system, consisting of points stationary relative to each other in the system, or even a liquid whose mean positions of the molecules are stationary relative to each other. In such a field, we may take $u$, $v$ and $w$ to be zero. Therefore, the potential distribution governing equation in a solid may be obtained from equation (1.4) as:

$$\frac{\partial}{\partial x}\left(k_x \cdot \frac{\partial \theta}{\partial x}\right) + \frac{\partial}{\partial y}\left(k_y \cdot \frac{\partial \theta}{\partial y}\right) + \frac{\partial}{\partial z}\left(k_z \cdot \frac{\partial \theta}{\partial z}\right) + (Q - H) = \rho \cdot C_p \cdot \frac{\partial \theta}{\partial t} \qquad (1.5)$$

## 1.5 THE CONDUCTION OF HEAT

Heat can be transferred by conduction, convection or radiation. The phenomenon of heat conduction in solids is usually interpreted as a simple molecular interchange of kinetic energy. Thus, if the molecules of the conducting material at one point are heated, they are set into rapid motion and these, in communicating by elastic impact with their neighbours of lower kinetic energy, set the latter into more violent motion, and so on throughout the conducting zone. In thermal problems, the level of kinetic energy is measured in terms of its temperature.

Consider any two neighbouring points which are at the same temperature; even though there may be exchange of heat, there will be no conduction of heat. Heat can only be conducted between these two points only if they are at different temperatures, and the direction of heat flow is always from high to low temperatures; in other words, heat flows only when there is a temperature gradient, and towards the direction of lower temperatures. Hence, the conduction of heat in solids can be considered as a potential field problem and is governed by an equation of the form of (1.5), where $\theta$ refers to the temperature and $k$ stands for the thermal conductivity.

Heat conduction problems are classified as linear and non-linear. When thermal conductivities depend on temperature, which we will be concerned with, the governing equation is non-linear (see Section 1.3). Hence, the problem is termed non-linear heat conduction. However, in linear heat conduction problems, thermal conductivities are independent of temperature. For example, consider a two-dimensional case in an isotropic material $(k_x = k_y)$; such a problem is then governed by a relation such as:

$$\frac{\partial^2 \theta}{\partial x^2} + \frac{\partial^2 \theta}{\partial y^2} = \frac{1}{k} \left( \rho \cdot C_p \cdot \frac{\partial \theta}{\partial t} + H - Q \right) \qquad (1.6)$$

where: $\qquad \frac{1}{k} \left( \rho \cdot C_p \cdot \frac{\partial \theta}{\partial t} + H - Q \right) = \mathcal{f}(x,y)$

Therefore, equation (1.6) is harmonic, similar to equation (1.3).

## 1.6  FORMULATION FOR A HEAT CONDUCTION PROBLEM

The conduction of heat in solids is generally governed by an equation of the form of (1.5), where $k_x$, $k_y$ and $k_z$ are known functions of $x$, $y$, $z$, $\theta$ and $t$ and stand for the thermal conductivities along the principal axes of the material, respectively.  $Q$ is also a known function of $x$, $y$, $z$, $\theta$ and $t$, which refers to the volumetric rate of heat generation.  Also, $H$ is known function of $x$, $y$, $z$, $\theta$ and $t$ which represents the volumetric rate of the thermal energy sink.  $\rho$ is the density, and $C_p$ is the specific heat under constant pressure.  Hence, we can solve the problem for the unknown quantity, $\theta$, which represents the temperature distribution all over the solution domain.  A unique solution to this problem can, in principle, be obtained for any given set of sufficient boundary conditions (see Table 1.2).

Boundary conditions for heat conduction problems may be classified, in general, into two basic groups, as follows.

In the first group, the temperature distribution (energy level) only is prescribed on the boundary $(S_1)$, which is termed as the "forced boundary", or the so-called "first kind of boundary condition", and it is shown as:

$$\theta = \theta_b \qquad \text{on } S_1 \qquad (1.7)$$

In the literature, it is called the Dirichlet type of boundary condition.

In the second group, the heat flux (energy flow) across the boundary surface is prescribed;  this group itself can be further sub-divided into three types, as follows.

(a) <u>Conductive Boundary</u>

When the neighbouring region is a conductor, we will have a conductive boundary surface $(S_2)$, through which the heat flux may be specified as:

$$q_2 = q_b \qquad \text{on } S_2 \qquad\qquad (1.8)$$

the so-called "second kind of boundary condition", and in the literature it is also named the Neumann type of boundary condition. The total flow of heat by conduction through the surface $S_2$ will be:

$$W_2 = \iint\limits_{S_2} q_2 \cdot dS \qquad\qquad (1.9)$$

(b) <u>Convective Boundary</u>

Heat may be transferred by a moving fluid through a boundary layer adjacent to the boundary surface $(S_3)$; it is termed the "convective boundary surface", through which the heat flux may be specified as:

$$q_3 = h \cdot (\theta - \theta_\infty) \qquad\qquad (1.10)$$

where $h$ is a prescribed heat transfer coefficient, and $\theta_\infty$ is the ambient temperature of the moving fluid. This type is the so-called "third kind of boundary condition", and is called in the literature the Cauchy type of boundary condition. The total flow of heat by convection through the surface $S_3$ will be:

$$W_3 = \iint\limits_{S_3} q_3 \cdot dS = \iint\limits_{S_3} h \cdot (\theta - \theta_\infty) \cdot dS \qquad\qquad (1.11)$$

(c) <u>Radiative Boundary</u>

Heat may also be exchanged by radiation through the "radiative boundary surface" $(S_4)$. The flow of heat which is transferred in this way is, in general, too difficult to formulate, but as a crude and ideal estimate, heat flux may be written as:

$$q_4 = \varepsilon \cdot \sigma \cdot (\theta^4 - \theta_w^4) \tag{1.12}$$

where $\varepsilon$ and $\sigma$ are the emissivity and the Stefan-Boltzmann constant, respectively. $\theta_w$ is the prescribed temperature of the radiating surface facing $S_4$. The flow of heat by radiation through the surface $S_4$ will be:

$$W_4 = \iint\limits_{S_4} q_4 \cdot dS = \iint\limits_{S_4} \varepsilon \cdot \sigma \cdot (\theta^4 - \theta_w^4) \cdot dS \tag{1.13}$$

This may be termed as the "fourth kind of boundary condition".

Any mixed combinations of these three latter kinds (a, b and c) are also possible at the same point (part) of the boundary surface. Therefore, in general, heat flux through a boundary surface of the second group may be expressed as a sum of these three heat fluxes $(q_2, q_3$ and $q_4)$, namely:

$$q = q_2 + q_3 + q_4 \tag{1.14}$$

On the other hand, heat flux at any point of the boundary surface is a vector which can be written as:

$$q = -\left(k_x \cdot \frac{\partial \theta}{\partial x} \cdot \ell_x + k_y \cdot \frac{\partial \theta}{\partial y} \cdot \ell_y + k_z \cdot \frac{\partial \theta}{\partial z} \cdot \ell_z\right) \tag{1.15}$$

where $\ell_x$, $\ell_y$ and $\ell_z$ are the direction cosines of the outward normal to the

boundary surface. Hence, at a boundary of the second group, where there is neither absorption nor liberation of heat (change of phase), the heat flux is given by equation (1.14) or equation (1.15); equating these two gives:

$$k_x \cdot \frac{\partial \theta}{\partial x} \cdot \ell_x + k_y \cdot \frac{\partial \theta}{\partial y} \cdot \ell_y + k_z \cdot \frac{\partial \theta}{\partial z} \cdot \ell_z + q_2 + q_3 + q_4 = 0 \qquad (1.16)$$

All these boundary conditions may be tabulated, as shown in Table 1.3.

A set of boundary conditions is said to be sufficient if the union of all the surfaces $(S_1, S_2, .., S_n)$, where the boundary conditions are imposed, form a closed surface $(S)$ which completely surrounds the region of interest. Hence:

$$S = S_1 \: U \: S_2 \: ..... \: U \: S_n \qquad . \qquad (1.17)$$

Note: Overlapping parts, as explained for equation (1.14), must be considered.


## 1.7 INCENTIVE OF THIS WORK

Almost all physical phenomena in solid mechanics are non-linear (including potential field problems). However, in general, the non-linearity may be due to material properties, solution domain geometry, or both. The material non-linearities (temperature-dependent properties, for example) are the easiest to visualise, especially for a fixed geometry. The geometric non-linearities refer to large deformations (body expansions, for example).

In steady-state heat conduction problems, no geometric changes take place, whereas they do exist in transient problems, although in very small proportions. For the present analysis here, only the material property

TABLE 1.3

The Boundary Condition Classifications in Heat Conduction Problems

| Boundary Conditions in Heat Conduction | | | |
|---|---|---|---|

1st Group      2nd Group

| | Prescribed Temperatures | Prescribed Heat Flux | | |

| Type | — | a | b | c |
|---|---|---|---|---|
| Nature of the Boundary | Forced | Conductive | Convective | Radiative |
| Expression | $\theta = \theta_b$ | $q_2 = q_b$ | $q_3 = h \cdot (\theta - \theta_\infty)$ | $q_4 = \varepsilon \cdot \sigma \cdot (\theta^4 - \theta_w^4)$ |
| Equation Number | (1.7) | (1.8) | (1.10) | ( 1.12 ) |
| Known in the Literature | Dirichlet | Neumann | Cauchy | — |
| The So-Called | 1st Kind | 2nd Kind | 3rd Kind | 4 th Kind |
| Imposed on | $S_1$ | $S_2$ | $S_3$ | $S_4$ |
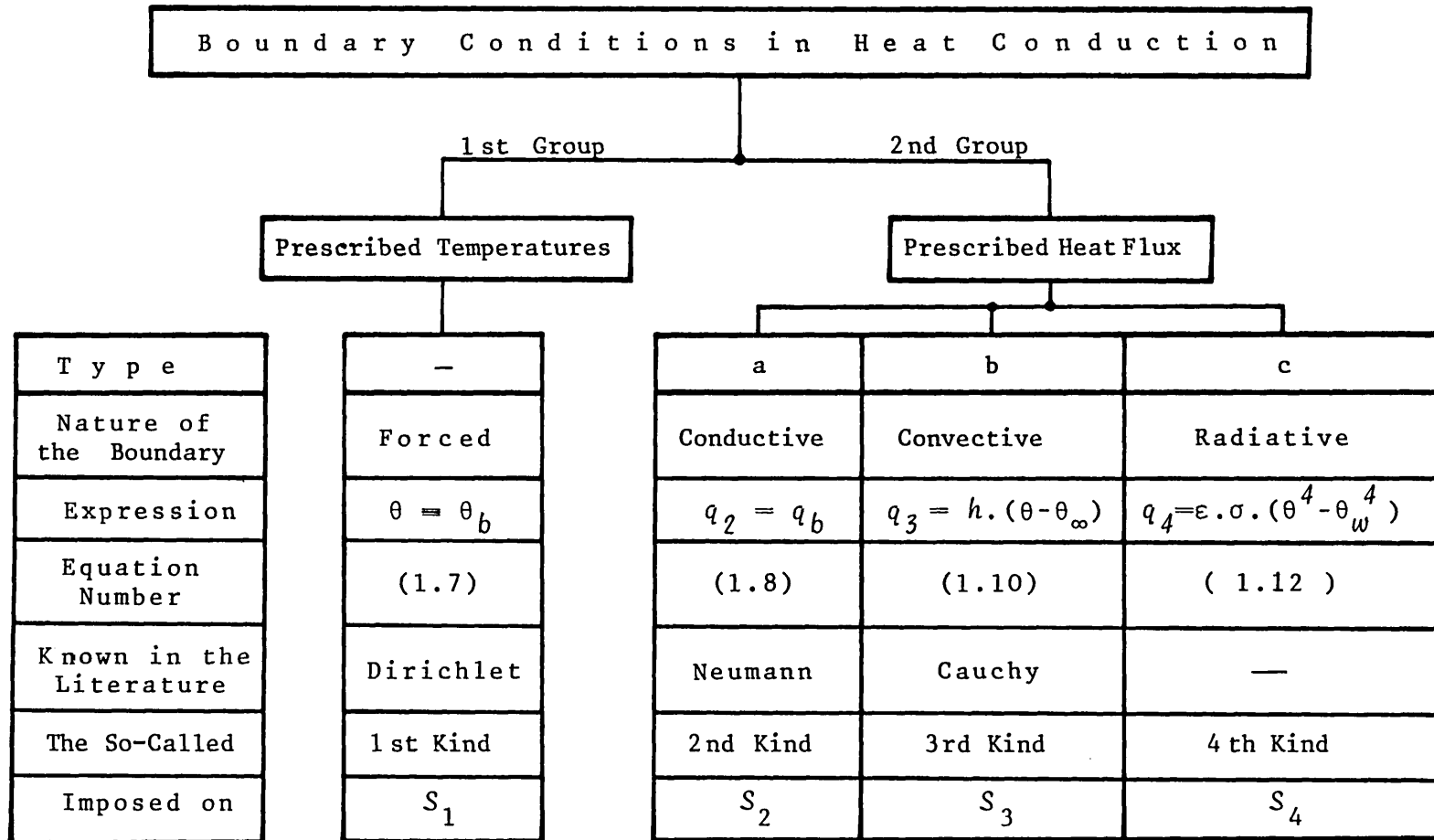
non-linearities are considered, and the geometric variations are neglected (fixed geometry).

As for non-linearities, any kind of irregularity makes the problem complicated. Their analytical solutions are often restricted to specific problems only and generalisations are either too cumbersome to handle, or are in very impractical forms to be of any use for practical applications. Hence, other methods have to be investigated, at least to have an acceptable solution in such a form which can be of more practical use. Therefore, a numerical approach is proposed in the following chapter.

## 1.8  OBJECTIVES OF THIS WORK

The objectives of this work is to numerically solve and develop a solution to heat conduction problems in multi-zones, involving temperature-dependent properties for both the steady-state case and the transient case. Moreover, change of phase is also considered, and interfaces (between any two neighbouring phases) are located at any time.  Therefore, free boundary problems are also solved here.

An application of this work can be mentioned as the conduction of heat (temperature distribution) through a nuclear reactor core (or its components), even for accidental cases which have a low probability of occurrence.

# CHAPTER 2

## NUMERICAL ANALYSIS:

## GENERAL FINITE ELEMENT FORMULATIONS FOR

## A POTENTIAL FIELD PROBLEM

ABSTRACT

A general finite element method is derived, in this chapter, for three-dimensional potential field problems with multiple boundary conditions. The method is then applied to a general heat conduction problem with all kinds of boundary conditions, except radiation.

## 2.1 INTRODUCTION

As discussed in the previous chapter, a potential field may be generally governed by a quasi-harmonic partial differential equation of the type of (1.5). A particular problem is then specified in a unique manner by its prescribed boundary conditions.

Analytically, one way of solving such potential field problems is by minimising the total energy of the system. This is done by defining a functional which involves both the governing equation and the boundary conditions. The integrated functional is then minimised all over the whole solution domain. The resulting solution also satisfies the governing equation and the boundary conditions. Therefore, it is the solution of the original problem. Although not many analytical solutions can be obtained by this method which are useful, this idea is used to form the basis of some numerical method, such as the finite element method.

A general potential field problem is analysed in the following sections of this chapter, and the method is then applied to a general heat conduction problem as a guideline. Although the generality of the treatment is mathematically acceptable, it has become too abstract for an

average engineering application. Therefore, to assist in the understanding of the method, similar analysis is also carried out in detail for (i) a two-dimensional case in Chapter 3 for a steady-state case, and for (ii) a transient case in Chapter 4    (iii) Change of phase: phase change is separately considered in the following chapters.

Heat conduction equations, in general, may be extracted from Section 1.6. They are rewritten here for convenience as:

$$\frac{\partial}{\partial x}\left(k_x \cdot \frac{\partial \theta}{\partial x}\right) + \frac{\partial}{\partial y}\left(k_y \cdot \frac{\partial \theta}{\partial y}\right) + \frac{\partial}{\partial z}\left(k_z \cdot \frac{\partial \theta}{\partial z}\right) + (Q - H) = \rho \cdot C_p \cdot \frac{\partial \theta}{\partial t} \qquad (2.1)$$

subject to the set of prescribed boundary conditions as:

$$\theta = \theta_b(t) \qquad \text{on } S_1 \qquad (2.2a)$$

and: $\ell_x \cdot \left(k_x \cdot \frac{\partial \theta}{\partial x}\right) + \ell_y \cdot \left(k_y \cdot \frac{\partial \theta}{\partial y}\right) + \ell_z \cdot \left(k_z \cdot \frac{\partial \theta}{\partial z}\right) + q_{cond}$

$$+ h \cdot (\theta - \theta_\infty) + \varepsilon \cdot \sigma \cdot (\theta^4 - \theta_w^4) = 0 \qquad \text{on } (S - S_1) \qquad (2.2b)$$

Equation (2.2b) refers to the heat flux through the portion of the boundary on which the temperatures are not prescribed $(S - S_1)$, and where $k_x$, $k_y$ and $k_z$ were equal (isotropic material), and $q_{cond}$, $h$ and $\varepsilon$ were zero. The well-known adiabatic (non-conducting)boundary condition is obtained as:

$$\frac{\partial \theta}{\partial \vec{n}} = 0$$

in which $\vec{n}$ is the normal to the boundary surface.

A particular problem is specified in a unique manner by the coupled equations (2.1) and (2.2), and a solution has to satisfy equation (2.1) all over the solution domain, together with the prescribed boundary

conditions (2.2) on the boundaries.  If the analytical form of the

solution for a particular problem was difficult or impractical, an

alternative formulation would be possible with the aid of the calculus of

variations, as follows.


## 2.2  VARIATIONAL FORM OF THE HEAT CONDUCTION EQUATION

The set of coupled equations (2.1) and (2.2) has been solved by

different methods (for instance, Gurtin and Galerkin [4,5]).  Here, we

have chosen to use the calculus of variations.  In essence, we look for a

variational functional, whose minimum is also a solution of equation (2.1),

together with the boundary conditions (2.2).  This is known as the

Euler's theorem of variational calculus [4], which is applied as follows.

Consider a variational functional (function of other functions) of the

form:

$$X = \iiint_V F(x,y,z,\theta,\theta'_x,\theta'_y,\theta'_z,t) \cdot dV + \iint_S G(\theta) \cdot dS \tag{2.3}$$

where $\theta(x,y,z,t)$ is the unknown function, and $\theta'_x$, $\theta'_y$ and $\theta'_z$ are defined as

$\theta'_x = \partial\theta/\partial x$, $\theta'_y = \partial\theta/\partial y$ and $\theta'_z = \partial\theta/\partial z$, which are treated as independent

variables distinct from $\theta$.  $F$ is some functional defined all over the

region of interest, $V$, which is surrounded by the boundary surface, $S$, on

which the functional $G$ is defined.

Let $\delta\theta$ be an arbitrary small variation of $\theta$ and its derivatives.

Therefore, the change, $\delta X$, of $X$ in equation (2.3) may be equated as:

$$\delta X = \iiint_V \left[ \frac{\partial F}{\partial \theta} \cdot \delta\theta + \frac{\partial F}{\partial \theta'_x} \cdot \delta(\theta'_x) + \frac{\partial F}{\partial \theta'_y} \cdot \delta(\theta'_y) + \frac{\partial F}{\partial \theta'_z} \cdot \delta(\theta'_z) \right] \cdot dV$$

$$+ \iint_S \left[ \frac{\partial G}{\partial \theta} \cdot \delta\theta \right] \cdot dS \tag{2.4}$$

where we may write:

$$\delta(\theta_x') \quad = \quad \delta(\frac{\partial\theta}{\partial x}) \quad = \quad \frac{\partial}{\partial x}(\delta\theta) \quad , \quad \text{etc.}$$

Hence, equation (2.4) becomes:

$$\delta X \quad = \quad \iiint\limits_V \left[\frac{\partial F}{\partial\theta} \cdot \delta\theta + \frac{\partial F}{\partial\theta_x'} \cdot \frac{\partial}{\partial x}(\delta\theta) + \frac{\partial F}{\partial\theta_y'} \cdot \frac{\partial}{\partial y}(\delta\theta) + \frac{\partial F}{\partial\theta_z'} \cdot \frac{\partial}{\partial z}(\delta\theta)\right] \cdot dV$$

$$+ \iint\limits_S \left[\frac{\partial G}{\partial\theta} \cdot \delta\theta\right] \cdot dS$$

The second term on the right hand side inside the volume integral can be integrated by parts, with respect to $x$, as follows:

$$\iiint\limits_V \left[\frac{\partial F}{\partial\theta_x'} \cdot \frac{\partial}{\partial x}(\delta\theta)\right] \cdot dV$$

$$= \iint\limits_S \left[\frac{\partial F}{\partial\theta_x'} \cdot \delta\theta \cdot \ell_x\right] \cdot dS - \iiint\limits_V \left[\frac{\partial}{\partial x}(\frac{\partial F}{\partial\theta_x'}) \cdot \delta\theta\right] \cdot dV$$

Because, if we take $U = \partial F/\partial\theta_x'$ and $W = \delta\theta$, we can write:

$$\int U \cdot \frac{\partial W}{\partial x} \cdot dx \quad = \quad U \cdot W - \int W \cdot \frac{\partial U}{\partial x} \cdot dx$$

A similar relation may be written only along the $x$-direction as:

$$\iiint\limits_V U \cdot \frac{\partial W}{\partial x} \cdot dx \cdot dy \cdot dz \quad = \quad \iint\limits_S U \cdot W \cdot dy \cdot dz - \iiint\limits_V W \cdot \frac{\partial U}{\partial x} \cdot dx \cdot dy \cdot dz$$

where $dx.dy.dz = dV$ and $dy.dz = \ell_x.dS$, and $\ell_x$ is the direction cosine of the normal to the surface surrounding the volume $V$ with the $x$ axis. Similar terms are obtained for others and, finally, we will have:

$$\delta X = - \iiint_V \left\{ \frac{\partial}{\partial x}\left(\frac{\partial F}{\partial \theta'_x}\right) + \frac{\partial}{\partial y}\left(\frac{\partial F}{\partial \theta'_y}\right) + \frac{\partial}{\partial z}\left(\frac{\partial F}{\partial \theta'_z}\right) - \left(\frac{\partial F}{\partial \theta}\right) \right\} . \delta\theta . dV$$

$$+ \iint_S \left[ \ell_x . \left(\frac{\partial F}{\partial \theta'_x}\right) + \ell_y . \left(\frac{\partial F}{\partial \theta'_y}\right) + \ell_z . \left(\frac{\partial F}{\partial \theta'_z}\right) + \left(\frac{\partial G}{\partial \theta}\right) \right] . \delta\theta . dS \qquad (2.5)$$

On the other hand, since $\delta\theta$ is taken as an arbitrary variation and cannot always be zero, then, if in equation (2.5) we had:

$$\frac{\partial}{\partial x}\left(\frac{\partial F}{\partial \theta'_x}\right) + \frac{\partial}{\partial y}\left(\frac{\partial F}{\partial \theta'_y}\right) + \frac{\partial}{\partial z}\left(\frac{\partial F}{\partial \theta'_z}\right) - \left(\frac{\partial F}{\partial \theta}\right) = 0 \qquad (2.6)$$

everywhere inside the region $V$, which is generally called the Euler-Lagrange equation, and, also, if we had:

$$\ell_x . \left(\frac{\partial F}{\partial \theta'_x}\right) + \ell_y . \left(\frac{\partial F}{\partial \theta'_y}\right) + \ell_z . \left(\frac{\partial F}{\partial \theta'_z}\right) + \left(\frac{\partial G}{\partial \theta}\right) = 0 \qquad (2.7)$$

for any value of $\theta$, then the value of $\delta X$ in equation (2.5) would be zero. These two conditions, (2.6) and (2.7), are required for the functional $X$, defined in (2.3), to be an extremum functional. Thus, we need to find a functional such that the conditions (2.6) and (2.7) are equivalent to the set of coupled equations (2.1) and (2.2), respectively.

Consider an expression for $F$, in equation (2.3), of the form:

$$F = \frac{1}{2}\left[ k_x . \left(\frac{\partial \theta}{\partial x}\right)^2 + k_y . \left(\frac{\partial \theta}{\partial y}\right)^2 + k_z . \left(\frac{\partial \theta}{\partial z}\right)^2 \right] - \left(Q - H - \rho . C_p . \frac{\partial \theta}{\partial t}\right) . \theta$$

in which $(Q - H - \rho.C_p.\partial\theta/\partial t)$ is assumed to be independent of $\theta$. And another expression for $G$ of the form:

$$G = q_{cond} . \theta + \frac{1}{2} . h . (\theta - \theta_\infty)^2 + \varepsilon . \sigma . \left(\frac{\theta^5}{5} - \theta_w^4 . \theta\right)$$

where $q_{cond}$, $h$, $\theta_\infty$, $\varepsilon$ and $\theta_w$ are also assumed to be independent of $\theta$.

Now, $\delta X$ from relation (2.5) can be evaluated as:

$$\delta X = - \iiint\limits_V \left\{\frac{\partial}{\partial x}(k_x \cdot \frac{\partial\theta}{\partial x}) + \frac{\partial}{\partial y}(k_y \cdot \frac{\partial\theta}{\partial y}) + \frac{\partial}{\partial z}(k_z \cdot \frac{\partial\theta}{\partial z}) - (Q - H - \rho \cdot C_p \cdot \frac{\partial\theta}{\partial t})\right\} \cdot \delta\theta \cdot dV$$

$$+ \iint\limits_S \left[\ell_x \cdot (k_x \cdot \frac{\partial\theta}{\partial x}) + \ell_y \cdot (k_y \cdot \frac{\partial\theta}{\partial y}) + \ell_z \cdot (k_z \cdot \frac{\partial\theta}{\partial z}) + q_{cond} + h \cdot (\theta - \theta_\infty)\right.$$

$$\left. + \varepsilon \cdot \sigma \cdot (\theta^4 - \theta_w^4)\right] \cdot \delta\theta \cdot dS \qquad (2.8)$$

Consequently, an associated extremum functional of the form of (2.3), corresponding to the set of coupled equations (2.1) and (2.2), may be written as:

$$X = \iiint\limits_V \left\{\frac{1}{2}\left[k_x \cdot (\frac{\partial\theta}{\partial x})^2 + k_y \cdot (\frac{\partial\theta}{\partial y})^2 + k_z \cdot (\frac{\partial\theta}{\partial z})^2\right] - (Q - H - \rho \cdot C_p \cdot \frac{\partial\theta}{\partial t}) \cdot \theta\right\} \cdot dV$$

$$+ \iint\limits_S \left[q_{cond} \cdot \theta + \frac{1}{2} \cdot h \cdot (\theta - \theta_\infty)^2 + \varepsilon \cdot \sigma \cdot (\frac{\theta^5}{5} - \theta_w^4 \cdot \theta)\right] \cdot dS \qquad (2.9)$$

whose value is stationary for any value of $\theta$, which is satisfying the coupled equations (2.1) and (2.2).

Hence, when this functional (2.9) is stationary, it is said to be equivalent to the set of heat conduction equations (2.1) and (2.2). Therefore, the problem is now changed to determining the minimum of the above functional $X$, (2.9), that is to solve for:

$$\frac{\partial X}{\partial \theta} = 0 \qquad (2.10)$$

This equation, (2.10), is always automatically satisfied on the boundary surface $S_1$, since the temperatures are prescribed over that surface (see equation (2.2a)). Therefore, the surface integral in the functional

applies only on the rest of the boundary surface $(S - S_1)$, where the boundary conditions (2.2b) are prescribed.

The finite element method is used here to numerically solve the above equation (2.10).

## 2.3  THE FINITE ELEMENT METHOD

### 2.3.1  The Finite Element Ideas

Consider a closed region which obeys the relation (2.10). Let the domain be subdivided into a number of small parts called elements. Since the relation (2.10) holds for all the domain, it also holds for each element.  In order to simplify further, we characterise each element by a number of points called nodes.  These nodes are of special interest, as will be shown later, but here we note that the relation (2.10) must also hold at these nodes.  In other words, the behaviour of the whole domain may be studied by looking at the behaviour of only the nodes.

These ideas formed a basis for a new method, in which each element was finite;  hence, it was called the "Finite Element Method", which has now become a very standard technique.  Therefore, we shall not expand on it.  Further detailed proof may be obtained in many numerical method text books (for example [4,5,6]).

### 2.3.2  Features of the Finite Element Method

The finite element method is based on the extremum method, when a functional representing an integrated quantity (the energy, for example) over the region of interest is defined.  It has been shown that the minimising of such a functional is equivalent to solving the original quasi-harmonic partial differential equation of the type (1.5).  This method is summarised in the following steps.

Firstly, the region of interest has to be finite;  therefore,

it must be confined by a closed surface. The domain is subdivided into a number of elements by a number of imaginary surfaces. Reversely, the union of all the elements in a certain order should be the domain itself, and their intersections must be a null set. Now, each element is enclosed by some parts of these imaginary surfaces, each of which is called a "face". Moreover, each intersection between any pair of faces is called a "side". A "boundary element" is any element which has at least one face on the approximation surface that forms (replaces) the boundary surface of the solution domain; the face is hence called the "boundary face". A "corner element" is any element which has more than one boundary face adjacent to each other. Each element which is finite and closed can also be considered individually and as a separate region. It may be characterised by knowing and calculating values at a finite number of points, the so-called "nodes" which are usually at the vertices of the element in question. The boundaries (sides) of all the elements in assemblage look like the skeleton of the domain, where the joints are at the vertices; it is traditionally called a "mesh". Hence, the whole solution domain may be replaced by a mesh interlinking the vertices of the elements and, consisting of a number of nodes, the domain will be studied only at those nodes. Nodes and elements are then numbered simply for reference. Thus, a typical element of the domain (element $e$, for example) with nodes $i,j,k$ will be governed by equation (2.10), including at its nodes, this can be expressed in a matrix form as:

$$\left\{\frac{\partial X}{\partial \theta}\right\}^e \equiv \left\{\begin{array}{c} \partial X/\partial \theta_i \\ \partial X/\partial \theta_j \\ \partial X/\partial \theta_k \end{array}\right\} = 0 \qquad (2.11)$$

If the relation (2.11) showed the contribution of the typical

element $e$ to the calculations, we may assemble them for the entire domain as:

$$\left\{\frac{\partial X}{\partial \theta}\right\}^{D} = \sum_{e=1}^{NEL} \left\{\frac{\partial X}{\partial \theta}\right\}^{e} \tag{2.12}$$

where $D$ refers to the whole solution domain, and $NEL$ is the number of all the elements [4]. This assemblage (2.12) can also be written in terms of the nodal values of $\theta$ as:

$$\left\{\frac{\partial X}{\partial \theta_{n}}\right\}^{D} = \sum_{e=1}^{NEL} \left\{\frac{\partial X}{\partial \theta}\right\}^{e} \equiv 0 \tag{2.13}$$

where $n = 1, \ldots, N$, and $N$ is the number of all the nodes. Therefore, any potential field (temperature distribution field, for example) can be analysed by relations (2.11) and (2.13) by examining it at the nodes.

In other words, equation (2.10) is to be satisfied at all the points inside the region of interest, whereas equation (2.13) is at least satisfied at the nodes. Moreover, equation (2.13) can be analysed if equation (2.11) is satisfied within each element individually.

For demonstration purposes, the method is applied to a particular heat conduction problem in the next section.

## 2.4  A HEAT CONDUCTION PROBLEM

Although this method has been fully generalised, only for mathematical convenience, it is developed herein for a case study having neither sink nor radiation. Therefore, the typical element $e$ will be governed by equation (2.11), where:

$$X = \iiint\limits_{V^{e}} \left\{\frac{1}{2}\left[k_x \cdot \left(\frac{\partial \theta}{\partial x}\right)^2 + k_y \cdot \left(\frac{\partial \theta}{\partial y}\right)^2 + k_z \cdot \left(\frac{\partial \theta}{\partial z}\right)^2\right] - \left(Q - \rho \cdot C_p \cdot \frac{\partial \theta}{\partial t}\right) \cdot \theta\right\} \cdot dV$$

$$+ \iint\limits_{S_2} \left(q \cdot \theta\right) \cdot dS + \iint\limits_{S_3} \left[\frac{1}{2} \cdot h \cdot \left(\theta - \theta_{\infty}\right)^2\right] \cdot dS \tag{2.14}$$

in which $V^e$ represents the volume of element $e$, $S_2$ refers to any conductive boundary face of the element with (prescribed) heat flux $q$, and $S_3$ is the convective boundary face of the element if applicable (see equation (2.9)). Hence, equation (2.11) can be written at node $i$ of the element $e$ as:

$$\frac{\partial X}{\partial \theta_i} = 0 = \frac{\partial}{\partial \theta_i} \iiint_{V^e} \{\frac{1}{2}\left[k_x \cdot (\frac{\partial \theta}{\partial x})^2 + k_y \cdot (\frac{\partial \theta}{\partial y})^2 + k_z \cdot (\frac{\partial \theta}{\partial z})^2\right]$$

$$- (Q - \rho \cdot C_p \cdot \frac{\partial \theta}{\partial t}) \cdot \theta\} \cdot dV$$

$$+ \frac{\partial}{\partial \theta_i} \iint_{S_2} (q \cdot \theta) \cdot dS + \frac{\partial}{\partial \theta_i} \iint_{S_3} \left[\frac{1}{2} \cdot h \cdot (\theta - \theta_\infty)^2\right] \cdot dS$$

where $dV$ and $dS$ are independent of $\theta_i$, since the geometry is assumed to be fixed. Moreover, we assume that each of the quantities $Q$, $\rho$, $C_p$, $q$, $h$, $\theta_\infty$ and $\partial\theta/\partial t$ are independent of $\theta$ (and thus of $\theta_i$). Therefore, we may rewrite the previous equation as:

$$\frac{\partial X}{\partial \theta_i} = \underbrace{\iiint_{V^e} \{\left[\frac{\partial}{\partial \theta_i}(\frac{\partial \theta}{\partial x})\right] \cdot k_x \cdot (\frac{\partial \theta}{\partial x})\} \cdot dV}_{I^e_{x_i}} + \underbrace{\iiint_{V^e} \{\left[\frac{\partial}{\partial \theta_i}(\frac{\partial \theta}{\partial y})\right] \cdot k_y \cdot (\frac{\partial \theta}{\partial y})\} \cdot dV}_{I^e_{y_i}}$$

$$+ \underbrace{\iiint_{V^e} \{\left[\frac{\partial}{\partial \theta_i}(\frac{\partial \theta}{\partial z})\right] \cdot k_z \cdot (\frac{\partial \theta}{\partial z})\} \cdot dV}_{I^e_{z_i}} - \underbrace{\iiint_{V^e} \left[Q \cdot (\frac{\partial \theta}{\partial \theta_i})\right] \cdot dV}_{F^e_{Q_i}}$$

$$+ \underbrace{\iiint_{V^e} \left[\rho \cdot C_p \cdot \frac{\partial \theta}{\partial t} \cdot (\frac{\partial \theta}{\partial \theta_i})\right] \cdot dV}_{F^e_{c_i}} + \underbrace{\iint_{S_2} \left[q \cdot (\frac{\partial \theta}{\partial \theta_i})\right] \cdot dS}_{F^e_{q_i}}$$

$$+ \underbrace{\iint_{S_3} \left[h \cdot \theta \cdot (\frac{\partial \theta}{\partial \theta_i})\right] \cdot dS}_{I^e_{h_i}} - \underbrace{\iint_{S_3} \left[h \cdot \theta_\infty \cdot (\frac{\partial \theta}{\partial \theta_i})\right] \cdot dS}_{F^e_{h_i}} = 0 \qquad (2.15)$$

The integrals are labelled in this particular notation simply for convenience later.

Similar equations to (2.15) can be written for other nodes of the same element $e$ to make up the set of equations (2.11), in which we require a relationship among $\theta^e$, the temperature at a point inside the element $e$, and $x$, $y$ and $z$, its coordinates, and $\theta_i$, $\theta_j$ and $\theta_k$, the nodal temperatures of the element in question. In general, it may be shown that:

$$\theta^e = \theta(x,y,z,\theta_i,\theta_j,\theta_k,\ldots,t) \tag{2.16}$$

which is equal to the exact solution to the governing equations (2.1) and (2.2).

Hence, we now need to model $\theta^e$ by a trial function such that it satisfies the equation (2.15). This procedure may be repeated for all the elements. Here, this trial function is termed as the "temperature model", and is chosen as follows.

### 2.4.1  The Temperature Model

The temperature distribution is always continuous throughout a region, but the temperature gradient is not always continuous all over that region. For instance, at a separating interface between two different parts having different properties, the temperatures are equal (conforming), whereas the temperature gradients are usually different, since they depend on the properties. Therefore, the trial function chosen for $\theta$, which approximates the temperature distribution within the typical element $e$, must have continuity all over the element in question, and also the temperatures must be compatible at the boundaries (sides) between adjacent elements to hold the continuity all over the solution domain.

The temperature at any point inside the element $e$ surely

depends on its position relative to the nodes (vertices), as well as on the nodal temperatures of the element in question (equation (2.16)). Therefore, the exact solution (2.16) can be approximated by a trial function, chosen piecewise to define uniquely the state of the temperature $\theta^e$ within the typical element $e$ in terms of its nodal temperatures expressed as:

$$\theta^e = \sum N_i \cdot \theta_i$$

where $i$ refers to the nodal numbers of the element in question, and $N$'s are the "position functions" referring to the position of the point in question whose temperature is $\theta^e$. These functions are geometrical (depending on space and time) and are usually called "shape functions". Here, they are independent of time, since the geometry is fixed and, in such cases, the nodal temperatures only depend on time. Then we may write:

$$\theta^e = \left[ N_{(x,y,z)} \right] \cdot \{\theta_t\}^e \tag{2.17}$$

where $\left[ N_{(x,y,z)} \right]$ is a row matrix as:

$$\left[ N_{(x,y,z)} \right] = \left[ \ldots, N_{i(x,y,z)}, \ldots, N_{j(x,y,z)}, \ldots, N_{k(x,y,z)}, \ldots \right]$$

and $\{\theta_t\}^e$ is a column matrix, listing only the nodal temperatures of the element $e$ as:

$$\{\theta_t\}^e = \begin{Bmatrix} \vdots \\ \theta_{i(t)} \\ \vdots \\ \theta_{j(t)} \\ \vdots \\ \theta_{k(t)} \\ \vdots \end{Bmatrix}$$

A general three-dimensional linear model can have the following form:

$$\theta = A + B \cdot x + C \cdot y + D \cdot z \qquad (2.18)$$

where $A$, $B$, $C$ and $D$ are constants. In order to evaluate these constants, we need to know the temperatures at least at four nodes. The most suitable three-dimensional element is a tetrahedron, since it has only four vertices. Hence, the four constant coefficients ($A$, $B$, $C$ and $D$) in relation (2.18) can uniquely be determined in terms of the temperatures at the four vertices of the tetrahedral element. The two-dimensional equivalent in the $x$-$y$ plane is a triangular element (Section 3.2) where $D$ is zero, and the one-dimensional equivalent in the $x$-direction is simply a straight line joining two nodes, here $C$ and $D$ are both zero.

For a tetrahedral element with the nodes at the vertices $i$, $j$, $k$ and $\ell$, we can obtain:

$$\theta^e = [N] \cdot \{\theta\}^e \qquad (2.19)$$

where $\theta^e$ is the temperature at a point $P_{(x,y,z)}$ inside the element, and:

$$[N] = [N_i \quad N_j \quad N_k \quad N_\ell] \qquad (2.20)$$

in which $N_i = V_i/V_e$, etc., where $V_i$ is the volume of the tetrahedron $pjk\ell$ (sub-element), and $V_e$ is the volume of the tetrahedron $ijk\ell$ (the main element). Obviously, since:

$$\sum_i V_i = V_i + V_j + V_k + V_\ell = V_e \qquad (2.21)$$

we will have: $\quad \sum_i N_i = N_i + N_j + N_k + N_\ell = 1$

where $i$ is the summation over all the nodes of the element.

For a two-dimensional triangular element $ijk$, the detailed proof is given in the next chapter, where we can obtain:

$$\theta^e = [N] \cdot \{\theta\}^e$$

where $\theta^e$ is the temperature at a point $P_{(x,y)}$ inside the element, and:

$$[N] = [N_i \quad N_j \quad N_k] \qquad (2.22)$$

in which $N_i = \Delta_i/\Delta_e$, etc., where $\Delta_i$ is the area of the triangle $pjk$ (sub-element), and $\Delta_e$ is the area of the triangle $ijk$ (the main element). Obviously:

$$\sum_i N_i = N_i + N_j + N_k = 1$$

$$(2.23)$$

since: $\qquad \sum_i \Delta_i = \Delta_i + \Delta_j + \Delta_k = \Delta_e$

Finally, for a one-dimensional element $ij$, we can obtain:

$$\theta^e = [N] \cdot \{\theta\}^e$$

where $\theta^e$ is the temperature at a point $P_{(x)}$ on the element, and:

$$[N] = [N_i \quad N_j] \qquad (2.24)$$

in which $N_i = \ell_i/\ell_e$, etc., where $\ell_i$ is the length of $pj$ (sub-element), and $\ell_e$ is the length of the element $ij$ (the main element). Obviously:

$$\sum_i N_i = N_i + N_j = 1$$

(2.25)

since: $\qquad \sum_i \ell_i = \ell_i + \ell_j = \ell_e$

## 2.4.2 Finite Element Formulations

The problem can be solved if equations (2.13) are satisfied; consequently, equations (2.11) must be satisfied over each element, and, therefore, equation (2.15) must also be satisfied at all the nodes of each element. Hence, the chosen temperature model (2.17) must satisfy equation (2.15) within the typical element $e$. To do so, some derivatives of $\theta$ and its gradients with respect to $\theta_i$ are required as follows:

$$\theta^e = [N].\{\theta\}^e = \ldots N_i \cdot \theta_i + \ldots N_j \cdot \theta_j + \ldots N_k \cdot \theta_k + \ldots$$

(2.26)

and:
$$\frac{\partial \theta^e}{\partial x} = \ldots + \frac{\partial N_i}{\partial x}.\theta_i + N_i.\frac{\partial \theta_i}{\partial x} + \ldots \frac{\partial N_j}{\partial x}.\theta_j + N_j.\frac{\partial \theta_j}{\partial x} + \ldots$$

$$+ \ldots \frac{\partial N_k}{\partial x}.\theta_k + N_k.\frac{\partial \theta_k}{\partial x} + \ldots$$

where $\partial \theta_i/\partial x = \partial \theta_j/\partial x = \partial \theta_k/\partial x = 0$, since the mesh is fixed. Hence:

$$\frac{\partial \theta^e}{\partial x} = \ldots \frac{\partial N_i}{\partial x}.\theta_i + \ldots \frac{\partial N_j}{\partial x}.\theta_j + \ldots \frac{\partial N_k}{\partial x}.\theta_k + \ldots$$

(2.27)

Similar relations to (2.27) can be written with respect to $y$ and $z$. They also can be expressed in matrix form as:

$$\frac{\partial \theta^e}{\partial x} = \left[\frac{\partial N}{\partial x}\right].\{\theta\}^e$$

(2.28)

Likewise:

$$\frac{\partial \theta^e}{\partial y} = \left[\frac{\partial N}{\partial y}\right] \cdot \{\theta\}^e \qquad (2.29)$$

and:

$$\frac{\partial \theta^e}{\partial z} = \left[\frac{\partial N}{\partial z}\right] \cdot \{\theta\}^e \qquad (2.30)$$

where:

$$\left[\frac{\partial N}{\partial x}\right] = \left[\ldots \frac{\partial N_i}{\partial x} \ldots \frac{\partial N_j}{\partial x} \ldots \frac{\partial N_k}{\partial x} \ldots\right] \qquad , \text{ etc.} \qquad (2.31)$$

Moreover, from relation (2.27), we may write:

$$\frac{\partial}{\partial \theta_i}\left(\frac{\partial \theta^e}{\partial x}\right) = \frac{\partial N_i}{\partial x} \qquad (2.32)$$

Similarly:

$$\frac{\partial}{\partial \theta_i}\left(\frac{\partial \theta^e}{\partial y}\right) = \frac{\partial N_i}{\partial y} \qquad (2.33)$$

and:

$$\frac{\partial}{\partial \theta_i}\left(\frac{\partial \theta^e}{\partial z}\right) = \frac{\partial N_i}{\partial z} \qquad (2.34)$$

Also, from equation (2.26), we may derive:

$$\frac{\partial \theta^e}{\partial \theta_i} = N_i \qquad (2.35)$$

Finally, from the relation (2.17) for a fixed geometry, we will have:

$$\frac{\partial \theta^e}{\partial t} = \frac{\partial}{\partial t}\left([N] \cdot \{\theta\}^e\right) = [N] \cdot \frac{\partial}{\partial t}\{\theta\}^e = [N] \cdot \left\{\frac{\partial \theta}{\partial t}\right\}^e \qquad (2.36)$$

Now, the equation (2.15) can be developed by using the relations (2.17) to (2.36). The integrals in equation (2.15) are then considered individually as follows.

The first volume integral in relation (2.15), which corresponds to the first term of equation (2.1), represents the conduction of heat along the x-direction, and it can be written as:

$$I^e_{x_i} = \iiint_{V^e} \left\{ \left[ \frac{\partial}{\partial \theta_i} \left( \frac{\partial \theta}{\partial x} \right) \right] \cdot k^e_x \cdot \left( \frac{\partial \theta}{\partial x} \right) \right\} \cdot dV$$

By using relations (2.28), (2.31) and (2.32), we may write:

$$I^e_{x_i} = \iiint_{V^e} \left\{ \left( \frac{\partial N_i}{\partial x} \right) \cdot k^e_x \cdot \left[ \frac{\partial N}{\partial x} \right] \cdot \{\theta\}^e \right\} \cdot dV$$

in which the nodal temperatures, $\{\theta\}^e$, may come out of the integral, since the geometry is fixed and the nodal temperatures are independent of the geometry. Therefore:

$$I^e_{x_i} = \left( \iiint_{V^e} \left\{ \frac{\partial N_i}{\partial x} \cdot k^e_x \cdot \left[ \frac{\partial N}{\partial x} \right] \right\} \cdot dV \right) \cdot \{\theta\}^e \tag{2.37}$$

The second and third volume integrals in relation (2.15) correspond to the second and third terms in equation (2.1) and represent the conduction of heat along the $y$-and $z$-directions, respectively. Similar relations to (2.37) can be obtained for them as follows:

$$I^e_{y_i} = \left( \iiint_{V^e} \left\{ \frac{\partial N_i}{\partial y} \cdot k^e_y \cdot \left[ \frac{\partial N}{\partial y} \right] \right\} \cdot dV \right) \cdot \{\theta\}^e \tag{2.38}$$

and: 
$$I^e_{z_i} = \left( \iiint_{V^e} \left\{ \frac{\partial N_i}{\partial z} \cdot k^e_z \cdot \left[ \frac{\partial N}{\partial z} \right] \right\} \cdot dV \right) \cdot \{\theta\}^e \tag{2.39}$$

The fourth volume integral in the relation (2.15), which corresponds to the fourth term in equation (2.1), represents the generation of heat (sources term) within the element in question, $e$, and by using the relation (2.35) it can be written as:

$$F^e_{Q_i} = \iiint_{V^e} (Q^e \cdot N_i) \cdot dV \tag{2.40}$$

The fifth volume integral in the relation (2.15), which corresponds to the last term of equation (2.1), represents the time effect in transient phenomena and, by using relation (2.35), it can be expressed as:

$$F^e_{c_i} = \iiint_{V^e} \left[ (\rho^e \cdot C^e_p \cdot \frac{\partial \theta}{\partial t}) \cdot N_i \right] \cdot dV$$

where, from the relation (2.36), we will have:

$$F^e_{c_i} = \iiint_{V^e} (N_i \cdot (\rho^e \cdot C^e_p) \cdot [N] \cdot \{\frac{\partial \theta}{\partial t}\}^e) \cdot dV$$

Again, since the geometry (mesh) is fixed, all the time derivatives of the nodal temperatures can be moved outside the volume integral, and therefore we can write:

$$F^e_{c_i} = ( \iiint_{V^e} \{N_i \cdot (\rho^e \cdot C^e_p) \cdot [N]\} \cdot dV) \cdot \{\frac{\partial \theta}{\partial t}\}^e \tag{2.41}$$

The sixth integral in the relation (2.15), which represents the contribution of node $i$ in the conduction of heat through the conductive boundary surface $(S_2)$, may be written by using relation (2.35) as:

$$F^e_{q_i} = \iint_{S_2} (q^e \cdot N_i) \cdot dS \tag{2.42}$$

where $S_2$ is only the conductive boundary face of the boundary elements.

The seventh integral in the relation (2.15), which represents the convection of heat passed out of element $e$ through the convective boundary surface $(S_3)$, may be written by using relations (2.17) and (2.35) as follows:

$$I^e_{h_i} = \iint_{S_3} \left[ N_i \cdot h^e \cdot ([N] \cdot \{\theta\}^e) \right] \cdot dS$$

When the geometry (mesh) is fixed, the nodal temperatures $\{\theta\}^e$ are independent of geometry, and we may write:

$$I_{h_i}^e = \left(\iint_{S_3} \{N_i \cdot h^e \cdot [N]\} \cdot dS\right) \cdot \{\theta\}^e \qquad (2.43)$$

Finally, the last integral of relation (2.15), which represents the contribution of node $i$ in the convective heat gained by the element $e$ through the convective boundary surface $(S_3)$, may be written by using relation (2.35) as:

$$F_{h_i}^e = \iint_{S_3} (h^e \cdot \theta_\infty \cdot N_i) \cdot dS \qquad (2.44)$$

where $S_3$, in both relations (2.43) and (2.44), is only the convective boundary face of the boundary elements.

Therefore, equation (2.15) is the sum of all the equations (2.37) to (2.44) as:

$$\frac{\partial X^e}{\partial \theta_i} = I_{x_i}^e + I_{y_i}^e + I_{z_i}^e + I_{h_i}^e - F_{Q_i}^e + F_{c_i}^e + F_{q_i}^e - F_{h_i}^e = 0$$

in which all the terms have already been discussed. Similar relations can be written for other nodes of the same element $e$, and they can then be arranged in matrix form as:

$$\begin{Bmatrix} \frac{\partial X}{\partial \theta_i} \\ \frac{\partial X}{\partial \theta_j} \\ \frac{\partial X}{\partial \theta_k} \end{Bmatrix} = \begin{Bmatrix} I_{x_i} \\ I_{x_j} \\ I_{x_k} \end{Bmatrix} + \begin{Bmatrix} I_{y_i} \\ I_{y_j} \\ I_{y_k} \end{Bmatrix} + \begin{Bmatrix} I_{z_i} \\ I_{z_j} \\ I_{z_k} \end{Bmatrix} + \begin{Bmatrix} I_{h_i} \\ I_{h_j} \\ I_{h_k} \end{Bmatrix} - \begin{Bmatrix} F_{Q_i} \\ F_{Q_j} \\ F_{Q_k} \end{Bmatrix} + \begin{Bmatrix} F_{c_i} \\ F_{c_j} \\ F_{c_k} \end{Bmatrix} + \begin{Bmatrix} F_{q_i} \\ F_{q_j} \\ F_{q_k} \end{Bmatrix} - \begin{Bmatrix} F_{h_i} \\ F_{h_j} \\ F_{h_k} \end{Bmatrix} = 0$$

which is identical to the equation (2.11) and can be expressed as:

$$\left\{\frac{\partial X}{\partial \theta}\right\}^{e} = \{I_{x}\}^{e} + \{I_{y}\}^{e} + \{I_{z}\}^{e} + \{I_{h}\}^{e} - \{F_{Q}\}^{e} + \{F_{c}\}^{e} + \{F_{q}\}^{e} - \{F_{h}\}^{e} = 0 \quad (2.45)$$

where the first term on the right hand side (see equation (2.37)) may be factorised as follows:

$$\{I_{x}\}^{e} = [K_{x}]^{e} . \{\theta\}^{e} \quad (2.46)$$

where, by using relations (2.29) and (2.37), we will have:

$$[K_{x}]^{e} = \iiint_{V^{e}} \left\{ \left[\frac{\partial N}{\partial x}\right]^{T} . k_{x}^{e} . \left[\frac{\partial N}{\partial x}\right] \right\} . dV \quad (2.47)$$

This matrix is usually termed as the "thermal conductivity matrix along the X-direction". It is always a symmetric matrix of size $n \times n$ for an element with $n$ nodes. A general term of this matrix can be shown as:

$$K^{e}_{x_{(i,j)}} = \iiint_{V^{e}} \left\{ (\frac{\partial N_{i}}{\partial x}) . k_{x}^{e} . (\frac{\partial N_{j}}{\partial x}) \right\} . dV \quad (2.48)$$

which is the thermal energy conducted between the two nodes $i$ and $j$ through the element $e$ only along the X-direction. Likewise, for the same element $e$, the thermal conductivity matrices along the $y$-and z-directions may be defined, which are also symmetric matrices of size $n \times n$. They can be shown as:

$$\{I_{y}\}^{e} = [K_{y}]^{e} . \{\theta\}^{e} \quad (2.49)$$

where: $\qquad [K_{y}]^{e} = \iiint_{V^{e}} \left\{ \left[\frac{\partial N}{\partial y}\right]^{T} . k_{y}^{e} . \left[\frac{\partial N}{\partial y}\right] \right\} . dV \quad (2.50)$

whose general term is:

$$K^e_{y(i,j)} = \iiint_{V^e} \{ (\frac{\partial N_i}{\partial y}) \cdot k^e_y \cdot (\frac{\partial N_j}{\partial y}) \} \cdot dV \qquad (2.51)$$

along the $y$-direction. Similarly, along the z-direction:

$$\{I_z\}^e = [K_z]^e \cdot \{\theta\}^e \qquad (2.52)$$

where:
$$[K_z]^e = \iiint_{V^e} \{ [\frac{\partial N}{\partial z}]^T \cdot k^e_z \cdot [\frac{\partial N}{\partial z}] \} \cdot dV \qquad (2.53)$$

whose general term is:

$$K^e_{z(i,j)} = \iiint_{V^e} \{ (\frac{\partial N_i}{\partial z}) \cdot k^e_z \cdot (\frac{\partial N_j}{\partial z}) \} \cdot dV \qquad (2.54)$$

Similarly, $\{I_h\}^e$ in relation (2.45), by using the relation (2.43), can be written as:

$$\{I_h\}^e = [H]^e \cdot \{\theta\}^e \qquad (2.55)$$

where:
$$[H]^e = \iint_{S_3} \{ [N]^T \cdot h^e \cdot [N] \} \cdot dS \qquad (2.56)$$

This matrix is also symmetric, of size $n \times n$, and it is called the "convective matrix", whose general term is:

$$H^e_{(i,j)} = \iint_{S_3} (N_i \cdot h^e \cdot N_j) \cdot dS \qquad (2.57)$$

This only accounts for the loss of heat (by convection) through a boundary face (side $ij$) of the element $e$. The gain of heat through the same face is described by the integral $F^e_{h_i}$, defined in equation (2.15), which is analysed later in Section 2.4.3.

The next matrix in relation (2.45), $\{F_Q\}^e$, may be considered together with relation (2.40) and leads to:

$$\{F_Q\}^e = \iiint_{V^e} \{Q^e . [N]^T\} . dV \qquad (2.58)$$

which is a column matrix with $n$ terms and lists the contribution of the internal sources distributed over the element $e$, lumped at the nodes of the element $e$, whose general term is as (2.40), which is rewritten as:

$$F_{Q_i}^e = \iiint_{V^e} (Q^e . N_i) . dV \qquad (2.40)$$

Another matrix in equation (2.45), $\{F_c\}^e$, is developed by using relation (2.41) in the following way:

$$\{F_c\}^e = [C]^e . \{\frac{\partial \theta}{\partial t}\}^e \qquad (2.59)$$

where: $\quad [C]^e = \iiint_{V^e} \{[N]^T . (\rho^e . C_p^e) . [N]\} . dV \qquad (2.60)$

This matrix is also symmetric, of size $n \times n$, which can be named the "thermal capacity matrix". Its general term can be written as:

$$C_{(i,j)}^e = \iiint_{V^e} \{(N_i) . (\rho^e . C_p^e) . (N_j)\} . dV \qquad (2.61)$$

which is the thermal energy capacity, due to the material, between nodes $i$ and $j$ within the element $e$ only. Obviously, this matrix is considered only in the transient problems.

The next matrix in equation (2.45), $\{F_q\}^e$, is developed by using relation (2.42) as:

$$\{F_q\}^e = \iint_{S_2} \{q^e . [N]^T\} . dS \qquad (2.62)$$

This is a column matrix with $n$ terms, each of which represents the contribution of the corresponding node in conduction of heat through the conductive boundary face of the element in question on the conductive boundary surface, $S_2$. All the terms corresponding to the nodes not on (off) the conductive boundary surface $S_2$ are zero in this matrix. It is a boundary load matrix and may be called the "conductive (boundary) load matrix", and it is only considered in the boundary elements with at least one face on the conductive boundary surface, $S_2$. Its general term can be shown as relation (2.42), which is rewritten as:

$$F_{q_i}^e = \iint_{S_2} (q^e . N_i) . dS \qquad (2.42)$$

Finally, the last term in equation (2.45), $\{F_h\}^e$, is considered together with relation (2.44). We may then write:

$$\{F_h\}^e = \iint_{S_3} \{h^e . \theta_\infty . [N]^T\} . dS \qquad (2.63)$$

which is also a column matrix with $n$ terms, each term representing the contribution of the corresponding node in the convection of heat gained by the element $e$ through the boundary face of the element $e$ on the convective boundary surface, $S_3$. All terms corresponding to the nodes off (not on) the convective boundary surface $S_3$ are zero in this matrix. This is, again, a boundary load matrix and may be called the "convective (boundary) load matrix". Its general term can be shown as relation (2.44), which is rewritten as:

$$F_{h_i}^e = \iint_{S_3} (h^e . \theta_\infty . N_i) . dS \qquad (2.44)$$

Consequently, equation (2.45) for the typical element $e$ with $n$ nodes may be re-arranged as:

$$[K]^e . \{\theta\}^e + [C]^e . \left\{\frac{\partial \theta}{\partial t}\right\} + \{F\}^e = 0 \qquad (2.64)$$

where: $\qquad [K]^e = [K_x]^e + [K_y]^e + [K_z]^e + [H]^e \qquad (2.65)$

which is usually termed the "thermal conductivity matrix" of the element $e$. Since each matrix on the right hand side is symmetric, of size $n \times n$, $[K]^e$ is also symmetric, of size $n \times n$, and $[C]^e$ is described as before by the relation (2.60). Finally, in relation (2.64):

$$\{F\}^e = - \{F_Q\}^e + \{F_q\}^e - \{F_h\}^e \qquad (2.66)$$

This is a column matrix with $n$ terms and is usually called the "load matrix" (see equations (2.58), (2.62) and (2.63)). These matrices are explained thoroughly and in detail in Section 2.4.3.

Each element may be governed by the equation (2.11), which is equivalent to the equation (2.64), and which is called the "elemental matrix equation".

Using a similar procedure used to obtain equation (2.13) from the relation (2.11), we may take the ensemble of all the elemental equations (2.64) and write them in the following form:

$$[K] . \{\theta\} + [C] . \left\{\frac{\partial \theta}{\partial t}\right\} + \{F\} = 0 \qquad (2.67)$$

where each matrix is directly formed by assembling all the corresponding matrices in the elemental matrix equation (2.64). The above equation (2.67) has been derived for an arbitrary number of elements with arbitrary

number of nodes. Also, the solution domain as well as each element can be of arbitrary shape.

For the entire solution domain with $N$ nodes, the relation (2.67) is called the "system matrix equation", in which $[K]$ and $[C]$ are both symmetric matrices of size $N \times N$. They are also named similar to the corresponding matrix in the elemental equation (2.64) as the thermal conductivity matrix and the thermal capacity matrix of the system, respectively. Moreover, $\{F\}$ can be called the load matrix of the system which is a column matrix with $N$ nodal loads.

### 2.4.3 Discretisation of the Loads

In the finite element method, a continuous solution domain is replaced by a mesh with a number of nodes. The problem is then numerically analysed only at the nodes. Therefore, the system of all the loads acting on the solution-domain also has to be replaced by an equivalent system of distinct loads acting only at those nodes (the nodal loads) in such a way that the overall balance of the system is conserved. The nature of loads can occur in many forms, such as weights, forces or even thermal loads. The analysis is very general and applicable to all types, but our primary concern here is to deal with the thermal loads. These loads are formulated here only for a typical element, as in equation (2.66). Then the system of loads on the whole solution-domain is just the sum of all the loads on each individual element (assemblage). In general, the loads acting on the solution-domain can be classified into two types as follows: (a) the loads that act at a point (point-loads), and (b) the loads that are distributed (distributive loads). Point-loads can easily be replaced by an equivalent system of distinct loads acting at the nodes, which is described later, but the distributed loads have to be dealt with more carefully.

Each term on the right hand side of equation (2.66) represents a particular type of load which may act on the typical element. Any system of scattered or distributed loads of each type acting on the element must be replaced by an equivalent system of distinct loads acting only at the nodes of that element. This can be achieved in two steps. Firstly, all the similar loads can be replaced by a single point-load ($\vec{F}_p^e$, their resultant) acting at a unique point ($P$, the load-centre), where the net moment due to that type of load is zero (conservation). Next, this is then treated as a point load which can be replaced by an equivalent system of distinct loads acting just at the nodes of the element (segmentation). Of course, great care has to be taken so that the basic laws of conservation and moment are not violated. This is explained in detail in Appendix A.

In the thermal problems, the distributed heat loads can either be internally generated inside the solution-domain, or can be externally applied to the solution-domain (imposed as the boundary conditions), namely, the body forces due to the potential flow passing through the boundary. These loads can be dealt with as before and may be combined by a relation similar to the relation (2.66), in which each vector matrix on the right hand side involves a particular distributed load, acting on the typical element. Hence, they are individually transformed to vectors that involve an equivalent system of nodal loads.

The first vector matrix on the right hand side of the relation (2.66), namely, $\{F_Q\}^e$, involves only the internally generated heat loads that are due to the production of heat by the distributed (or point) sources within the element. Consider a typical element with a general load distribution with a local density $\vec{Q}^e$ per unit volume. All this distributed load can be replaced by a point-load as described for the relations (A.1a) and (A.1b). This load is taken to act at a unique point

(the load-centre) located by the relation (A.2). Next, this point-load

has to be replaced by an equivalent system of distinct loads acting at the

nodes of the same element, $e$, such that the relations (A.7) and (A.8) are

both satisfied. This must lead to the same results as given by the

relation (A.16). If the element is a tetrahedron and the load is

uniformly distributed, then equation (A.24) has to be used, which is:

$$\{F_Q\}^e = \frac{\vec{Q}^e \cdot V^e}{4} \cdot \begin{Bmatrix} 1 \\ 1 \\ 1 \\ 1 \end{Bmatrix} \tag{2.68}$$

The second vector matrix on the right hand side of the relation

(2.66), namely, $\{F_q\}^e$, which is a boundary load matrix and involves some

of the externally applied body forces. It consists of only the nodal

loads due to the conduction of heat through a boundary face $(S_e)$ of a

boundary element, associated with the approximated surface representing

the conductive boundary surface $(S_2)$, referred to as the Neumann type of

boundary condition. Consider a typical boundary face, $S_e$, of a boundary

element $e$ with a continuous heat flux distribution, $\vec{q}_{S^e}$, across the face

$S_e$. The total heat load due to this heat flux is equivalent to a point-

load determined by the relations (A.3a), (A.3b) and (A.4). Next, this

point-load has to be replaced by an equivalent system of distinct loads

acting at the nodes of the same element, $e$, preferably at the nodes on the

same boundary face, $S_e$. Again, the relations (A.7) and (A.8) both have

to be satisfied. This must lead to the same results as given by the

relation (A.17). If the face $S_e$ is triangular and the heat flux is

uniform through it, then equation (A.29) has to be used, which is:

$$\{F_q\}^e = \frac{\vec{q}_{S^e} \cdot \Delta e}{3} \cdot \begin{Bmatrix} 1 \\ 1 \\ 1 \end{Bmatrix} \tag{2.69}$$

Finally, the third vector matrix on the right hand side of the relation (2.66), namely, $\{F_h\}^e$, which is also a boundary load matrix and involves only some of the body forces externally applied to the solution-domain across the boundary surface $S_3$. It consists of the nodal loads which represent only the influx of the potential flow through a boundary face. In the thermal problems, they are due to the heat flow by convection from the ambient to the solution domain, and they refer to the second term in relation (1.10), termed as the Cauchy type of boundary condition. Of course, the flow of heat transferred from the solution-domain to the ambient through the same boundary face, $S^e$, which refers to the first term on the right hand side of the relation (1.10), was accounted for in the thermal conductivity matrix as the $H$ matrix given by the relation (2.56).

The matrix $\{F_h\}^e$ can be analysed similarly to the previous one, namely, $\{F_q\}^e$, where the local heat flux is taken to be:

$$\vec{q}_{S^e} = h^e_{S^e} \cdot \theta^e_\infty$$

in which $h^e_{S^e}$ is the prescribed heat transfer coefficient on the boundary face $S^e$ of the element $e$, and $\theta^e_\infty$ is the prescribed ambient temperature effective on $S^e$. This must lead to the same results as given by the relation (A.18), or, in the case of uniformity, the relation (A.29) can be used.


## 2.5 CALCULATIONS

After the solution domain has been replaced by a mesh and a known distribution of loads has been replaced by an equivalent system of distinct loads acting only at some selected (or all of the) nodes of the mesh, the unknown potentials, $\theta$, can be calculated at the nodes. Finite

element equations in the form of (2.64) are then derived for each element, involving its nodal potentials (temperatures, for example) as the unknowns. For a solution domain with $N$ nodes, the ensemble (2.67) yields $N$ linear algebraic simultaneous equations (involving $N$ known nodal loads and $N$ unknown nodal potentials), which can then be solved by well-established matrix solving methods. A typical $i$th equation of such a set may be written as:

$$\sum_{j=1}^{N} K_{(i,j)} \cdot \theta_j + \sum_{j=1}^{N} C_{(i,j)} \cdot \frac{\partial \theta_j}{\partial t} + F_i = 0 \qquad (2.70)$$

This set of equations is solved here by a computationally very economic, hybrid, Gauss-Seidel iteration method, which also automatically optimises an over-relaxation factor within each iteration. The technique is similar to the one proposed by Carré,B.A.[8].

## 2.6  THE PERFORMANCE OF THE METHOD

The actual generation of numerical results can depend on many factors. However, the system matrix equation (2.67) is stable and has a unique solution. The accuracy of the method depends on the number of elements, number of nodes, order of the mathematical model, etc. The speed of convergence of the solution is related to the actual method used to solve the matrix equation (2.67). In this respect, a lot of research has been carried out by mathematical analysts. The hybrid Gauss-Seidel iteration method has many advantages over other methods.

Some factors which affect the method are sometimes conflicting, and therefore particular attention has to be paid to optimise the achievement of a satisfactory result in each case. For instance, the number of elements is essentially a compromise between two conflicting demands. On one hand, the solution-domain has to be discretised into a number of

elements small enough to ensure that the mathematical modelling adequately

approximates the exact solution.   On the other hand, the number of

elements, as well as the number of nodes, will be limited by the storage

capacity of the available computer used.   Moreover, any increase in the

number of elements increases the computational time and effort, and hence

makes it more expensive.   In a scalar potential (temperature, for example)

field, each node carries only one scalar quantity, whereas in a vector

potential field each node carries a vector whose two or three components

(in two or three-dimensional cases, respectively) have to be stored.

Thus, the requirements (or limitations of the capacity) of the computer

storage depends on the nature of the problem.   Further, the number of

equations in (2.67) is doubled or tripled in two-or three-dimensional

vector potential field problems.

Although the method is fully independent of the grid, the careful

choice of the mesh can enable us to produce better results, often at less

computer expense.   For example, in the directions with higher rates of

change in the potentials (temperatures), closer nodes (smaller dimensions

of the elements) give better quality of the solution, and in other

directions farther nodes (larger dimensions of the elements) give smaller

numbers of elements.   Thus, each problem may have its own special recipe

of optimal parameters for computational effort.   Hence, it is very

difficult to generalise for every situation.   On the shape of the

elements, many authors have considered a generally accepted idea of

"aspect-ratio", which is a characteristic of discretisation that affects

the finite element solution.   It describes the shape of the element in

the assemblage, it implies the sharpness or narrowness of the element, and

it can be defined as the ratio of the length of its largest dimension to

the length of its smallest dimension.   The optimum aspect-ratio of an

element at any location within the grid depends largely on the difference

in the rate of change of the potentials (temperature) in different
directions.  If the potentials (temperature) vary at about the same rate
in each direction, then the closer the aspect-ratio to unity, the better
the quality of the solution.  Moreover, sharp and narrow elements, as
well as concave elemtns, should be avoided since their volumes may not be
calculated accurately enough and it may take a longer computational time to
converge to a good solution, or even fail to converge.

The system matrix equation (2.67), which governs all the solution-
domain, is the ensemble of all the elemental equations (2.64), which is
employed piecewise over each element individually and is also fully
independent of the physical and geometrical properties of other elements.
This makes the method so useful and so powerful for solving almost any
type of potential field problem.  It can be applied to most physical
problems with non-linearities involving inhomogeneous situations,
anisotropic materials, and irregular geometries of the solution-domain, as
well as arbitrary boundary conditions ( see Table 1.3 ).  This is
especially helpful in multi-phase (transient) problems, since the
interfaces (between any two neighbouring phases) can be very irregular and
also shift with respect to time.  The same method can be used to solve
both steady-state and transient problems, as well as for single or multi-
phase problems.

Although the finite element method has been applied to a vast range
of problems, there are still many problems for which this method has to be
developed.  In conclusion, however, we may say in brief that the quality
of the (finite element) solution depends mostly on the following criteria.


(a)  Smallness of the elements, refinements are needed in zones of

     steep potential (temperature) gradients, or abrupt changes in

     the geometry or source distributions, as well as in the physical

properties.   Refinements are also recommended where more
accuracy is demanded.

(b)   The order of the mathematical model (the trial function);   the
      higher the order we choose, the more accurate the solution we
      achieve, but the more difficult the formulations.

(c)   The shape of the elements;   for a typical element, the closer
      the aspect-ratio is to its optimal, the more accurate the
      solution will be.

(d)   The number of nodes and elements;   the more nodes and elements
      we look at, the more accurate the representations of the
      solution-domain we obtain and the better quality of the solution.
      However, the more equations (in (2.67)) to be solved, the more
      expensive the solution.


A two-dimensional version of this method is explained in the following
chapters for steady-state and transient problems, as well as for the
moving boundary problems.

# CHAPTER 3

## TWO-DIMENSIONAL FORMULATIONS

The finite element method, proposed in Chapter 2, is applied to a general two-dimensional heat conduction problem, with temperature-dependent thermal conductivity, for the time-independent (steady-state) case. The first, second and third kinds of boundary conditions are included.

## 3.1  INTRODUCTION

The finite element method, as described in the previous chapter, may be applied to any type of potential field problem, including vector potential field problems, although more attention has to be paid to that type of problem. A general heat conduction problem, as considered in Section 2.4, requires only the calculation of the temperature distribution, which is a scalar potential field problem. The analysis for the vector potential field problems has not been included.

In this chapter, a general two-dimensional steady-state heat conduction problem is analysed by the same method as introduced in Chapter 2. The method is formulated for a very general case, involving an arbitrary shape of the solution-domain, as well as physical material non-linearities (temperature-dependent properties, or different materials, for example).

Moreover, the formulations are arranged such that they are applicable to both cartesian and axi-symmetric systems with minimal changes. In a cartesian system, any arbitrary element ($e$) with the cross-section sketched in the ($x,y$) plane (Figure 3.1(a)) will represent a vertical prism of height $\ell^e$ along the z-direction (perpendicular to the ($x,y$) plane). The volume of such a prism is:
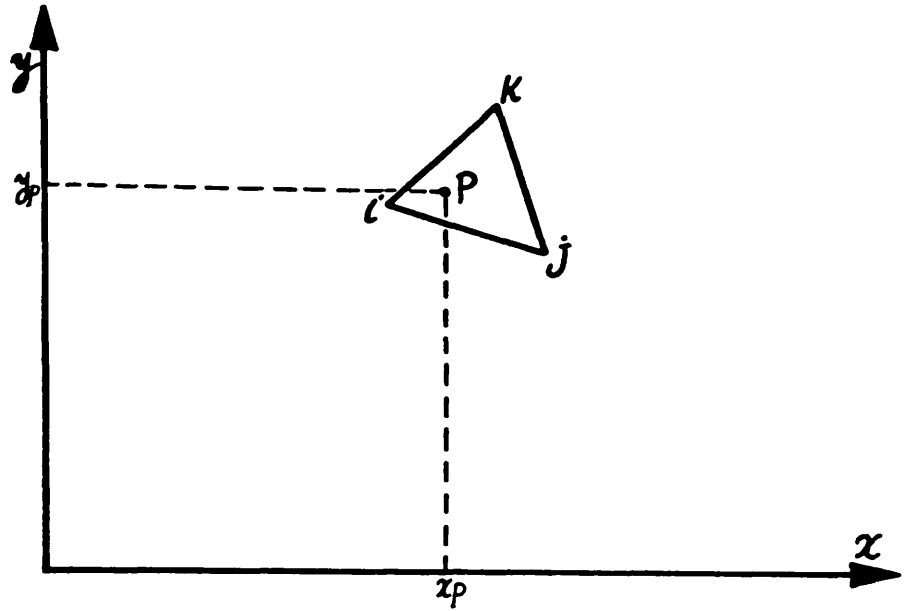
(a) A two-dimensional element in $X$-$Y$ Plane, cartesian system.
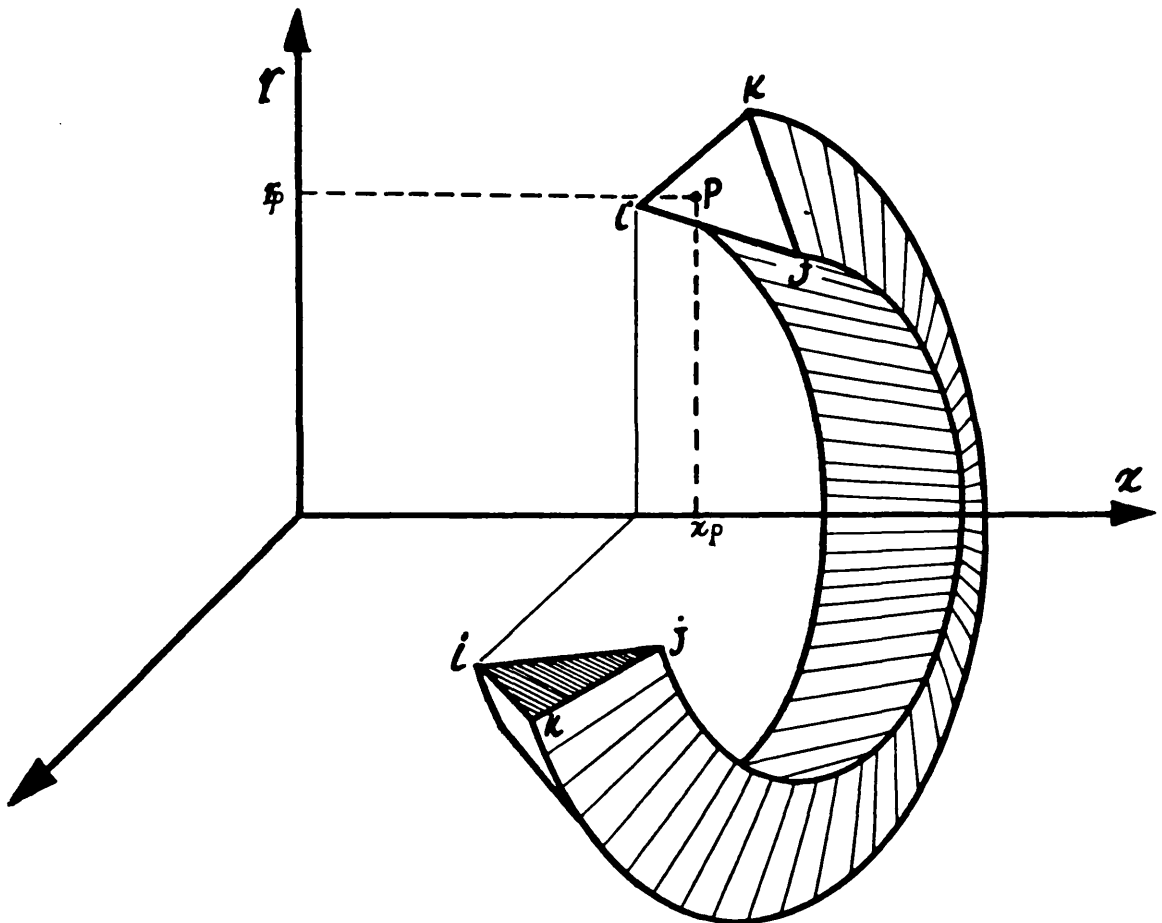


(b) A two-dimensional element in $X$-r Plane, axi-symmetrical system

Figure 3.1:

$$V^e = \ell^e \cdot \iint\limits_{S^e} dS = \ell^e \cdot \iint\limits_{S^e} dx\, dy \qquad (3.1)$$

where $S^e$ is the area of the cross-section of the element $e$ on the $(x,y)$ plane. The area of a lateral face (on side $ij$, for example) on the boundary surface of the prism is:

$$S_{ij} = \ell^e \cdot \int\limits_{ij} dc \qquad (3.2)$$

while, in an axi-symmetric system, any arbitrary element $e$ with the cross-section sketched in the $(x,\imath)$ plane (Figure 3.1(b)) will represent a toroidal section of mean radius $\imath_m^e$ generated by rotating it around the $x$-axis. The volume of such a toroidal section is:

$$V^e = \psi \cdot \imath_m \cdot \iint\limits_{S^e} dS = \psi \cdot \imath_m^e \cdot \iint\limits_{S^e} dx\, d\imath \qquad (3.3)$$

where $\psi$ is the angle subtended by the toroidal section at the axis of gyration in radians. The area of a lateral face (on side $ij$, for example) on the boundary surface of this toroidal section is:

$$S_{ij} = \psi \cdot \imath_m^e \cdot \int\limits_{ij} dc \qquad (3.4)$$

where $\imath_m^e$ is, here, the mean radius of the axi-symmetric surface generated by rotation of the side $ij$ around the axis of gyration.

From the similarities between Figures 3.1(a) and 3.1(b), relations (3.1) and (3.3), as well as relations (3.2) and (3.4), the $(x,y)$ plane of a cartesian system may be replaced (in the formulations) by the $(x,\imath)$ plane in the axi-symmetric system, where the $x$-axis is the axis of revolution. Namely, $\ell^e$ must simply be replaced by $\psi \cdot \imath_m^e$ and the $y$

coordinate has to be replaced by the $\hbar$ coordinate in order to change the formulations from the cartesian system to the axi-symmetric system. Thus, it suffices to explain the formulations only in the cartesian system.

For plotting purposes, the solution domain is represented by a finite area, which is the cross-section of the actual solution-domain in the $(x,y)$ plane. This is termed the "solution plane". Since the temperature of any point within the solution-domain is a scalar quantity, it can be plotted along the third direction, perpendicular to the solution plane, which is called the "solution direction". Plotting the actual temperature distribution at all the points on the solution-domain will form a continuous surface. This surface is termed the "exact solution surface". A similar surface obtained by the analytical solution to the differential equation (2.1) for the same problem should also coincide with the first surface. Theoretically, it is possible to obtain a numerical solution surface, which is also close enough to the same surface by taking a sufficiently small refinement of the solution-domain. When the solution-domain is discretised into a finite number of smaller elements, similar subdivisions can also be obtained on the exact solution surface, such that each section is projected entirely on one element. Thus, the number of these sections on the solution surface is the same as the number of elements in the solution-domain. For instance, this discretisation is shown in Figure 3.2 for a special case of triangular elements for a particular solution-domain. This is only for the ease of understanding later. The problem is now able to obtain a solution surface as close as possible to the exact solution surface using a finite number of sections. Hence, each of these sections needs to be approximated as accurately as possible by temperature modelling.
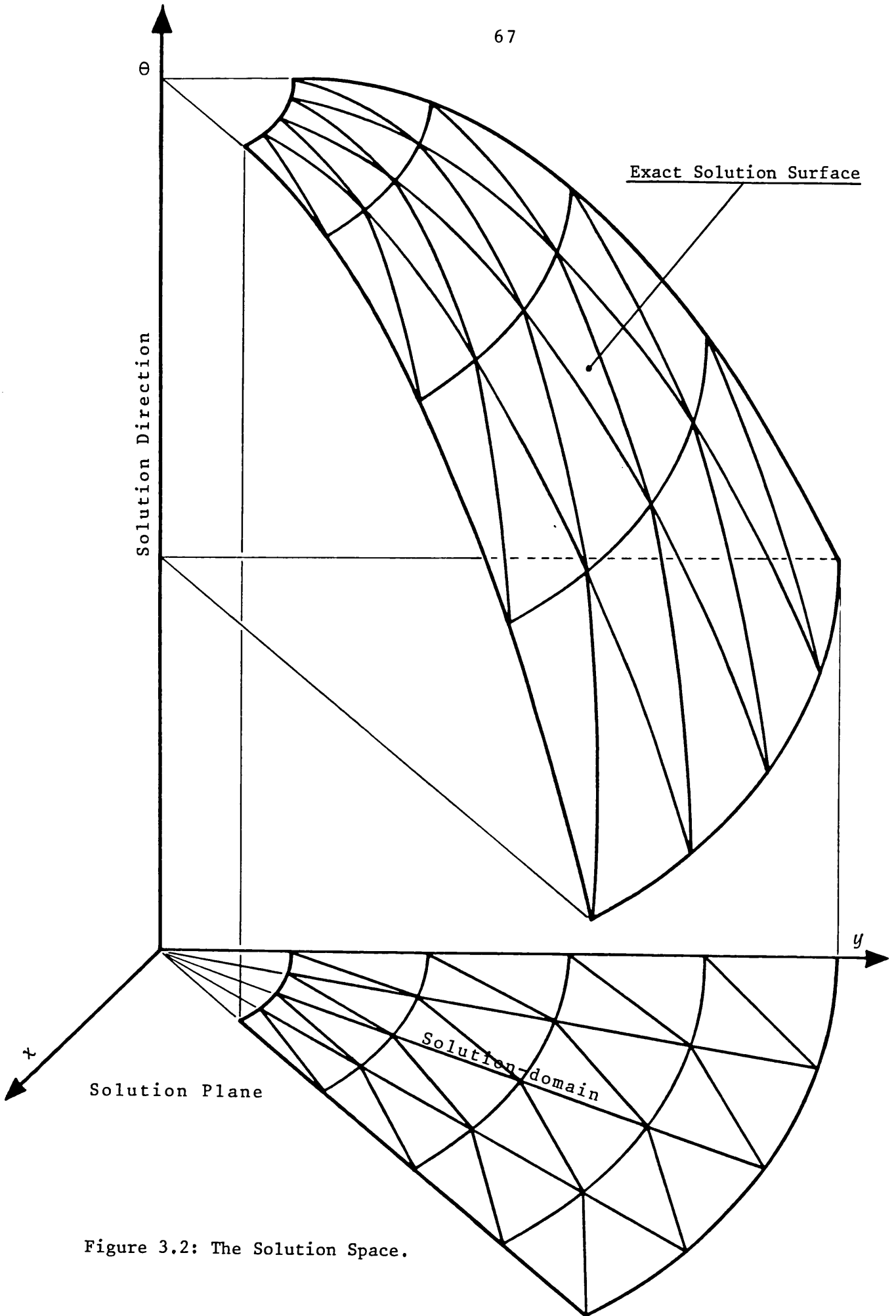
θ

Solution Direction

Exact Solution Surface

y

x

Solution Plane

Solution domain

Figure 3.2: The Solution Space.

## 3.2 TEMPERATURE MODELLING

### 3.2.1 Temperature Model for an Element with Three Nodes

Let the solution-domain be replaced by a triangular mesh with nodes at its joints (vertices); then, by the same method described in the previous section, the exact solution surface can be subdivided into the same number of triangular sections as the number of elements of the mesh (see Figure 3.2). Each section of the exact solution surface, which can also be projected on a unique element, can be replaced by an approximate solution surface, defined by the exact temperatures at the nodes of that element. This can be done only by defining a (polynomial type) relation to express an approximate solution surface close enough to the exact solution surface. The mathematical form of this relation is called the "trial function", which is also termed the "temperature model". Obviously, the accuracy of the approximation depends on the form of this trial function. Each element has to be dealt with individually, and independently.

Consider a typical triangular element $e$ (of the solution-domain), as shown in Figure 3.3, with nodes $i$, $j$ and $k$ at its vertices. The exact temperature distribution over that element can be plotted as shown by a curved triangle $(\theta_i \; \theta_j \; \theta_k)$, the "exact solution surface" (curved lines). A plane triangle $(\theta_i \; \theta_j \; \theta_k)$ is fitted passing through the exact temperatures at the vertices as defined in Figure 3.3, the "approximate solution surface" (straight lines). Both of these curved and plane triangles must project on the same element, $e$. The latter, which is also unique, is taken to be an approximate temperature distribution over the element $e$. Therefore, the exact solution surface over the typical element (the curved triangle) can be replaced by this approximate solution surface (the plane triangle). Of course, any point $P$ within the element $e$ has an exact temperature, $PB$, as shown in Figure 3.3, and an approximate temperature as $PA$, where the error at that point $P$ is defined as $\varepsilon$.
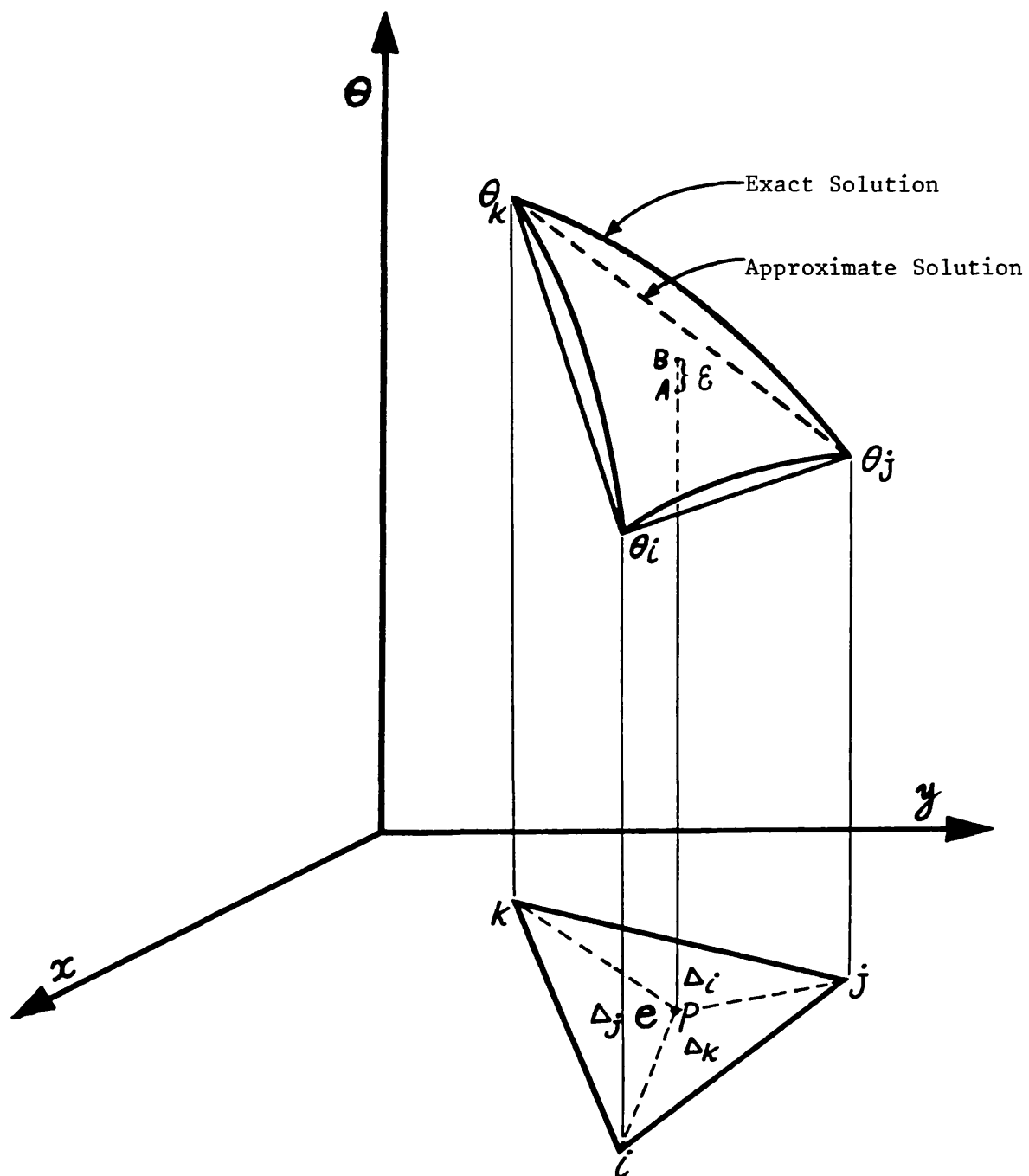
Figure 3.3: A typical triangular Element with three Nodes at its

vertices and using a Linear Temperature Model.
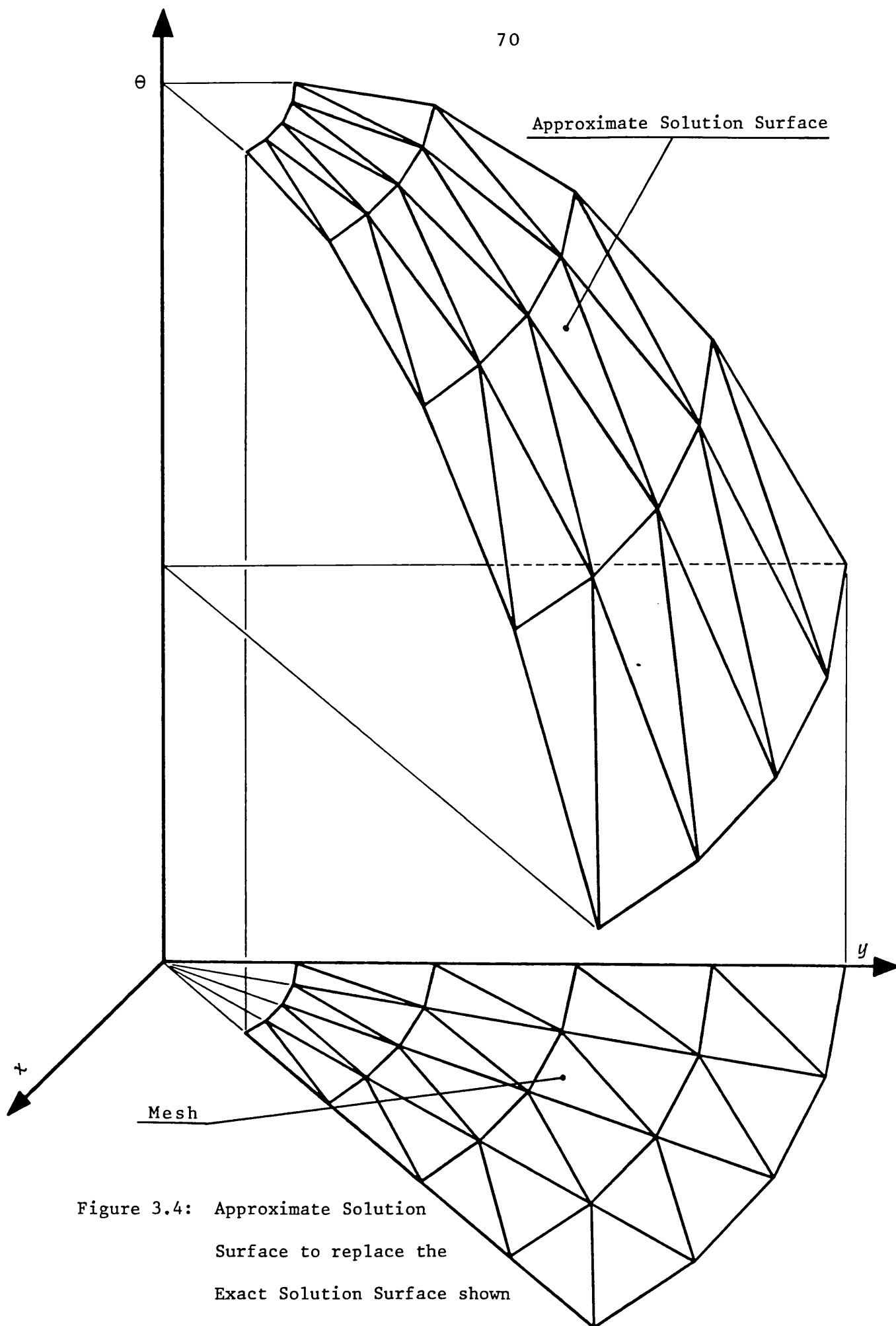
Figure 3.4: Approximate Solution Surface to replace the Exact Solution Surface shown in Figure 3.2, using Linear Temperature Model and triangular Elements.

For example, Figure 3.4 may show the assemblage of such approximations over each element for the same case as shown in Figure 3.2. This is a "crystal-like" surface imagination of the replacement to the exact solution surface.

Mathematically, the exact solution surface over the element $e$ may be expressed by some relation, say:

$$\theta^e = \theta(x,y) \qquad (3.5)$$

and the approximate solution surface (the plane triangle, $\theta_i$ $\theta_j$ $\theta_k$) over the same element $e$ can be expressed by a linear relation of the form:

$$\theta^e = A + B.x + C.y \qquad (3.6)$$

where $A$, $B$ and $C$ are constant, which can uniquely be determined in terms of the exact values of the nodal temperatures ($\theta_i$, $\theta_j$ and $\theta_k$ at nodes $i$, $j$ and $k$, respectively) by solving the following simultaneous equations:

$$\theta_i = A + B.x_i + C.y_i$$

$$\theta_j = A + B.x_j + C.y_j \qquad (3.7)$$

$$\theta_k = A + B.x_k + C.y_k$$

This can be solved to yield:

$$A = \frac{1}{2.\Delta_e} . [a] . \{\theta\}^e$$

$$B = \frac{1}{2.\Delta_e} . [b] . \{\theta\}^e \qquad (3.8)$$

$$C = \frac{1}{2.\Delta_e} . [c] . \{\theta\}^e$$

where $\Delta_e$ is the area of the element $e$, and:

$$[a] = [a_i \quad a_j \quad a_k]$$

$$[b] = [b_i \quad b_j \quad b_k] \quad \text{and} \quad \{\theta\}^e = \begin{Bmatrix} \theta_i \\ \theta_j \\ \theta_k \end{Bmatrix} \qquad (3.9)$$

$$[c] = [c_i \quad c_j \quad c_k]$$

These are termed as the element characteristic matrices, where $a$, $b$ and $c$ are called the "element characteristics" and may be tabulated as follows:

TABLE 3.1

The Characteristics of the Typical Triangular Element

$ijk$ in Figure 3.3 [9]

| Corresponding to | $a$ | $b$ | $c$ |
|---|---|---|---|
| Node $i$ | $a_i = (x_j \cdot y_k - x_k \cdot y_j)$ | $b_i = (y_j - y_k)$ | $c_i = (x_k - x_j)$ |
| Node $j$ | $a_j = (x_k \cdot y_i - x_i \cdot y_k)$ | $b_j = (y_k - y_i)$ | $c_j = (x_i - x_k)$ |
| Node $k$ | $a_k = (x_i \cdot y_j - x_j \cdot y_i)$ | $b_k = (y_i - y_j)$ | $c_k = (x_j - x_i)$ |

Substituting relations (3.8) in equation (3.6) and re-arranging the terms, we obtain:

$$\theta^e = \left[ (\frac{a_i + b_i \cdot x + c_i \cdot y}{2 \cdot \Delta_e}) \cdot \theta_i + (\frac{a_j + b_j \cdot x + c_j \cdot y}{2 \cdot \Delta_e}) \cdot \theta_j + (\frac{a_k + b_k \cdot x + c_k \cdot y}{2 \cdot \Delta_e}) \cdot \theta_k \right]$$

This can finally be written in matrix form as:

$$\theta^e = [N] \cdot \{\theta\}^e \qquad (3.10)$$

where:

$$[N] = [N_i \quad N_j \quad N_k]$$

and:

$$N_i = (a_i + b_i \cdot x + c_i \cdot y)/(2 \cdot \Delta_e)$$

$$N_j = (a_j + b_j \cdot x + c_j \cdot y)/(2 \cdot \Delta_e) \qquad (3.11)$$

$$N_k = (a_k + b_k \cdot x + c_k \cdot y)/(2 \cdot \Delta_e)$$

These are the position functions or the interpolation functions to be used for locating the unique point $P(x,y)$. Equation (3.10) is now similar to equation (2.19) described in Section 2.4.1 for a general case.

Consider a point $P(x,y)$ within the typical triangular element with vertices $ijk$ (Figure 3.3); then the area of the triangle $jpk$ ($\Delta_i$) is determined as follows:

$$\Delta_i = \tfrac{1}{2} \cdot \det \begin{bmatrix} x & y & 1 \\ x_j & y_j & 1 \\ x_k & y_k & 1 \end{bmatrix} = \tfrac{1}{2} \cdot [x \cdot (y_j - y_k) + y \cdot (x_k - x_j) + (x_j \cdot y_k - x_k \cdot y_j)]$$

By referring to Table 3.1, it can be shown that:

$$\Delta_i = \tfrac{1}{2} \cdot (a_i + b_i \cdot x + c_i \cdot y)$$

From the definition of $N_i$ in relation (3.11), we will have:

$$N_i = \frac{\Delta_i}{\Delta_e}$$

$$(3.12)$$

Similarly: $\qquad N_j = \dfrac{\Delta_j}{\Delta_e} \qquad$ and $\qquad N_k = \dfrac{\Delta_k}{\Delta_e}$

Due to the above results, $N_i$, $N_j$ and $N_k$ are also referred to as the area

coordinates.    From relations (3.12), we may write:

$$N_i + N_j + N_k = \frac{\Delta_i + \Delta_j + \Delta_k}{\Delta_e} = 1 \qquad (3.13)$$

Given the unique coordinates of $P(x,y)$, we can use any two of

the equations of (3.11) to determine the $N$'s, since the third is a

function of the other two, determined by relation (3.13).    Conversely, if

any two of the $N$'s were known $(N_i$ and $N_j$, for example), then the third

$(N_k)$ is also known by relation (3.13).    Thus, we can solve the system to

determine $x$ and $y$ uniquely as follows:

$$x = N_i \cdot x_i + N_j \cdot x_j + N_k \cdot x_k$$

$$\qquad (3.14)$$

$$y = N_i \cdot y_i + N_j \cdot y_j + N_k \cdot y_k$$

Since we are only interested in the solution within each

element, the point $P$ must be confined inside the element.    This implies

that the above-mentioned areas shall never be negative, and, consequently,

none of the $N$'s can be negative or greater than unity.    Hence, equation

(3.10) is only valid for the points on the plane triangle $(\theta_i \; \theta_j \; \theta_k)$

projecting on the element $ijk$ in Figure 3.3, and the excess plane defined

by equation (3.6) is automatically neglected.    Namely, equations (3.6)

and (3.10) are equivalent only and only over the element in question.

Therefore, it suffices to store either only the $x$ and $y$ for any point $P$,

or any two of $N_i$, $N_j$ and $N_k$, and the others can be obtained by using

relations (3.11) or (3.14).    In the finite element method, the latter are

more useful.

At this stage, some special relations are introduced which

will be used later, between the position of the point $P$ and the

corresponding $N$'s.    If the point $P$ coincides with the element centroid,

then by the properties of a triangle:

$$\Delta_i = \Delta_j = \Delta_k = \frac{1}{3} \cdot \Delta_e$$

Hence:$\qquad\qquad\qquad N_i = N_j = N_k = \frac{1}{3}$ $\qquad\qquad\qquad$ (3.15)

If the point $P$ lies on the mid-point of any side (side $ij$, for example),

then $\Delta_k = 0$ and $\Delta_i = \Delta_j = \frac{1}{2} \cdot \Delta_e$.    Thus:

$$N_i = \frac{1}{2} \quad , \quad N_j = \frac{1}{2} \quad \text{and} \quad N_k = 0 \qquad\qquad (3.16)$$

In brief, the temperature distribution over each triangular

element can be approximated by a linear relation of the form (3.6), which

is uniquely defined over the element, and can be expressed in matrix form

as (3.10).    The complete approximate solution surface then obtained

globally over the solution-domain looks similar to the one plotted in

Figure 3.4.    This is an approximation to the exact solution surface,

similar to the one plotted in Figure 3.2.    At this stage, it may be noted

that the temperatures obtained at the "seams" (boundaries) of the

adjoining elements are equal.    This makes the approximated solution

surface to be piecewise continuous (and compatible between adjacent

elements), which is the necessary condition as explained in Section 2.4.1

for the formulation to be valid.

## 3.2.2  Basic Outline

Next, we introduce this temperature model into our finite

element formulations described in the previous chapter.    The conductivity

matrix ([K]) is a sum of three matrices, two of them dealing with the conduction of heat inside the domain along the $x$ and $y$ directions (see relations (2.47) and (2.50), respectively), and the third dealing with the convection at the boundaries of the domain (see equation (2.56)). The load matrix ({F}) is also composed of three parts, namely: (i) the internally distributed loads (see relation (2.58)), (ii) the conductive loads through the boundaries of the domain (see relation (2.62)), and (iii) the convective loads through the boundaries of the domain (see relation (2.63)). After constructing each of these matrices, we shall end up with a system of simultaneous linear equations, in which $\theta$ (the nodal temperatures) are the only unknowns. Thus, the system can then be solved.

## 3.3 FINITE ELEMENT FORMULATIONS

### 3.3.1 The Elemental Formulations in Two Dimensions

A general steady-state heat conduction problem in the frame of the finite element method is considered, for which the elemental equation (2.64) becomes:

$$[K]^e . \{\theta\}^e + \{F\}^e = 0 \tag{3.17}$$

where, for the two-dimensional case ($x$ and $y$, for example), the thermal conductivity matrix (relation (2.65)) can be written as:

$$[K]^e = [K_x]^e + [K_y]^e + [H]^e \tag{3.18}$$

Using the definitions (2.47), (2.50) and (2.56) for $K_x$, $K_y$ and $H$, respectively, they can be written as follows:

$$[K_x]^e = \ell^e . \iint_{S^e} \{ \left[\frac{\partial N}{\partial x}\right]^T . k_x^e . \left[\frac{\partial N}{\partial x}\right] \} . dS \tag{3.19a}$$

$$[K_y]^e = \ell^e \cdot \iint\limits_{S^e} \left\{ \left[\frac{\partial N}{\partial y}\right]^T \cdot k_y^e \cdot \left[\frac{\partial N}{\partial y}\right] \right\} \cdot dS \tag{3.19b}$$

and: $$[H]^e = \ell^e \cdot \int\limits_{c_3} \left\{ [N]^T \cdot h^e \cdot [N] \right\} \cdot dc \tag{3.19c}$$

where, here, the volume $V^e$ is now replaced by the surface $S^e$ (the integration limits over the surface of the element $e$), and the elemental volume $dV$ becomes $\ell^e.dS$, where $dS$ is the elemental area for the two-dimensional case (see equation (3.1)). Similarly, the surface $S_3$ has to be replaced by a curve $c_3$ (the only integration limits of the convective boundary of the solution domain), and the elemental area $dS$ now becomes $\ell^e.dc$, where $dc$ is the elemental curve.

For the heat load vector, relation (2.66) is rewritten as:

$$\{F\}^e = -\{F_Q\}^e + \{F_q\}^e - \{F_h\}^e \tag{3.20}$$

where $F_Q$, $F_q$ and $F_h$ are the same as those defined by the expressions (2.58), (2.62) and (2.63), respectively. For two-dimensional cases, by introducing similar notation as before, they can be written as follows:

$$\{F_Q\}^e = \ell^e \cdot \iint\limits_{S^e} \left\{ Q^e \cdot [N]^T \right\} \cdot dS \tag{3.21a}$$

$$\{F_q\}^e = \ell^e \cdot \int\limits_{c_2} \left\{ q^e \cdot [N]^T \right\} \cdot dc \tag{3.21b}$$

and: $$\{F_h\}^e = \ell^e \cdot \int\limits_{c_3} \left\{ h^e \cdot \theta_\infty^e \cdot [N]^T \right\} \cdot dc \tag{3.21c}$$

where the surface $S_2$ is now replaced by the curve $c_2$ (the conductive boundary of the solution-domain). Starting from equation (3.18), these matrices can be explained individually as follows.

### 3.3.2  The Thermal Conductivity Matrix, $[K]^e$

In order to formulate the thermal conductivity matrix of a
typical element $e$ (relation (3.18)), we must be able to establish relations
(3.19).  To do so, we need to study the thermal conductivity properties
($k_x^e$ and $k_y^e$) of the material within the element, and also the effective
heat transfer coefficient, $h^e$, on the convective boundary face of the
element has to be prescribed.  In general, these can depend on various
interior factors, such as the temperature, the direction, the radiation,
the position $(x, y)$, and also on the external factors (pressure, for
example).  Ideally, we would like to use a method which incorporates all
these factors, but this is almost impossible because of the vast number
of experiments that would have to be studied in detail for each material.
However, the variation of thermal conductivity of some materials with
respect to temeprature has been studied.  Once the variation of the
thermal conductivity with temperature is established, then for any given
temperature the corresponding value of thermal conductivity can be
determined.  We can then incorporate this value into our solution
procedure by modelling the temperature for each element.  For instance,
one can use the nodal temperatures of the element, which are already known.
One obvious method is to determine the centroid temperature of the element
by using its nodal temperatures.  When the temperature model is linear
(as explained in Section 3.2.1), the centroid temperature is just the
average of the nodal temperatures.  This value is then used to determine
the temperature related to the physical properties of the element.  This
type of modelling makes the method isotropic ($k_x^e = k_y^e = k^e$, see Section
1.4), and also homogeneous, over each element.  Hence, for any particular
temperature, the corresponding value of the thermal conductivity, $k^e$, for
each element can now be used in the matrices (3.19) as follows.

By substituting relation (2.31) into relation (3.19a), we will

have:

$$[K_x]^e = \ell^e \cdot \iint_{S^e} \left( \begin{Bmatrix} \partial N_i/\partial x \\ \partial N_j/\partial x \\ \partial N_k/\partial x \end{Bmatrix} \cdot k^e \cdot \begin{bmatrix} \dfrac{\partial N_i}{\partial x} & \dfrac{\partial N_j}{\partial x} & \dfrac{\partial N_k}{\partial x} \end{bmatrix} \right) \cdot dS$$

From equations (3.11), this can be rewritten as:

$$[K_x]^e = \ell^e \cdot \iint_{S^e} \left( \frac{1}{2 \cdot \Delta_e} \begin{Bmatrix} b_i \\ b_j \\ b_k \end{Bmatrix} \cdot k^e \cdot \frac{1}{2 \cdot \Delta_e} \begin{bmatrix} b_i & b_j & b_k \end{bmatrix} \right) \cdot dS$$

This relation can be re-arranged as:

$$[K_x]^e = \frac{k^e \cdot \ell^e}{4 \cdot (\Delta_e)^2} \cdot \begin{Bmatrix} b_i \\ b_j \\ b_k \end{Bmatrix} \cdot \begin{bmatrix} b_i & b_j & b_k \end{bmatrix} \cdot \iint_{S^e} dS$$

since all the variables involved do not vary with respect to $dS$ over each element. Substituting $\Delta e$ for $\iint_{S^e} dS$, we finally obtain a matrix for $[K_x]^e$ of the form:

$$[K_x]^e = \frac{k^e \cdot \ell^e}{4 \cdot \Delta_e} \cdot \begin{bmatrix} b_i^2 & b_i\,b_j & b_i\,b_k \\ b_j\,b_i & b_j^2 & b_j\,b_k \\ b_k\,b_i & b_k\,b_j & b_k^2 \end{bmatrix} \tag{3.22}$$

and, similarly, for $K_y$:

$$[K_y]^e = \frac{k^e \cdot \ell^e}{4 \cdot \Delta_e} \cdot \begin{bmatrix} c_i^2 & c_i\,c_j & c_i\,c_k \\ c_j\,c_i & c_j^2 & c_j\,c_k \\ c_k\,c_i & c_k\,c_j & c_k^2 \end{bmatrix} \tag{3.23}$$

The $K_\chi$ and $K_y$ matrices are volumetric integrals (relations (2.47) and (2.50), respectively), and they involve all the elements throughout the solution-domain (see also relations (3.19a) and (3.19b)), whereas the $H$ matrix (relations (2.56) or (3.19c)) is applied only to the boundary elements with convective boundary face. This matrix is a surface integral, in contrast to the $K_\chi$ and $K_y$ matrices, which are volumetric integrals. It is integrated simply over the convective boundary faces (the approximated surface, $S_3$) of the boundary elements.

Let us consider a boundary face, $ij$, of a typical triangular boundary element $e$ with nodes $ijk$ at its vertices, as defined in Figure 3.5, for example, which is part of the approximated surface, $S_3$. For such an element, the $H$ matrix (relation (3.19c)) is written as:

$$[H]^e = \ell^e \cdot \int_{ij} \{ [N]^T \cdot h_{ij}^e \cdot [N] \} \cdot dc \tag{3.24}$$

where $h_{ij}^e$ stands for the heat transfer coefficient on the face $ij$ which has to be prescribed. If this coefficient is considered to be uniform on the face $ij$, then this relation can be rewritten as follows:

$$[H]^e = \ell^e \cdot h_{ij}^e \cdot \int_{ij} \{ [N]^T \cdot [N] \} \cdot dc \tag{3.25}$$

where: 
$$[N] = [N_i \quad N_j \quad N_k]$$

and, from Figure 3.5:

$$N_i = 1 - \frac{c}{L_{ij}} \quad , \quad N_j = \frac{c}{L_{ij}} \quad \text{and} \quad N_k = 0 \tag{3.26}$$

in which $L_{ij}$ is the length of the lateral side $ij$ of the element in question $(e)$. Hence, it can be rewritten as:
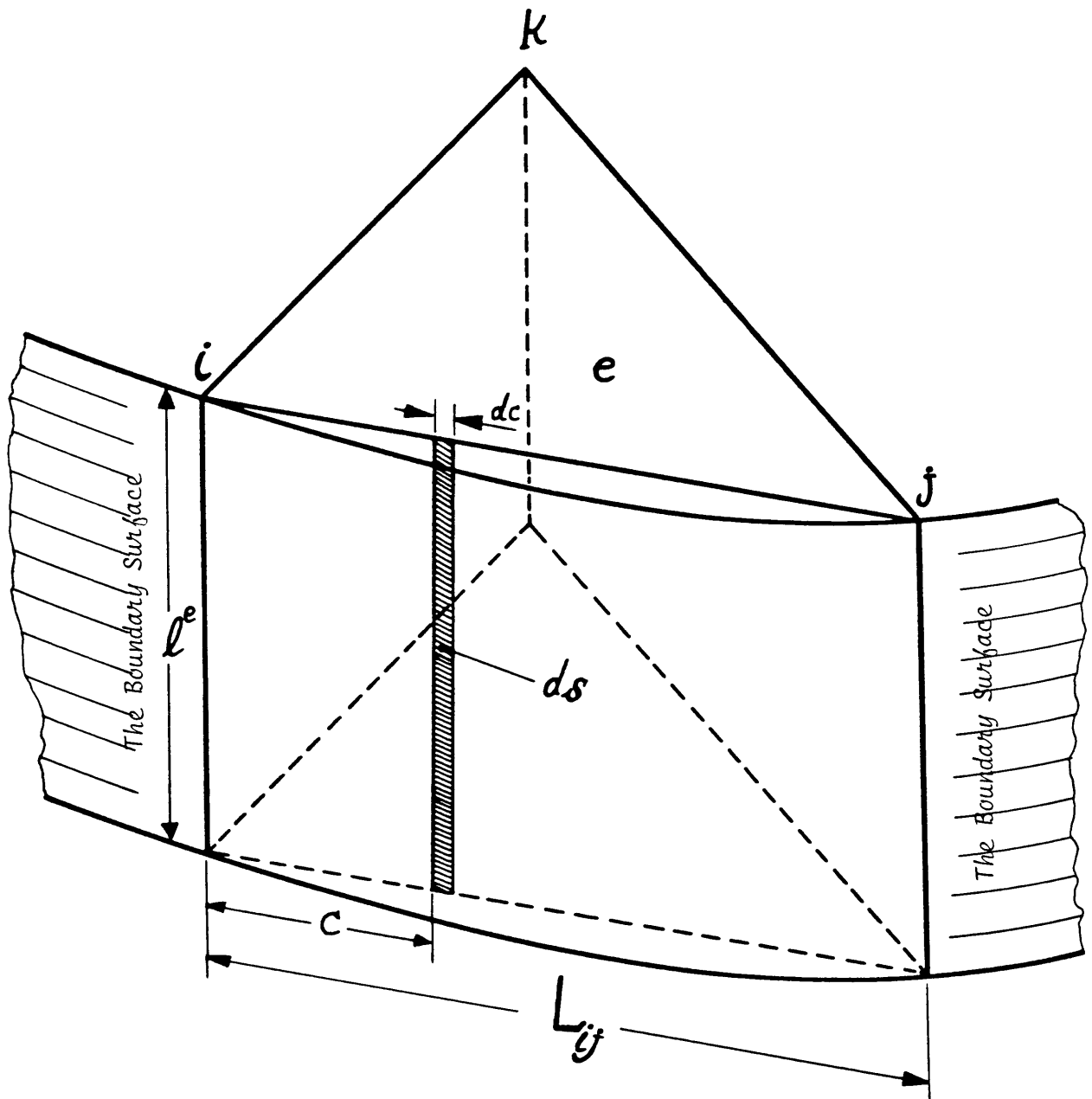
Figure 3.5: A Two-dimensional Boundary Element, e, with a rectangular boundary face based on side $ij$.

$$[H]^e = \ell^e \cdot h^e_{ij} \cdot \int_0^{L_{ij}} \left( \left\{ \begin{matrix} (1 - \frac{c}{L_{ij}}) \\ \frac{c}{L_{ij}} \\ 0 \end{matrix} \right\} \cdot \left[ (1 - \frac{c}{L_{ij}}) \quad \frac{c}{L_{ij}} \quad 0 \right] \right) \cdot dc \qquad (3.27)$$

Multiplying the vectors and integrating them term by term on the face $ij$, we finally obtain:

$$[H]^e_{on\ face\ ij} = \frac{\ell^e \cdot h^e_{ij} \cdot L_{ij}}{6} \begin{bmatrix} 2 & 1 & 0 \\ 1 & 2 & 0 \\ 0 & 0 & 0 \end{bmatrix} \qquad (3.28)$$

Here, it is noted that any node ($K$, for example) off the convective boundary, $S_3$, has no contribution in the $H$ matrices (3.27) and (3.28) as must be the case.

The $H$ matrix of the type (3.28) is obtained for each convective boundary face. For the remaining faces (non-convecting), this matrix would be equal to zero. Therefore, in general, for each trianglar element $e$ with nodes $ijk$, the elemental $H$ matrix will be the sum of the $H$ matrices of each of its faces:

$$[H]^e = [H]^e_{on\ face\ ij} + [H]^e_{on\ face\ jk} + [H]^e_{on\ face\ ki} \qquad (3.29)$$

Consequently, the thermal conductivity matrix of the typical element (equation (3.18)) can finally be obtained by summing the relations (3.22), (3.23) and (3.29).

### 3.3.3 The Heat Load Matrix, $\{F\}^e$

Next, we need to evaluate the heat load matrix $\{F\}^e$ in

equation (3.17). $\{F\}^e$ consists of three vector matrices and is described by the relation (3.20), in which each vector matrix represents the system of the nodal loads equivalent to a particular type of load acting on a typical element. All the loads acting off the nodes of the respective element must be replaced by an equivalent system of nodal loads acting at the nodes of the same element. This can be achieved, for each type of load, by the same method as explained in Section 2.4.3 with the usual changes for converting it to a two-dimensional problem, as was described in Section 3.1.

The first vector matrix on the right hand side of the relation (3.20), namely, $\{F_Q\}^e$, consists of the system of the nodal loads equivalent to the internally generated heat loads, due to the distributed heat sources within the element $e$. This vector matrix, in general, can be evaluated by the relation (A.16), where the total heat load is given by relations of the form (A.1a) or (A.1b), and the load-centre is located by the relation (A.2). In two-dimensional problems, the total heat load can be expressed by:

$$\vec{F_Q^e} = \ell^e . \iint\limits_{S^e} \vec{Q^e} . dS \qquad (3.30)$$

If the heat sources are uniformly distributed:

$$\vec{F_Q^e} = \vec{Q^e} . \ell^e . \Delta_e \qquad (3.31)$$

where $\Delta_e$ is the area of the element, and the load-centre coincides with the centroid of the element (c). By substituting the relation (3.31) into the relation (A.16), we obtain:

$$\{F_Q\}^e = (\vec{Q^e} . \ell^e . \Delta_e) . [N_{(c)}]^T \qquad (3.32)$$

where the $N_{(c)}$'s are the values of the position functions evaluated at the centroid of the element.

For a triangular element with three nodes at its vertices ($i$, $j$ and $k$, for example), as shown in Figure 3.3, with a uniform heat source (thermal load) distribution, $\vec{Q}^e$, per unit volume, the values of the $N_{(c)}$'s are given by the relation (3.15). Hence, relation (3.32) can be written for such an element as:

$$\{F_Q\}^e = \begin{Bmatrix} F_i \\ F_j \\ F_k \end{Bmatrix}^e = \frac{\vec{Q}^e \cdot \ell^e \cdot \Delta_e}{3} \cdot \begin{Bmatrix} 1 \\ 1 \\ 1 \end{Bmatrix} \qquad (3.33)$$

We can obtain a similar generalised result for a uniform load distribution acting upon a two-dimensional multi-sided polygonal element, but, by a different approach, it can also be proved that the conservation law and the moment law are satisfied. For this, we first require the following mathematical theorem as explained in Appendix B.

The second vector matrix on the right hand side of the relation (3.20), namely, $\{F_q\}^e$, which is a boundary load matrix and represents the system of the nodal loads equivalent to the thermal loads due to the conduction of heat through the boundary face(s) $S^e$ of a boundary element $e$, which is a member of the approximated surface for the conductive boundary surface $S_2$. Consider a typical boundary element $e$ of height $\ell^e$ with a polygonal cross-section and a lateral boundary face $S^e$. For example, a triangular element $ijk$ with a rectangular boundary face based on a side ($ij$, for example) as defined in Figure 3.5. Let this face be a member of the approximation surface of the conductive boundary surface $S_2$ of the solution-domain. The system of nodal loads equivalent to the thermal loads due to the conduction of heat through this face $S^e$ (side $ij$) can be calculated by the relation (3.21b) as:

$$\{F_q\}^e_{on\ ij} = \ell^e \cdot \int_0^{L_{ij}} \{\vec{q}_{ij} \cdot [N]^T\} \cdot dc \qquad (3.34)$$

where $L_{ij}$ is the length of the boundary side $ij$, which is the interval of integration, where $N_k = 0$ everywhere on side $ij$. For a uniform heat flux, $\vec{q}_{ij}$, distribution passing through that face (side $ij$), by using similar reasoning as before, we can finally obtain:

$$\{F_q\}^e_{on\ ij} = \begin{Bmatrix} F_i \\ F_j \\ F_k \end{Bmatrix}^e = \frac{\vec{q}_{ij} \cdot \ell^e \cdot L_{ij}}{2} \cdot \begin{Bmatrix} 1 \\ 1 \\ 0 \end{Bmatrix} \qquad (3.35)$$

(see relation (A.32)). The node $k$ off the boundary face $ij$ has no direct contribution in the conduction of heat through that face ($ij$), and thus its corresponding term, $\vec{F}_k$, is zero in relation (3.35).

This nodal load vector matrix is obtained for all the faces of the element on the approximation surface of the conductive boundary surface $S_2$. For all the rest of the faces, and hence for all the nodes not on this boundary surface, this vector is zero. Thus, for each triangular element, vectors of the form (3.35) or zero vectors are added for each side, depending on whether the side is a member of the approximation surface $S_2$ or not, respectively. Therefore:

$$\{F_q\}^e = \{F_q\}^e_{on\ ij} + \{F_q\}^e_{on\ jk} + \{F_q\}^e_{on\ ki} \qquad (3.36)$$

For a two-dimensional multi-sided polygonal element ($ijk\ell \dots n$, for example), the relation (3.35) can be written as:

$$\{F_q\}^e_{on \; ij} = \begin{Bmatrix} F_i \\ F_j \\ F_k \\ \vdots \\ \vdots \\ F_n \end{Bmatrix} = \frac{\vec{q}_{ij} \cdot \ell^e \cdot L_{ij}}{2} \cdot \begin{Bmatrix} 1 \\ 1 \\ 0 \\ \vdots \\ \vdots \\ 0 \end{Bmatrix} \qquad (3.37)$$

and the relation (3.36) can be written as:

$$\{F_q\}^e = \{F_q\}^e_{on \; ij} + \{F_q\}^e_{on \; jk} + \{F_q\}^e_{on \; k\ell} + \cdots \{F_q\}^e_{on \; ni} \qquad (3.38)$$

such that, in each component, we have only two non-zero terms.

These nodal loads can also be obtained by the relations (A.19), (A.30) and (A.32), when only the boundary faces (the boundary sides) on the conductive boundary surface $S_2$ are concerned.

Some of the terms of relations (3.36) or (3.38) corresponding to faces on $S_2$ may also be zero if they represent an adiabatic boundary face ($\vec{q}_{ij} = 0$ on side $ij$, for example).

Finally, the third vector matrix on the right hand side of the relation (3.20), namely, $\{F_h\}^e$, which is a boundary load matrix. This represents the system of the nodal loads equivalent to the thermal loads only due to the influx of heat from the ambient to the element $e$ through the convective boundary surface $S_3$ of the solution-domain. Consider a boundary polygonal element with a boundary face $S^e$ being on the approximation surface $S_3$. For example, a triangular element as defined in Figure 3.5. The thermal loads due to the heat flow from the ambient to this element, passing through that face ($S^e$), can be represented by a similar procedure as that described for the relation (3.34), where the heat flux is:

$$q_{ij} = h^e_{ij} \cdot \theta^{ij}_{\infty} \qquad (3.39)$$

where $h^e_{ij}$ is the heat transfer coefficient on the face $S^e$ (side $ij$), and $\theta^{ij}_{\infty}$ is the ambient temperature adjacent to the same face (side $ij$). Hence, for a uniform case, a similar relation to (3.35) is obtained as:

$$\{F_h\}^e_{on\ ij} = \begin{Bmatrix} F_i \\ F_j \\ F_k \end{Bmatrix}^e = \frac{h^e_{ij} \cdot \theta^{ij}_{\infty} \cdot \ell^e \cdot L_{ij}}{2} \cdot \begin{Bmatrix} 1 \\ 1 \\ 0 \end{Bmatrix} \qquad (3.40)$$

As before, for each element, vectors of the form (3.40) or zero vectors are added for each face (side), depending on whether it is a member of the approximation surface $S_3$ (convective boundary) or not, respectively. Hence, for the triangular element, it can be written:

$$\{F_h\}^e = \{F_h\}^e_{on\ ij} + \{F_h\}^e_{on\ jk} + \{F_h\}^e_{on\ ki} \qquad (3.41)$$

For a two-dimensional multi-sided polygonal element ($ijk\ell \ldots n$, for example), the relation (3.40) is written as:

$$\{F_h\}^e_{on\ ij} = \begin{Bmatrix} F_i \\ F_j \\ F_k \\ \vdots \\ F_n \end{Bmatrix}^e = \frac{h^e_{ij} \cdot \theta^{ij}_{\infty} \cdot \ell^e \cdot L_{ij}}{2} \cdot \begin{Bmatrix} 1 \\ 1 \\ 0 \\ \vdots \\ 0 \end{Bmatrix} \qquad (3.42)$$

and the relation (3.41) becomes:

$$\{F_h\}^e = \{F_h\}^e_{on \ ij} + \{F_h\}^e_{on \ jk} + \{F_h\}^e_{on \ k\ell} + \cdots \{F_h\}^e_{on \ ni} \qquad (3.43)$$

such that, in each component, we have only two non-zero terms.

Relations (3.37) and (3.42) show, as expected, that the nodes off the boundaries do not contribute to the boundary conditions. Hence, the vectors representing the loads at the nodes not on the boundaries, in the boundary load matrices, are taken to be zero.

Finally, therefore, the heat load matrix for each element, as given by the relation (3.20), will be the sum of relations (3.32), (3.38) and (3.43). In particular, for a triangular element, they are relations (3.33), (3.36) and (3.41), respectively.

### 3.3.4 Assemblage

So far, in this chapter, we have established some property matrices for a typical element such as the thermal conductivity matrix $[K]^e$, which is a sum of three component matrices (relation (3.18)) and the heat load vector matrix $\{F\}^e$, which is also a sum of three component vector matrices (relation (3.20)). Both together incorporate all kinds of the boundary conditions, except radiation.

The elemental matrix equation (3.17) yields a set of $n$ linear algebraic simultaneous equations for an element, $e$, with $n$ nodes, involving $n$ unknown nodal temperatures. In particular, a set of three linear algebraic simultaneous equations for each triangular element ($ijk$, for example), with only three unknown nodal temperatures ($\theta_i$, $\theta_j$ and $\theta_k$, for example). For such an element, the relation (3.17) can be written as:

$$\begin{bmatrix} K_{ii} & K_{ij} & K_{ik} \\ K_{ji} & K_{jj} & K_{jk} \\ K_{ki} & K_{kj} & K_{kk} \end{bmatrix}^e \cdot \begin{Bmatrix} \theta_i \\ \theta_j \\ \theta_k \end{Bmatrix}^e + \begin{Bmatrix} F_i \\ F_j \\ F_k \end{Bmatrix}^e = 0 \qquad (3.44)$$

There are as many sets of these equations as there are elements in a particular region or in the whole solution-domain, but, since the union of these elements forms the solution-domain itself (Section 2.3.2), there are many nodes that are common among several elements. Therefore, for a domain with $N$ nodes, there would be many common nodes that exist in more than one set of those equations. Each set (relation (3.44), for example) can be incorporated into a system of $N$ linear algebraic simultaneous equations by including all the $N$ unknown nodal temperatures in the $\theta$ vector matrix in equations (3.17) or (3.44). This requires an expansion of the $[K]^e$ matrix into an $N \times N$ matrix, and also the $\{F\}^e$ matrix into a vector matrix with $N$ components. All the nodes not featured in the elemental equations are obviously taken to be zero to complete the matrix. This does not affect each individual elemental equation ((3.44), for example), and hence it can be shown as:

$$
\begin{array}{c}
\begin{array}{ccccccccccc} 1 & 2 & 3 & \cdots & i & \cdots\cdots & j & \cdots & k & \cdots & N \end{array}\\
\begin{array}{c} 1\\2\\3\\ \vdots \\ i \\ \vdots \\ \vdots \\ j \\ \vdots \\ k \\ \vdots \\ N \end{array}
\left[
\begin{array}{ccccccccccc}
\cdot & \cdot & \cdot & \cdot & \cdot & \cdot & \cdot & \cdot & \cdot & \cdot & \cdot\\
\cdot & \cdot & \cdot & \cdot & \cdot & \cdot & \cdot & \cdot & \cdot & \cdot & \cdot\\
\cdot & \cdot & \cdot & \cdot & \cdot & \cdot & \cdot & \cdot & \cdot & \cdot & \cdot\\
& & & & & & & & & & \\
\cdot & \cdot & \cdot & K_{ii} & \cdot & \cdot & K_{ij} & \cdot & K_{ik} & \cdot & \cdot\\
& & & & & & & & & & \\
& & & & & & & & & & \\
\cdot & \cdot & \cdot & K_{ji} & \cdot & \cdot & K_{jj} & \cdot & K_{jk} & \cdot & \cdot\\
& & & & & & & & & & \\
\cdot & \cdot & \cdot & K_{ki} & \cdot & \cdot & K_{kj} & \cdot & K_{kk} & \cdot & \cdot\\
& & & & & & & & & & \\
\cdot & \cdot & \cdot & \cdot & \cdot & \cdot & \cdot & \cdot & \cdot & \cdot & \cdot
\end{array}
\right]
\cdot
\left\{
\begin{array}{c} \theta_1\\ \theta_2\\ \vdots \\ \theta_i \\ \vdots \\ \theta_j \\ \vdots \\ \theta_k \\ \vdots \\ \theta_N \end{array}
\right\}
+
\left\{
\begin{array}{c} \cdot\\ \cdot\\ \vdots \\ F_i \\ \vdots \\ F_j \\ \vdots \\ F_k \\ \vdots \\ \cdot \end{array}
\right\}
= 0
\end{array}
\tag{3.45}
$$

This set of $N$ equations (3.45) is equivalent to the set of $n$ equations in (3.44), and the solution for each set is unique only for the $n$ nodes that it originally described. Finally, we combine all these expanded elemental systems, which are all of the same size, to obtain a unique set of $N$ linear algebraic simultaneous equations involving $N$ unknown nodal temperatures. This is the system equation, obviously, since the solution domain can be dealt with as a single element with $N$ nodes; the final assemblage thus obtained has to be also of the form (3.17) with a unique solution. Therefore, the system equation can be written as:

$$[K] \cdot \{\theta\} + \{F\} = 0 \tag{3.46}$$

where $[K]$ is the sum of all the expanded $[K]^e$'s for all the elements, and $\{F\}$ is the sum of all the expanded $\{F\}^e$'s for all the nodes. This method

is usually called the "direct assembling" and the expansive description

of this method may be found in reference [9] by Eysink,B.J.

## 3.4  VALIDATION STUDY

### 3.4.1  Outline for Validation Study

Heat conduction phenomena are very important in engineering,

particularly in nuclear engineering, which is a very sensitive subject

both from civil and military viewpoints.  On one hand, due to safety, the

nuclear reactor components have to be carefully studied, but on the other

hand, because of commercial security reasons, some information is not made

freely available.  Hence, it is hard to get access to real data.  Often

published results can be mis-interpreted and also may cause unnecessary

concern.  Therefore, reliable sets of data for more realistic situations

are almost impossible to come by in the normal literature.  Simplified

problems of steady-state heat conduction have been studied and validated

using a similar method by Eysink.  His overall conclusions showed that

the finite element method had performed very well [9].  The solutions

obtained have been for highly idealised situations and thus in most cases,

for real life, they have limited usefulness.

The formulations presented in this chapter are very generalised

for non-linear steady-state problems.  The method is applicable to the

problems with any shape of geometry, physical non-linearities and all

kinds of boundary conditions except radiation.  Like most non-linear

problems, exact solutions are either non-existent or too complicated to be

of any practical use.  Throughout this work, we have tried to use the

LMFBR fuel element to demonstrate the capabilities of the proposed method

in various stages.  We have started with the fuel pellet to establish the

validity of the method, because it was possible to derive an analytical

solution for it, as will be shown in the next section (3.4.2).  This was

then extended to include the cladding with a uniform gap. All these geometrical configurations have been subjected to various non-axisymmetric boundary conditions and different internal rates of thermal energy generation. Finally, in this chapter, the gap is made non-uniform. When we come to consider the multi-phase problems, we shall continue to use the LMFBR fuel element for uniformity.

### 3.4.2 Analytical Solution for an Axisymmetric Non-Linear Problem with Internal Sources and Validation of the Proposed Numerical Method

A similar method has been tested thoroughly for steady-state linear problems (for example, [9,10]). Since the proposed method is applicable to non-linear problems, we need to verify its validity and to check its accuracy against a non-linear problem for which an analytical solution can be established. Harwell, UK, have recently released some relationships regarding the properties of the LMFBR fuel element components. We can incorporate these relationships into our formulations. We can also obtain analytical solutions to calculate the temperature distribution inside the fuel pellet subject to axisymmetric conditions.

The geometry of the fuel pellet is considered as a long hollow circular cylinder. Half of its cross-section is as shown in Figure 3.6, where $r_1$ and $r_2$ are the inner and the outer radii, respectively. The thermal conductivity ($k$) variations of the fuel pellet with respect to temperature ($T$) is given by a relation of the form:

$$k = (a + b \cdot T)^{-1} + c \cdot T^3 \tag{3.47}$$

where $k$ is measured in $W.m^{-1}.{}^{\circ}K^{-1}$, and $T$ is measured in ${}^{\circ}K$ [11]. The (constant) values of $a$, $b$ and $c$ are given in Table 3.2, and $k$ in relation
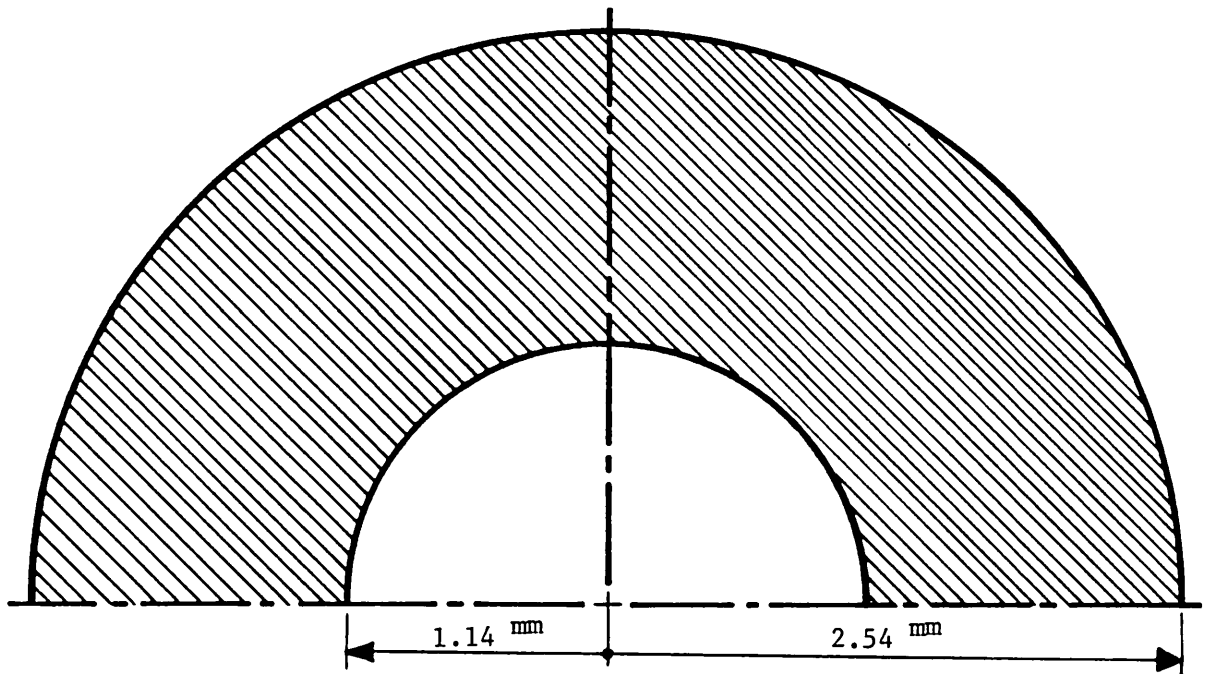
1.14 $^{mm}$    2.54 $^{mm}$

Figure 3.6:  An LMFBR Fuel Pellet Geometry (half cross-section is shown).
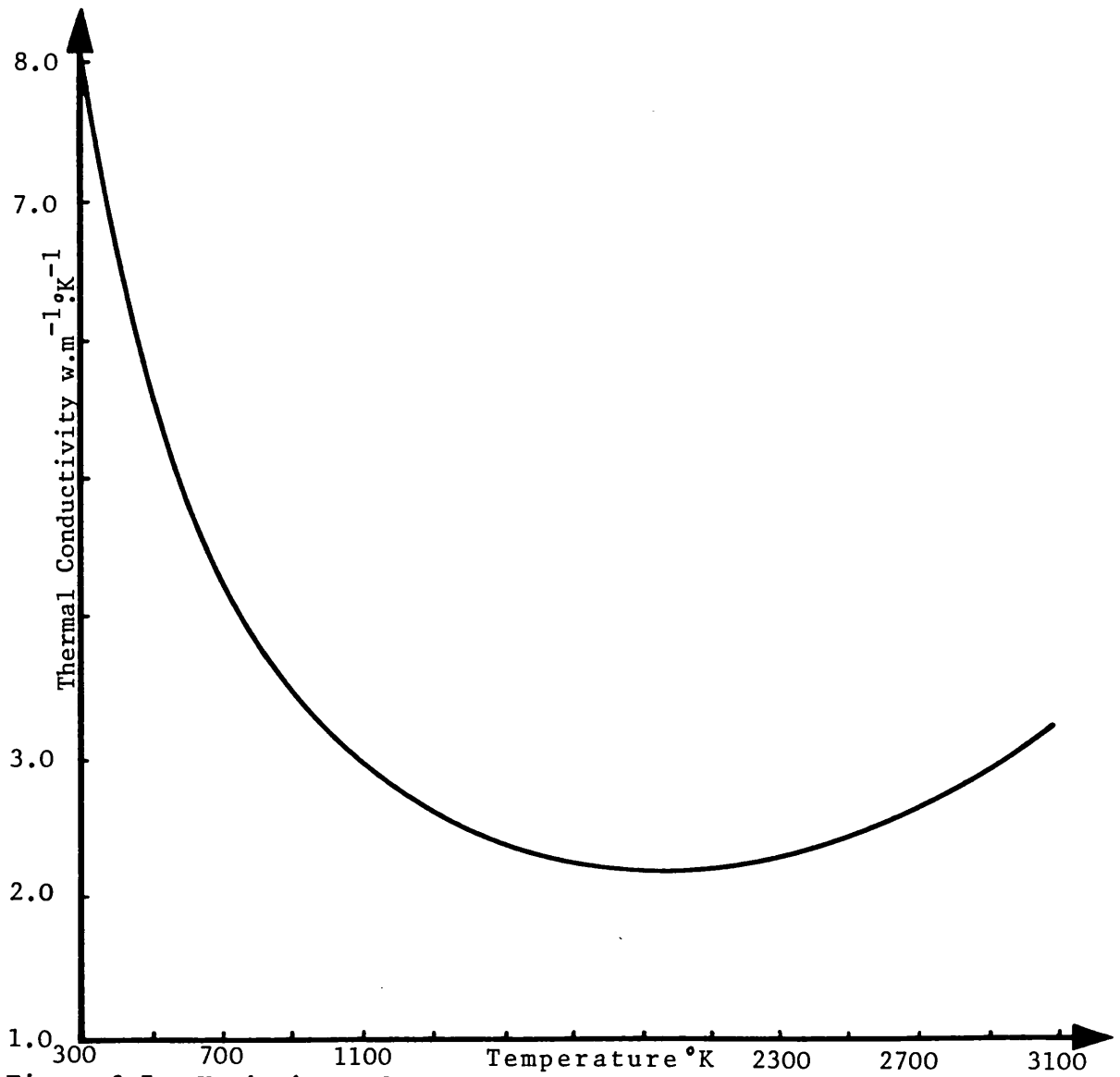


Figure 3.7:  Variations of $UO_2$ thermal conductivity versus Temperature.

TABLE 3.2

Properties of the LMFBR Fuel Pellet, Recently Released

by Harwell, UK [11]

---

Thermal Conductivity:  Defined by a relation of the form of (3.47),

where the constants are:

$$a = 0.042$$

$$b = 2.71 \times 10^{-4}$$

$$c = 69.0 \times 10^{-12}$$

---

The maximum (volumetric) rate of thermal energy generation is:

$$\dot{Q}_{max} = 0.27 \times 10^{10} \ W.m^{-3}$$

---

Geometry:  Tubular with half cross-section as shown in Figure 3.6,

where:

the inner radius is  : $h_1$ = 0.00114 m

the outer radius is  : $h_2$ = 0.00254 m

(3.47) is plotted against $T$ in Figure 3.7. The thermal energy source distribution is assumed to be uniform throughout the fuel pellet. The boundary conditions are prescribed temperature distribution $(T_2)$ on the outer surface ( defined as the first kind of boundary conditions ) and prescribed heat flux $(q_1)$ passing through the inner surface (defined as the second kind of boundary conditions). Since the problem is axisymmetric, the boundary conditions are also axisymmetric, namely, uniform temperature distribution on the outer surface and uniform heat flux passing through the inner surface.

The boundary conditions are assumed to be such that all the inner surface is adiabatic, $q_1 = 0$, and all the outer surface is kept at $T_2 = 1073°K$.

The governing equation for this case may be written as follows:

$$\frac{1}{\pi} \cdot \frac{\partial}{\partial \pi} (\pi \cdot k \cdot \frac{\partial T}{\partial \pi}) + Q = 0 \qquad (3.48)$$

where $\pi$ is the radius. Integrating this relation leads to a relation of the form:

$$k \cdot \frac{\partial T}{\partial \pi} = -\frac{Q}{2} \cdot \pi + c_1 \cdot \frac{1}{\pi} \qquad (3.49)$$

Since the inner surface is assumed to be adiabatic:

$$c_1 = \frac{Q}{2} \cdot \pi_1^2 \qquad (3.50)$$

Further integration of relation (3.49), using relations (3.47) and (3.50), gives:

$$\left| \frac{1}{b} \cdot \ln (a + b.T) + \frac{c}{4} \cdot T^4 \right|_{T_2}^{T} + \left| \frac{Q}{4} \cdot \pi^2 - \frac{Q}{2} \cdot \pi_1^2 \cdot \ln (\pi) \right|_{\pi_2}^{\pi} = 0 \qquad (3.51)$$

where $\hbar_2$ and $T_2$ are the radius and temperature of the outer surface,
respectively. Finally, relation (3.51) can be written as:

$$\frac{1}{b}\cdot\ln\left(\frac{a+b.T}{a+b.T_2}\right) + \frac{c}{4}\cdot(T^4-T_2^4) + \frac{Q}{4}\cdot(\hbar^2-\hbar_2^2) + \frac{Q}{2}\cdot\hbar_1^2\cdot\ln\left(\frac{\hbar_2}{\hbar}\right) = 0 \qquad (3.52)$$

This is the exact solution to the problem, but the explicit relationship

for $T$ (as a function of $\hbar$) is too difficult. Hence, the left hand side

of relation (3.52) is equated to $\varepsilon$, and then for each value of $\hbar$, the

respective value for $T$ is computed by iteration until $\varepsilon$ is small enough.

This value of $T$ is then taken to be the solution at the given radius $\hbar$.

Figure 3.8 shows the radial temperature distributions for some selected

percentages of the maximum rate of thermal energy generation, namely, 0%,

25%, 50%, 75% and 100%, of $Q_{max}$.

This problem is also solved by the (finite element)

formulations proposed in this chapter. Since the problem is axisymmetric,

it can be solved only for a small sector of the cross-section of the fuel

pellet (see Figure 3.9), thus saving on computing time while maintaining

the two-dimensionality of the problem. Of course, both sides of this

sector are to be considered as adiabatic boundaries. The radial

temperature distributions (profiles) for the same values of the rate of

thermal energy generation as used before are plotted again in the same

figure (Figure 3.8).

The results (of the proposed method) were in excellent

agreement with the exact solution (relation (3.52)), where as few as eight

(8) nodes in the radial direction were used (Figure 3.9). The solutions

were achieved after about five (5) iterations. The method is capable of

solving more complex non-linear problems and, as the above example has
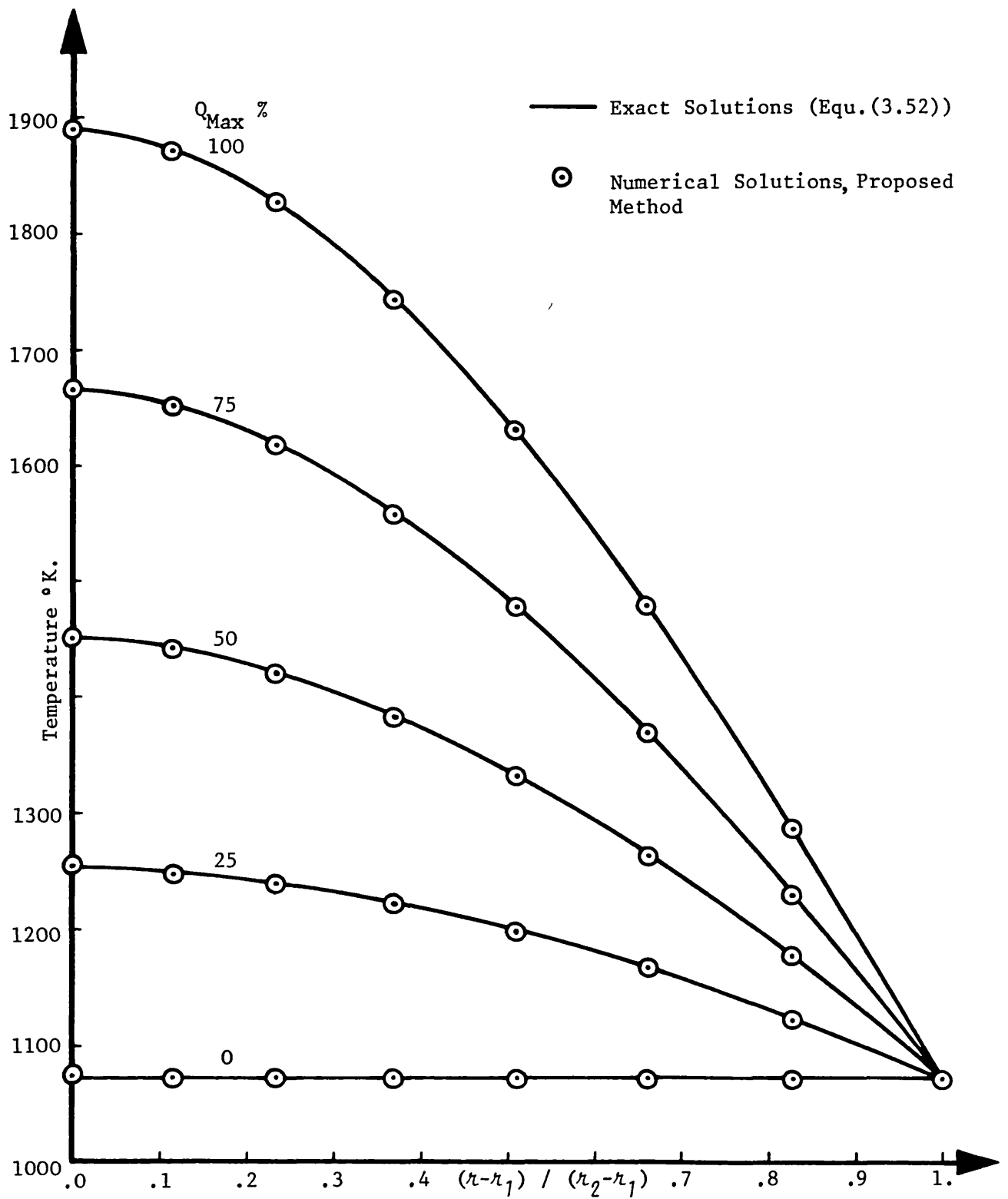
shown, it is very accurate, stable and economical.

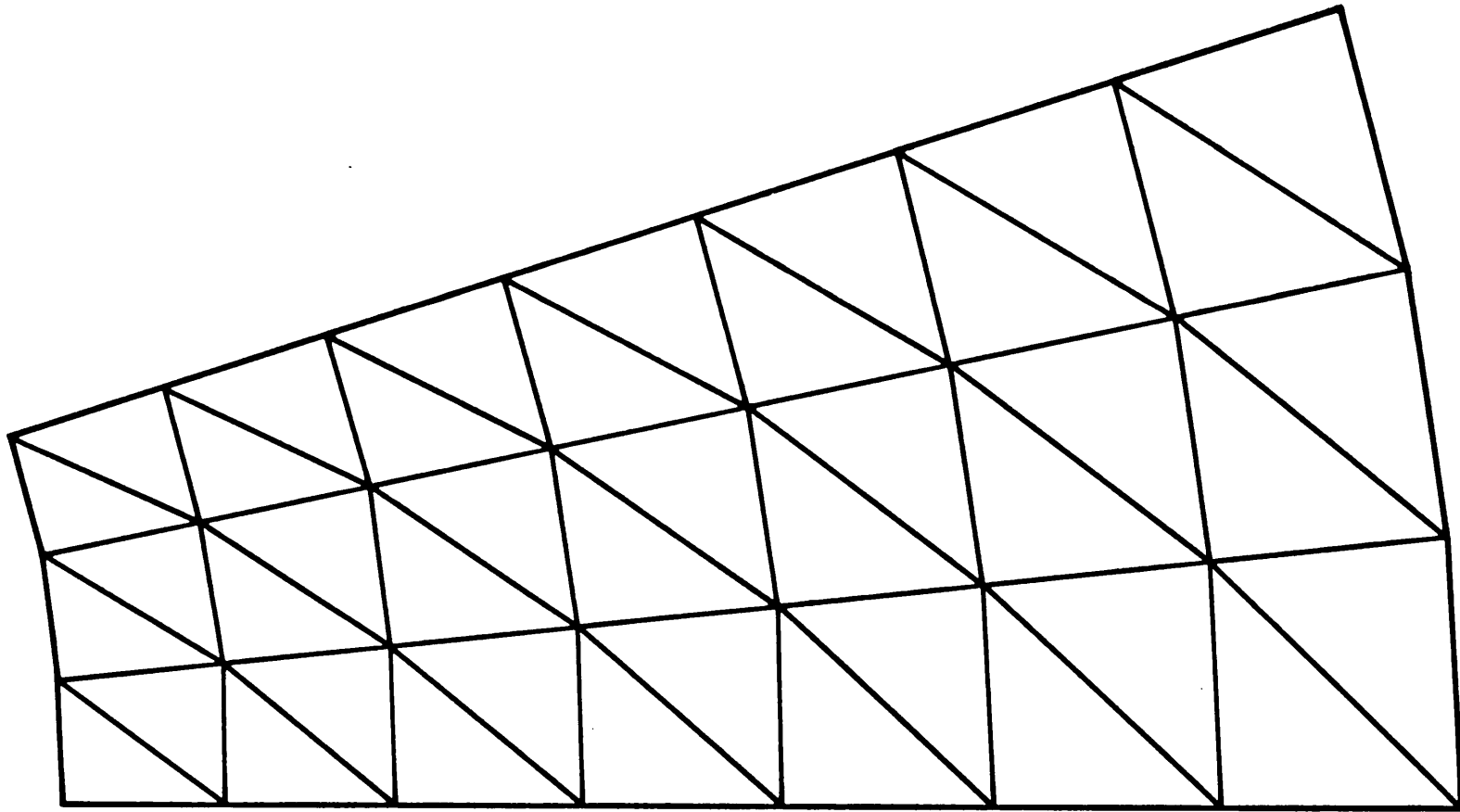Figure 3.8: Radial Temperature Profiles inside the Pellet.

Figure 3.9:

## 3.5 APPLICATION OF THE METHOD TO SOME MORE GENERAL EXAMPLES

The performance and capabilities of the proposed method is illustrated here by its application to some selected examples of the actual LMFBR fuel element components, as follows.

### 3.5.1 The Temperature Distribution within a Fuel Pellet Situated in a Linearly Varying Temperature Environment and with Adiabatic Inner Surface

The same sample as that defined in Section 3.4.2 is considered here again.  The method is valid for any prescribed boundary condition. For example, the fuel pellet may be assumed to be situated in a linearly varying temperature environment.  Thus, there would be a unique diameter (AB), the "symmetry diameter", joining the hottest point (A) and the coldest point (B), both on the outer surface of the pellet (Figure 3.10). The temperature $(T_p)$ at any point $(p)$ on the outer surface of the pellet may be determined by projecting it onto this diameter and interpolating between $T_A$ and $T_B$, the temperatures at A and B, respectively (see Figure 3.10).  The problem, in general, is only symmetric about the unique symmetry diameter (AB).  Hence, we have to calculate for at least half of the cross-section of the fuel pellet.  Of course, such a symmetry diameter is now considered as an adiabatic boundary.

Four different examples of this type are selected with the environmental temperature distributions along the symmetry diameter prescribed as shown in Figure 3.11, while the inner surface is always assumed to be an adiabatic boundary surface as before.  The temperature distribution inside the fuel pellet is then calculated for each case (at its maximum rate of thermal energy generation), but only the temperature profiles along the unique symmetry diameter are plotted in Figure 3.12. Corresponding curves in Figures 3.11 and 3.12 are labelled with the same
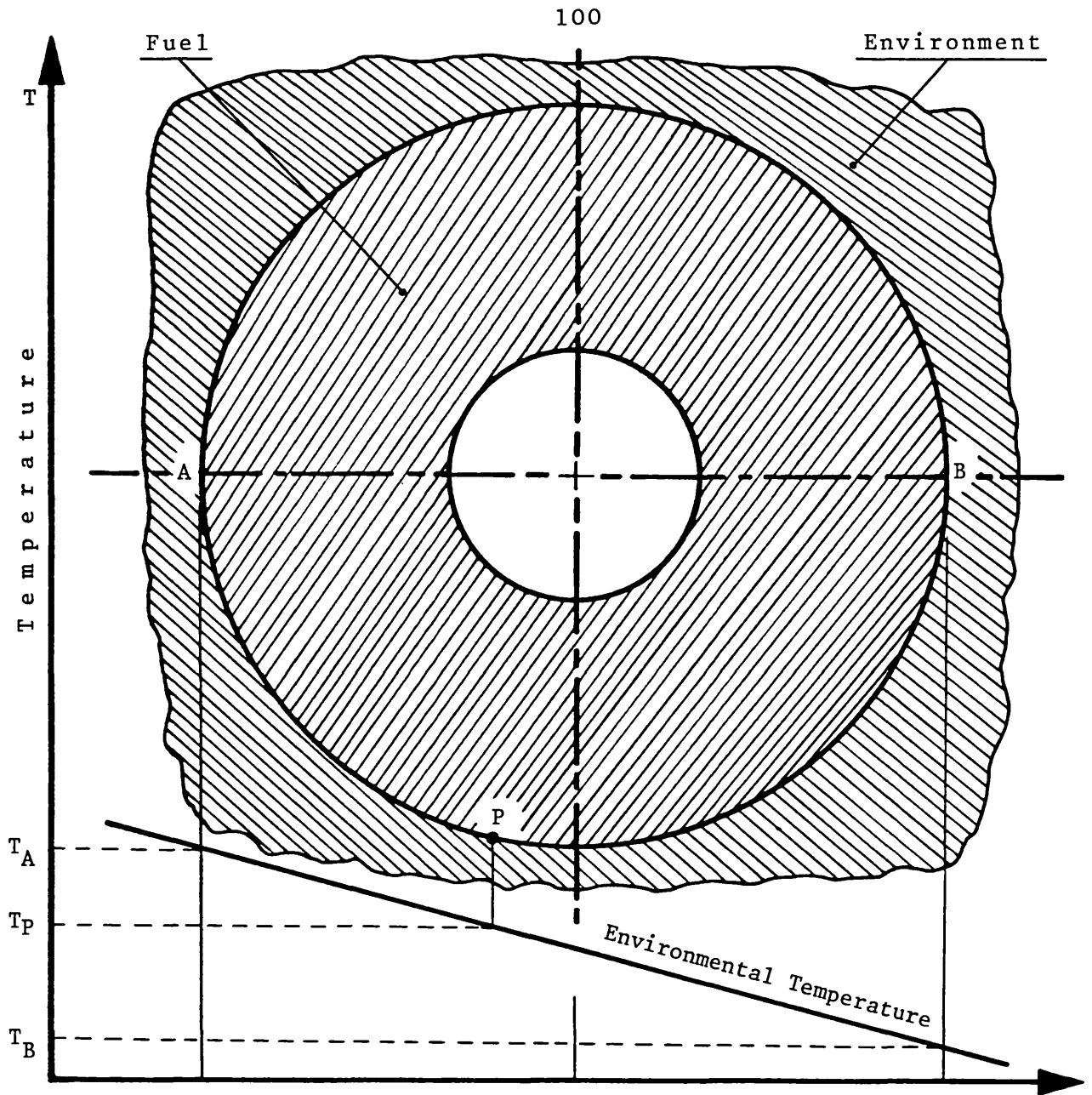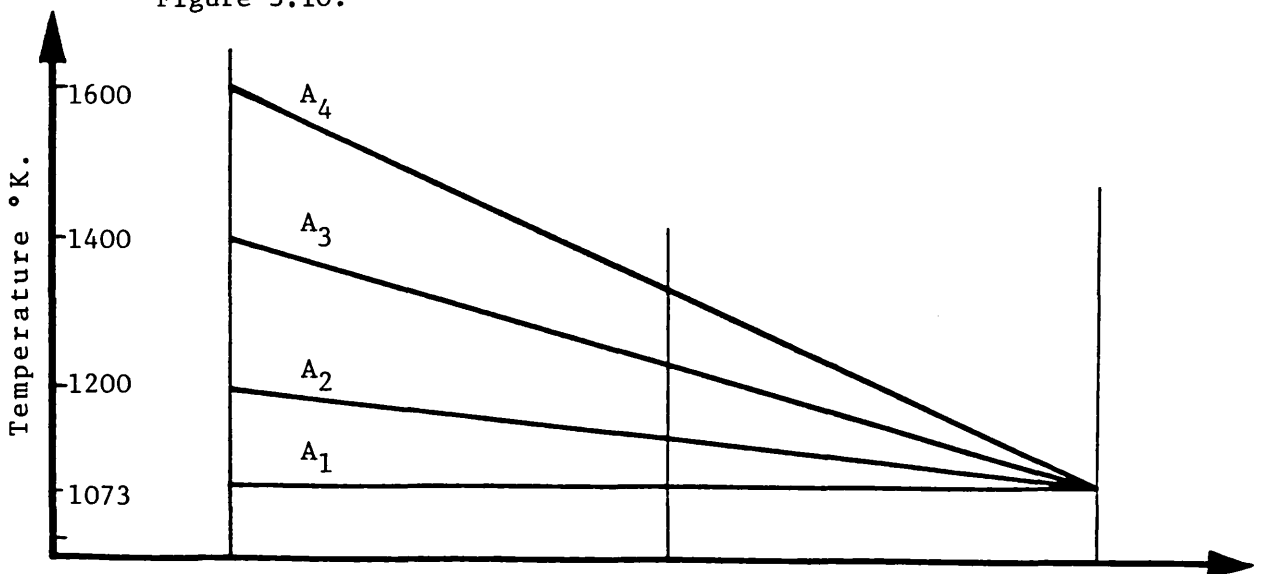
Figure 3.10:



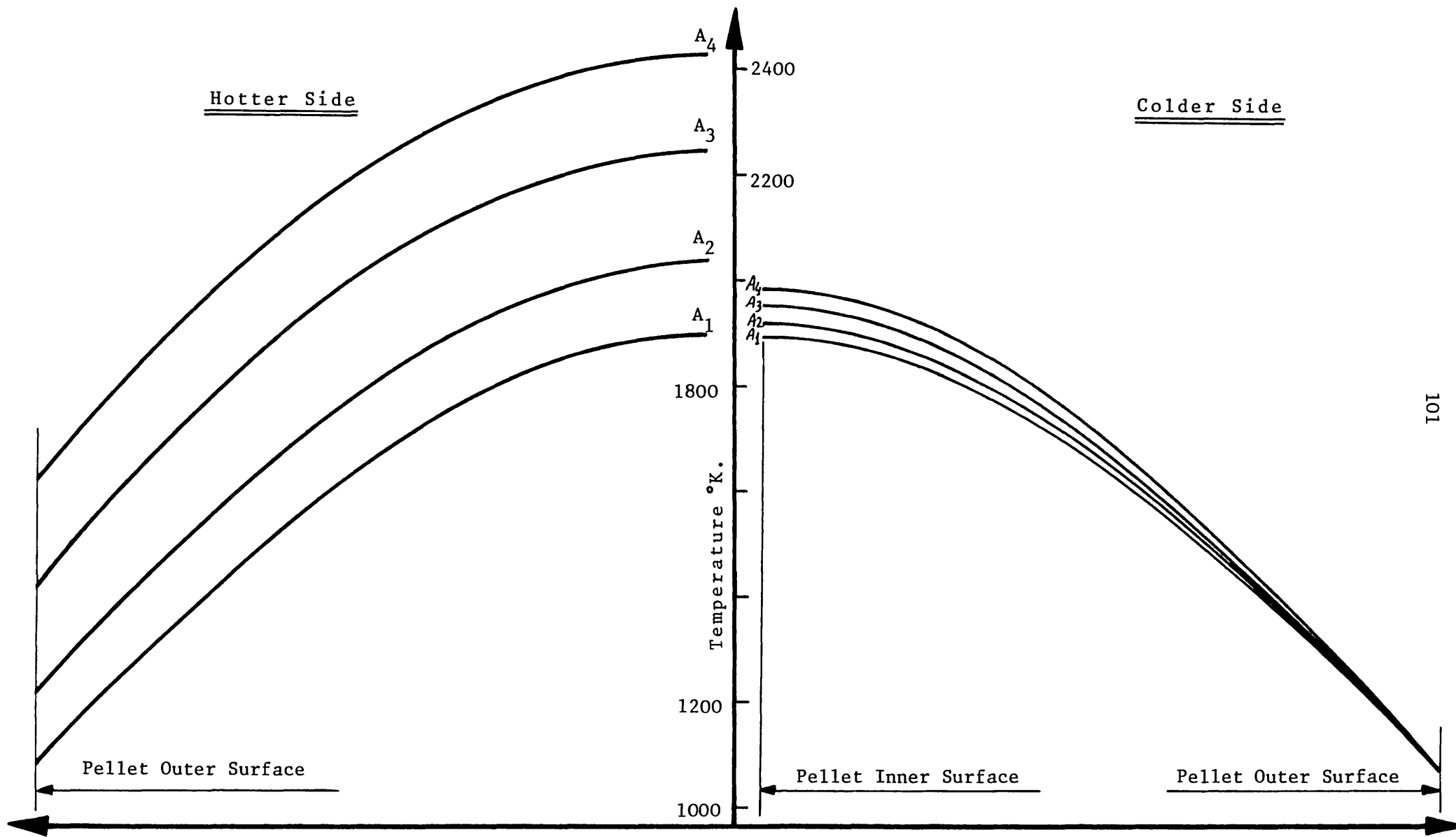Figure 3.11:  Environmental Temperature Distributions on the Outer Surface.

Figure 3.12: Temperature Distributions (along the symmetry diameter) inside the Pellet with Environmental Temperatures as defined in Figure 3.11.

symbols (A), where the curves labelled $A_1$ both refer to an axisymmetric problem.

### 3.5.2 The Temperature Distribution within a Fuel Element Situated in a Linearly Varying Temperature Environment and with Adiabatic Inner Surface

Let us consider a concentrically-mounted conventional fuel element of an LMFBR with the same fuel pellet as that defined in Section 3.4.2, whose geometry is defined in Figure 3.13 where half of its cross-section is shown. The inner and outer radii as well as the thermal conductivity of the clad, according to the data released by Harwell, UK [11], are tabulated in Table 3.3. Moreover, the existing (uniform) gap

### TABLE 3.3

### Properties of the Clad of an LMFBR Fuel Element [11]

| Thermal Conductivity: |
|---|
| 20.0 $W.m^{-1}.^{\circ}K^{-1}$ |

| Geometry: Tubular with: |
|---|
| the inner radius : $\hbar_{c1}$ = 0.00260 m |
| the outer radius : $\hbar_{c2}$ = 0.00298 m |

(of 0.00006 m) between the cladding and the fuel pellet is assumed to have an effective thermal conductivity, in which the effects of conduction and
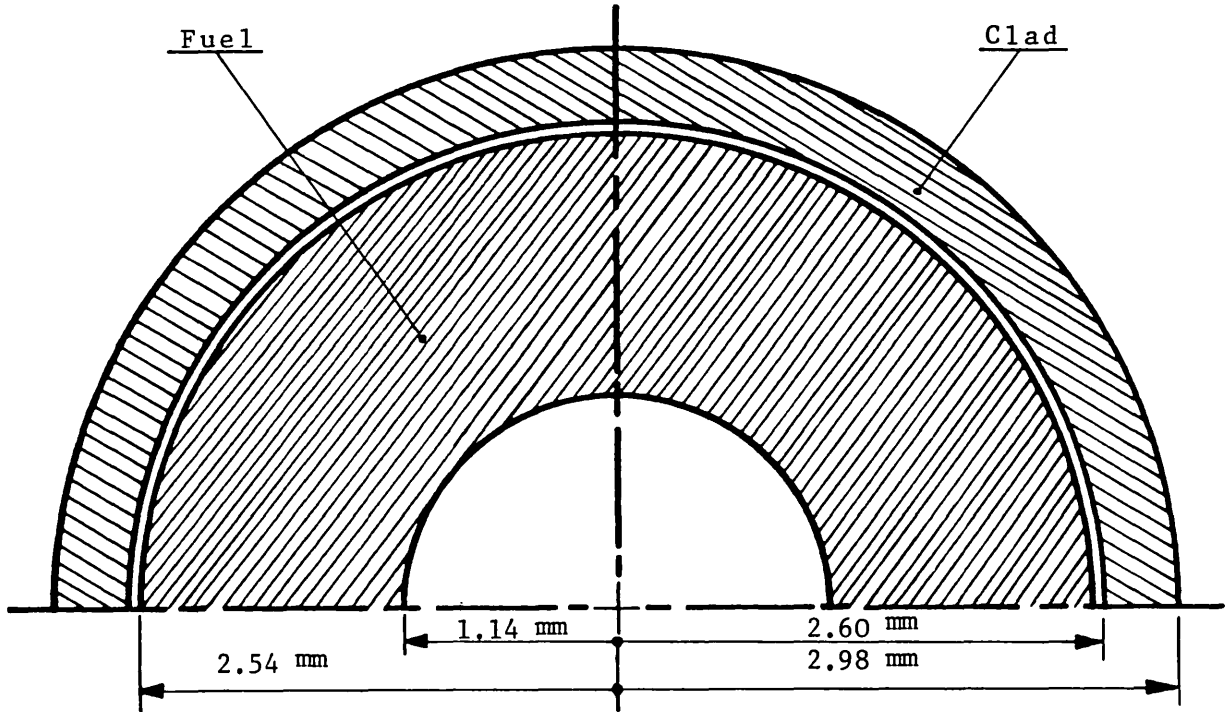
Figure 3.13: Fuel element Geometry (half cross-section is shown).
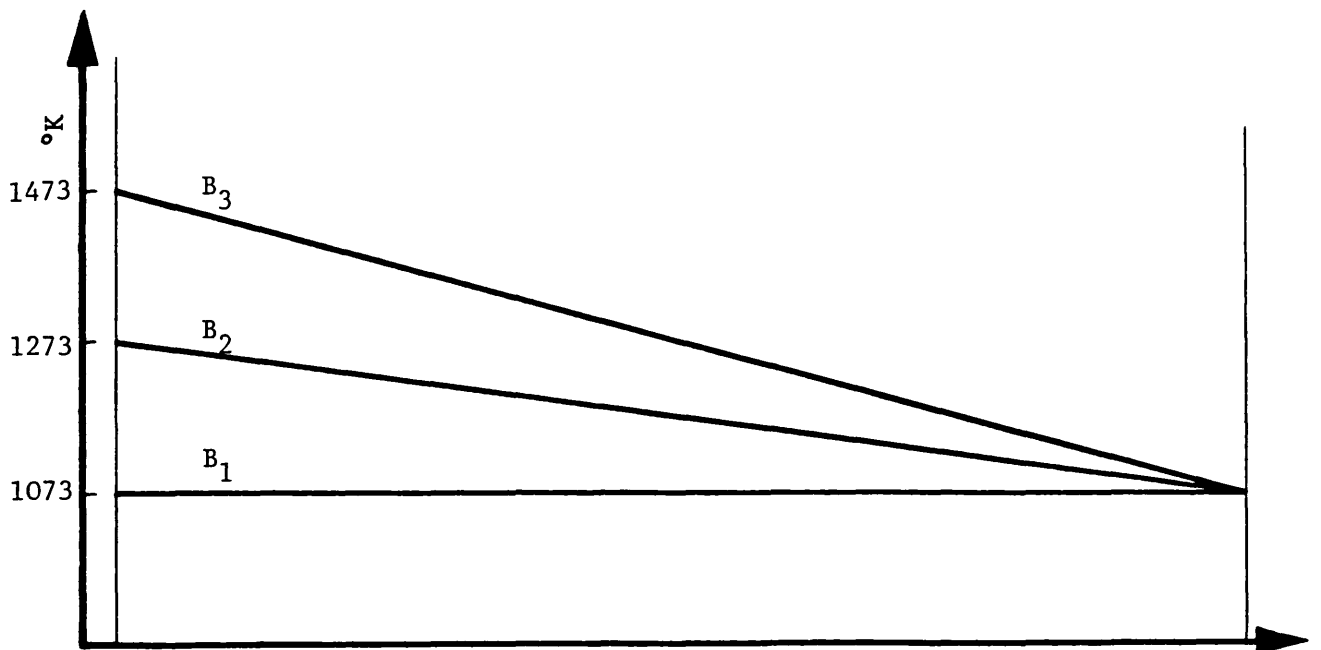


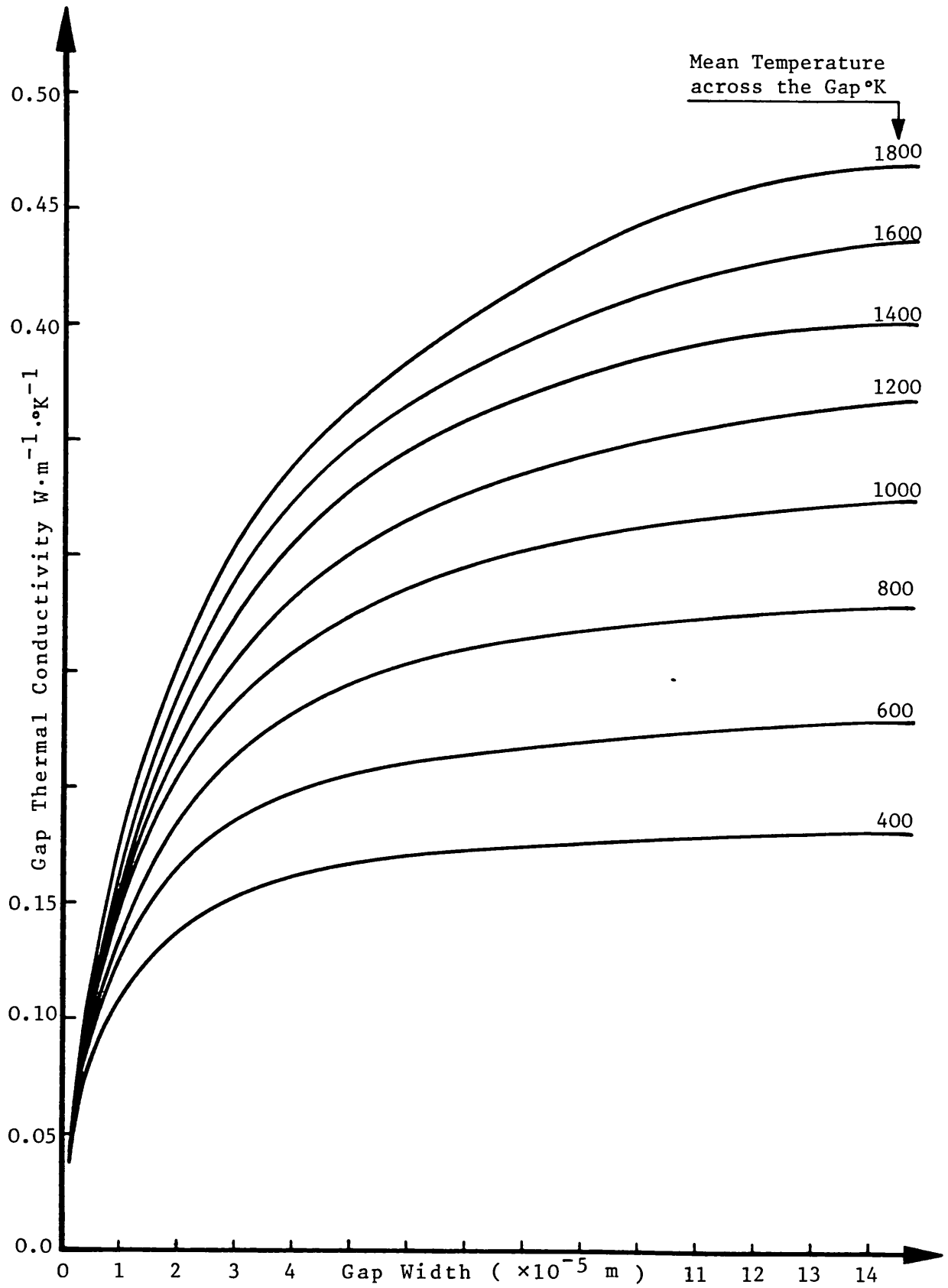Figure 3.15: Environmental Temperature Distributions around the Fuel Element.

Figure 3.14: Gap Thermal Conductivity variations of an LMFBR Fuel Element.
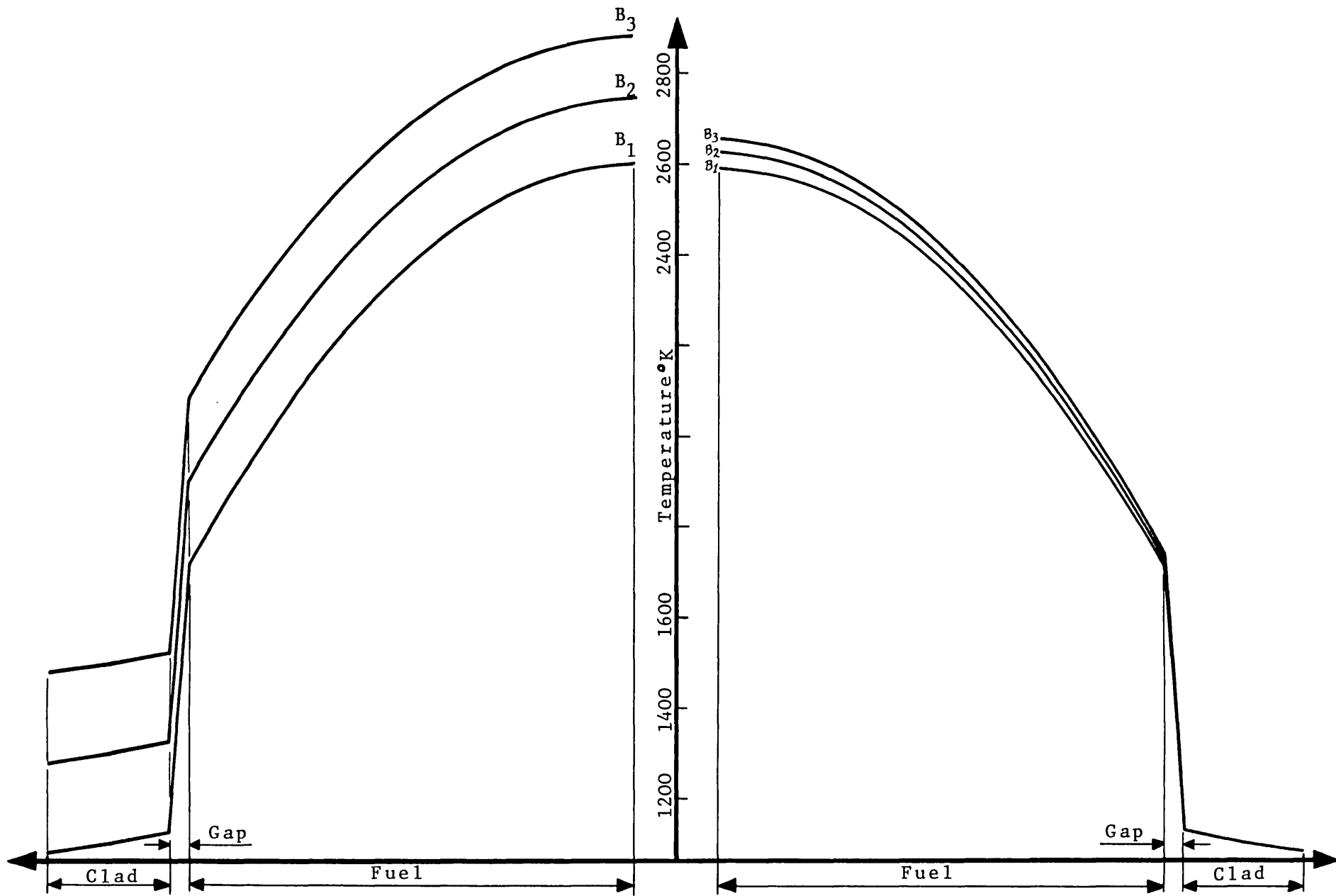
Figure 3.16:  Temperature Distributions, along the symmetry Diameter, inside the Fuel Element with Environmental temperatures as defined in Figure 3.15.

radiation across the gap are included. The effective gap thermal conductivity depends heavily on many factors, including the gas composition and the nature of the surface, both of which vary with burn-up. Figure 3.14 shows representative curves of the effective gap thermal conductivity as a function of gap width and gas temperature [11].

The boundary conditions are assumed to be similar to the case explained in Section 3.5.1, namely, the inner surface (of the fuel pellet) is adiabatic, while the fuel element is situated in a linearly varying temperature environment. Thus, the temperature at any point on the outer surface (of the clad) is linearly interpolated on the unique symmetry diameter, joining the hottest point and the coldest point, both on the outer surface of the clad (see Section 3.5.1). The problem, in general, is only symmetric about the unique symmetry diameter, and hence at least half of the cross-section of the fuel element has to be considered in the calculations. Of course, as before, such symmetry diameter is considered as an adiabatic boundary.

Three different examples of this type are selected with the environmental temperature distributions along the symmetry diameter prescribed as shown in Figure 3.15, while the inner surface of the pellet is always assumed to be adiabatic as before. The temperature distribution inside the fuel element is then calculated for each case (at its maximum rate of thermal energy generation), but only the temperature profiles along the unique symmetry diameter are plotted in Figure 3.16. Corresponding curves in Figures 3.15 and 3.16 are again labelled with the same symbols ($B$), where the curves labelled $B_1$ both refer to an axisymmetric example. The mesh used here was similar to the one shown in Figure 3.19 with 615 nodes and 1120 triangular elements. Each example converged after eight (8) iterations.

### 3.5.3 The Temperature Distribution within a Fuel Element with Uniform Temperatures on the Outer Surface and with Adiabatic Inner Surface, when the Pellet is Eccentrically Situated (Non-Uniform Gap)

Let us consider the same fuel element as explained in Section 3.5.2, in which the fuel pellet has been eccentrically situated. Figure 3.17 shows half of its cross-section. The outer surface of the cladding is assumed to be kept at a uniform temperature of 800°K, while the inner surface of the pellet is assumed to be adiabatic. Moreover, its rate of thermal energy generation is maximum. The problem, in general, is only symmetric about a unique diameter (AB), the "symmetry diameter", passing through the narrowest and the widest gaps. Therefore, at least half of the cross-section must be considered in the calculations. Of course, as before, such a symmetry diameter is considered as an adiabatic boundary. The temperature distribution inside the fuel element can then be calculated for any value of eccentricity. For instance, these temperatures are calculated here for six selected values of eccentricity. The temperature profiles along only the unique symmetry diameter, for each case, are shown in Figure 3.18, in which curves no. 1 refer to an axisymmetric example. Figure 3.19 shows the mesh used for these examples, consisting of 615 nodes and 1120 triangular elements. The solutions were achieved after about nine (9) iterations.
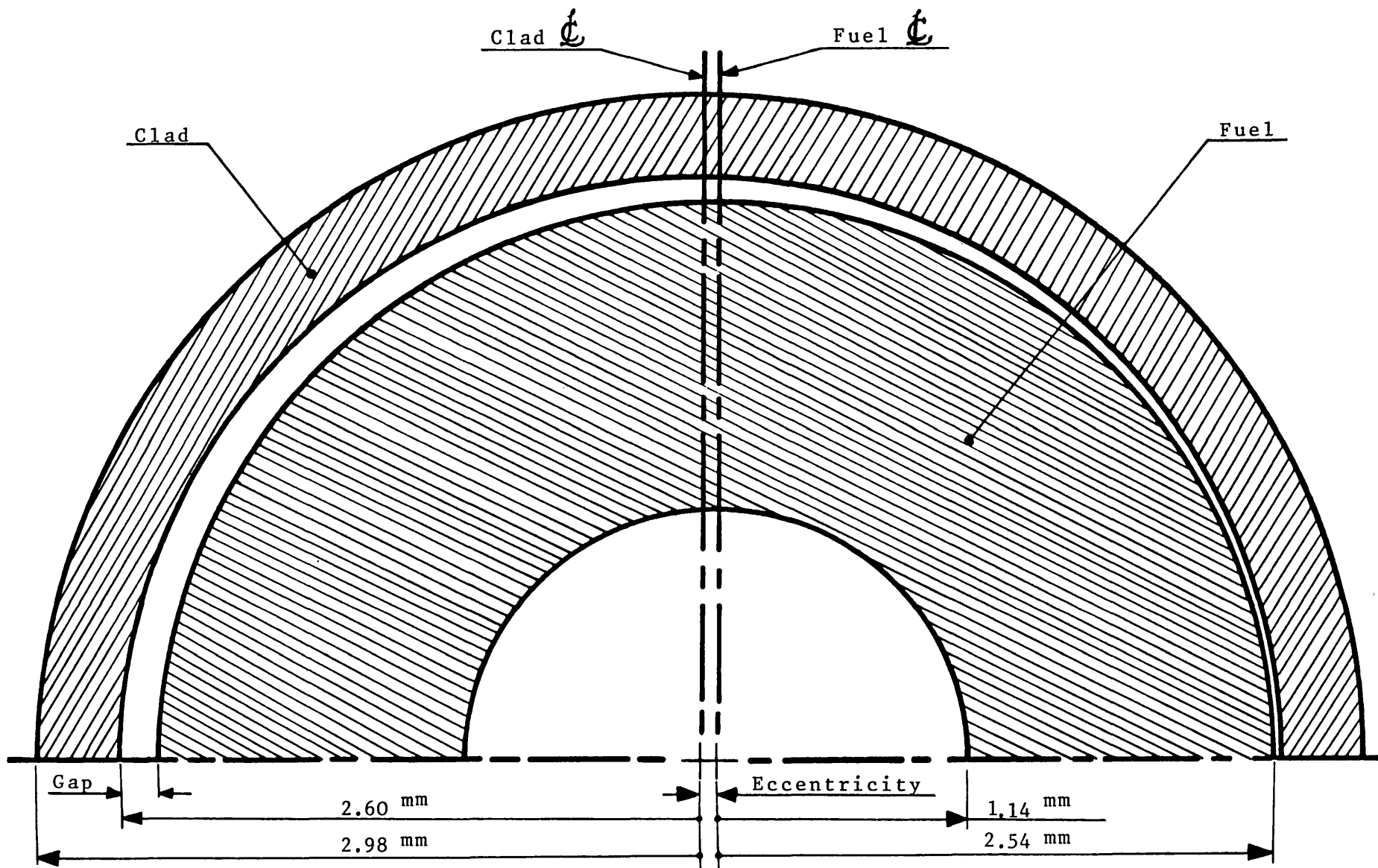
Figure 3.17:  Schematical Diagram of an LMFBR Fuel Element when the Pellet is eccentrically situated.  Half cross-section, along the symmetry diameter, is shown ( non-uniform Gap ).

Key:

| Curve No. | Eccentricity |
|-----------|--------------|
| 1 | $0.0 \times 10^{-6}$ m |
| 2 | 5.0 $//$ |
| 3 | 10.0 $//$ |
| 4 | 15.0 $//$ |
| 5 | 20.0 $//$ |
| 6 | 25.0 $//$ |
| 7 | 30.0 $//$ |

Figure 3.18:   Temperature Distributions along the Symmetry Diameter, inside the Fuel Element, due to various eccentricities.
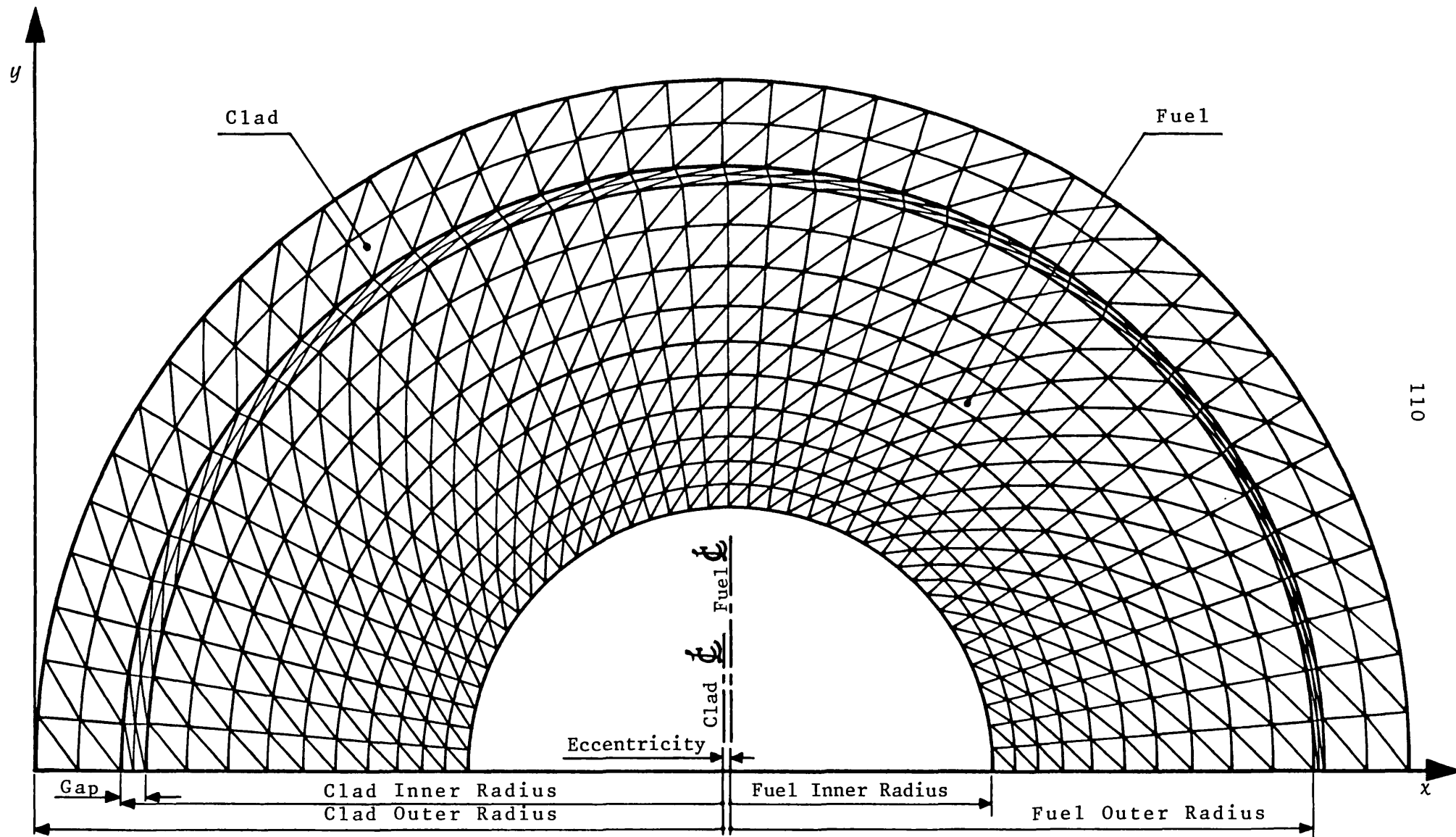
Figure 3.19:

# CHAPTER 4

## TIME-DEPENDENT PROBLEMS:

## FINITE ELEMENT FORMULATIONS FOR GENERAL

## TWO-DIMENSIONAL TRANSIENT HEAT CONDUCTION PROBLEMS

ABSTRACT

The finite element formulations, proposed in the previous chapters, are applied to very general two-dimensional transient heat conduction problems, involving single-phase media. Multi-phase problems (both steady-state and transient) are dealt with in the following chapter. Various material properties (temperature dependence, for example) can be handled by the proposed method, except for the geometrical variations, which are considered to be negligible.

## 4.1 INTRODUCTION

Transient field problems have been formulated in Chapter 2 within the framework of the finite element method, where it was shown that the solution to a transient heat conduction problem is governed by a system of first order linear differential equations of the form:

$$[K] \cdot \{\theta\} + [C] \cdot \left\{\frac{\partial \theta}{\partial t}\right\} + \{F\} = 0 \qquad (4.1)$$

(see equation (2.67)). In Chapter 3, a general steady-state heat conduction problem was solved by simply setting all the terms of the matrix $\{\partial \theta / \partial t\}$, in equation (2.67), equal to zero.
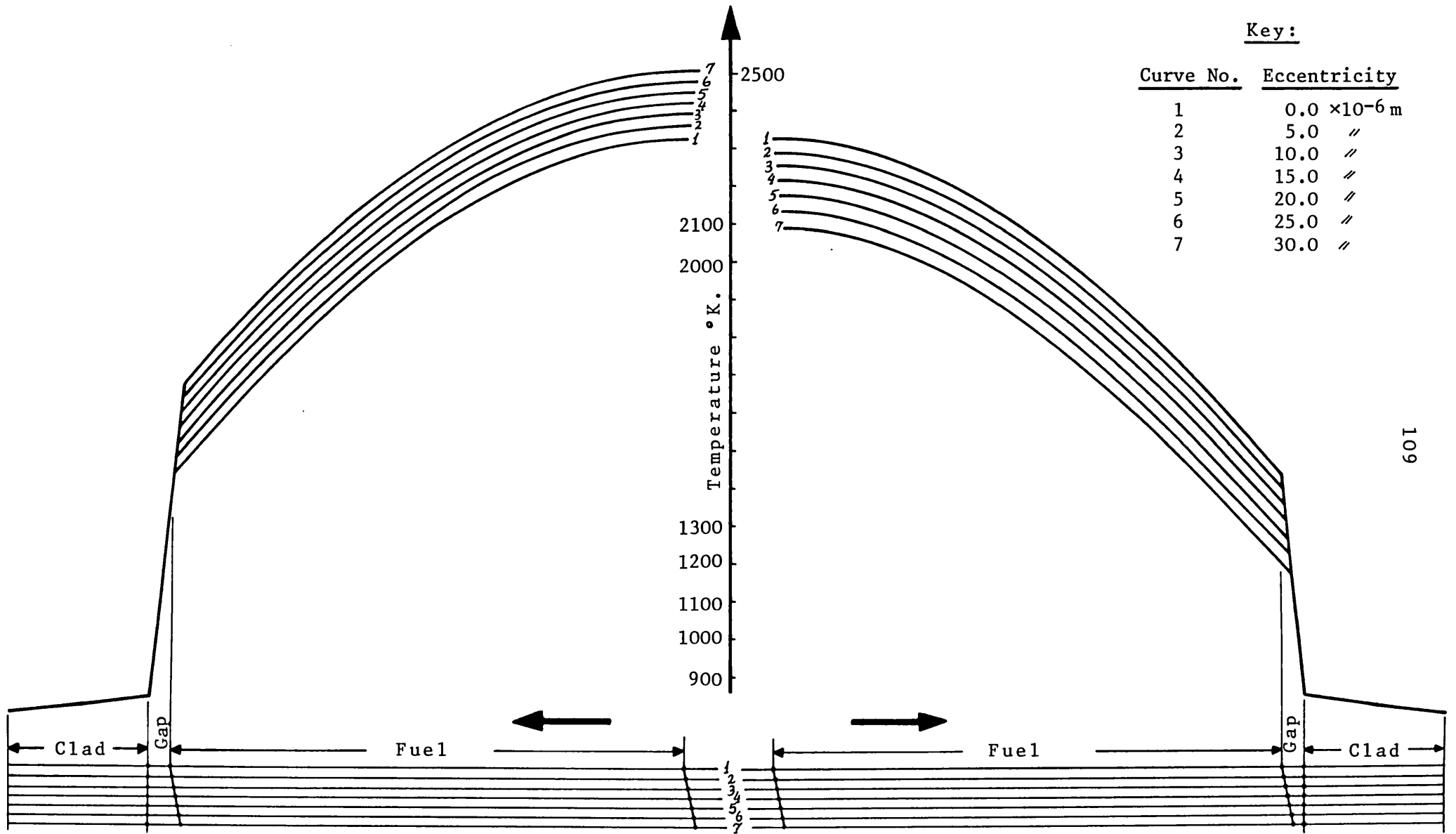
As was the case in Chapter 2, the geometry was assumed to be time-independent. If, of course, the geometry were to be time-dependent (which, in fact, is due to thermal expansion in transient problems), then the analytical (and also numerical) solution would be even more complicated.

A lot of work has been done involving transient field problems and many methods have been developed using special features of each individual problem. For example, Mazumdar [12] derived a two-dimensional method based on the concept of isothermal contours. Another formulation was proposed by Nijsing and Eifler [13] for axi-symmetric problems, but even in this case the method is highly complicated and involved. Extension to non-axisymmetric problems becomes a formidable task. The two most tried and tested methods are (a) the Crank-Nicholson method, and (b) the Galerkin method. The Crank-Nicholson method has been successfully used by Wilson and Nickell [14], and the Galerkin method has been used with equal success by Zienkiewicz and Parekh [15] using the mid-interval values.

A study to compare both of these methods was carried out by Donea [16] and his overall conclusion was that, for short-time steps, the Galerkin method produces more accurate results, but it is more expensive than the Crank-Nicholson method. We would like to derive a procedure here which combines the efficiency, accuracy, stability and economy of both methods.

Although the methods of Crank-Nicholson and Galerkin look distinctly different, it was found (as will be shown later) that the two methods can easily be generalised by one formulation. Using a parameter in the general formulation, one can then easily interchange between one method and the other, or produce a mixture of both. We have tried to derive a very general formulation capable of handling non-linear physical properties as well. In this method, time is regarded as one of the dimensions of the problem. For the numerical solution, as before, the time-dimension has to be discretised into a number of time-elements, which need not necessarily be equal. The so-called "time-step" and the end-points (the initial and final ends of each time-step) are called "time-nodes". The solution is then manipulated at these distinct time-nodes. If the solution at any intermediate instant is required, then the variable can be

interpolated in the usual way (relation (4.2), for example). A flat model, which assumes any variable to have a constant value over each time-step, by taking either the initial or the final value, or even a mid-interval value, is too simple and has a disadvantage that it will be discontinuous at the time-nodes, for the variables that are not constant. For spatial dimensions (see Section 2.4), since the level of approximations for other variables is assumed to be linear, the model for the temperature variation with respect to time is also assumed to be linear (Figure 4.1). This has an added advantage that the other variables will be piecewise continuous with respect to the time-dimension as well. Associated with this extra time derivative, there are the usual problems of convergence, stability and the magnitude of the time-step which have to be carefully monitored (more carefully than as has been described in detail in Chapter 3 for the spatial variables). The accuracy and the stability of the method will, of course, clearly depend on the size of the time-step chosen, and it is essential to test it. On the other hand, in transient problems, especially in phase-change problems (Chapter 5), where the field problem is governed by a non-linear quasi-harmonic equation, we must bear in mind that (in non-linear problems):

(a)  non-uniqueness of the solution may arise;

(b)  convergence can never be, *a priori*, guaranteed;

(c)  the cost of computation time for the solution is considerably greater than for linear problems, due to the many iterations in almost all parts of the program;  and

(d)  the time-steps have to be sufficiently small in order to obtain significant results, but too small time-steps can lead to wasteful computational effort, machine rounding off errors and occasionally even to unstable solution.
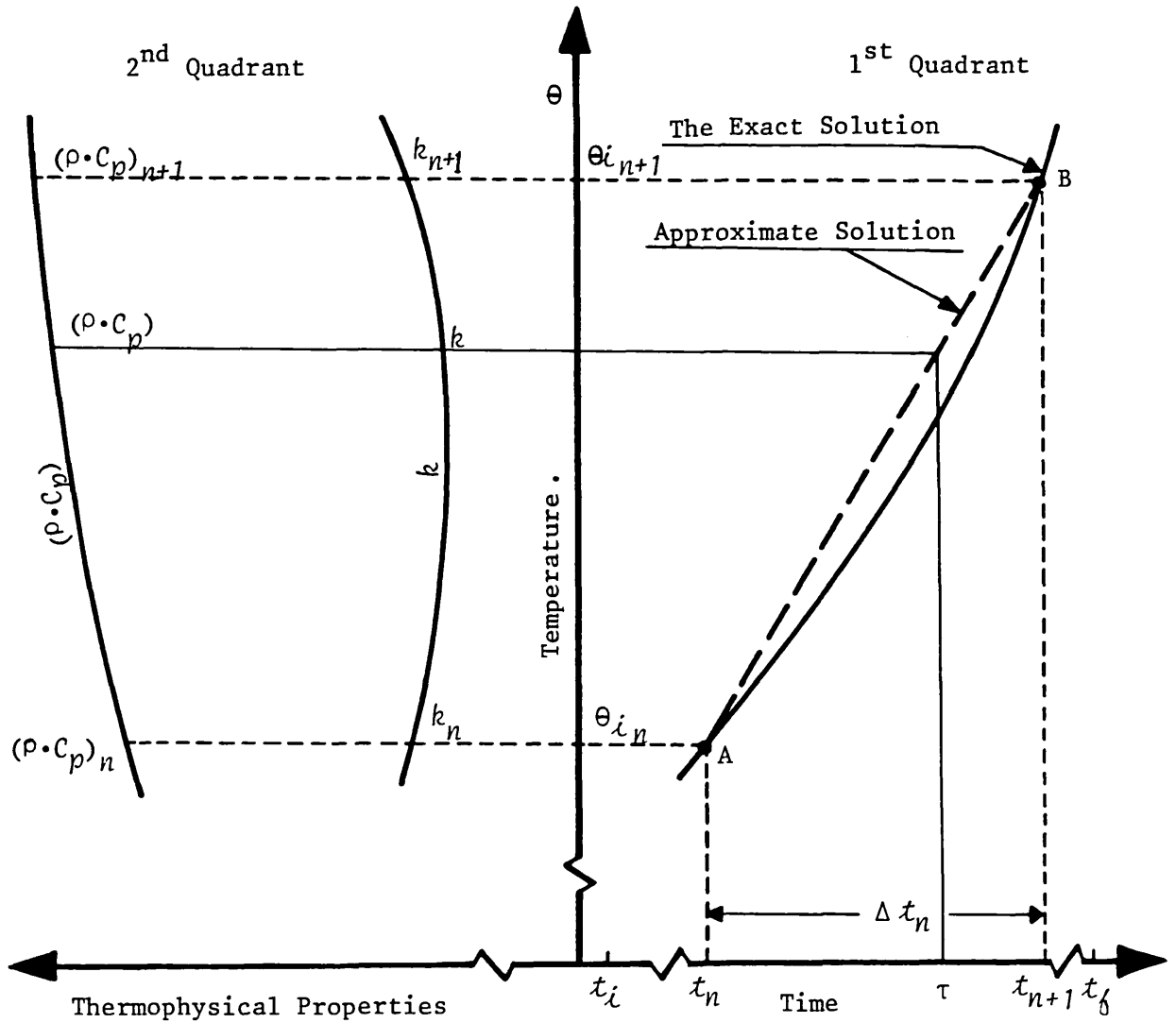
Figure 4.1:   $k$ and $(\rho \cdot C_p)$ represent the thermal conductivity and thermal energy capacity, respectively;   $\Theta_i$ is the temperature at node $i$ and $t$ is time.

A general recurrence formula is therefore derived using a parameter

$\lambda$, which for $\lambda$ equals unity yields the Crank-Nicholson formula, and for $\lambda$

equals two yields the Galerkin formula. Both are discussed in detail

later in this chapter, where for both cases the thermal properties are

taken to be constant over each time-step and usually the mid-time step

values are used.


## 4.2 FORMULATIONS

### 4.2.1 A General Case

At any time, the problem is governed by equation (4.1), which

is parabolic or hyperbolic (see Section 1.3) in the time-dimension.

Therefore, the state of any particular problem at a given time-node is

sufficient to determine the state of the problem at the next time-node.

Since in this method we shall be marching forward by time-steps, the

method may be called a step-by-step method, or a time-stepping method.

The time region is from $t_i$ to $t_\emptyset$ and will be discretised into a number of

time-steps. Then the initial time-node is $t_i$ and the final time-node is

$t_\emptyset$.

For a typical time-step, $\Delta t_n$, for instance, between time-nodes

$t_n$ and $t_{n+1}$, the exact temperature ($\theta$) at an arbitrary point (node $i$)

inside the solution-domain may typically vary as the curve shown in the

first quadrant in Figure 4.1. This is modelled to vary linearly as shown

by the straight line in the same quadrant. Simultaneously, the second

quadrant of the same graph (Figure 4.1) shows schematically how the

thermal properties (for example, thermal conductivity ($k$) and thermal

energy capacity ($\rho.C_p$)) also vary with temperature $\theta$ during the same time-

step. From Figure 4.1, it can be seen that at a particular time, $\tau$,

there is a unique value for $\theta$. Likewise, for a particular temperature, $\theta$,

there is a unique value for $k$ and a unique value for $\rho.C_p$.

In this formulation, the physical properties ($k$ and $\rho.C_p$, for example), loads, $F$, and temperature, $\theta$, are considered to vary continuously. Hence, for any time-step, $\Delta t_n$, between two time-nodes $t_n$ and $t_{n+1}$, these variables will attain their nodal values as time, $\tau$, approaches $t_n$ or $t_{n+1}$, either from the left or right hand side limits, respectively (see Table 4.1).

TABLE 4.1

Values of the Field Variables at

the Time-Nodes $t_n$ and $t_{n+1}$

| $\tau$ | $t_n$ | $t_{n+1}$ |
|---|---|---|
| $\theta$ | $\theta_n$ | $\theta_{n+1}$ |
| $k$ | $k_n$ | $k_{n+1}$ |
| $\rho.C_p$ | $(\rho.C_p)_n$ | $(\rho.C_p)_{n+1}$ |
| $F$ | $F_n$ | $F_{n+1}$ |

Since $\theta$ does not actually vary linearly with respect to time, the values of the gradient at these limits are different, depending on whether the limit is approached from the left or right hand side. However, for a given time-step, we may assume that the temperature varies linearly with respect to time and the right hand limit for the gradient of $\theta$ is then given by:

$$\frac{\theta_{n+1} - \theta_n}{t_{n+1} - t_n} \tag{4.2}$$

(the Euler approximation). This is also the same for the left hand limit

of the same time-step.

Therefore, for the whole system, using the forward difference approach at time-node $t_n$, equation (4.1) becomes:

$$[K_n] \cdot \{\theta_n\} + [C_n] \cdot \{\frac{\theta_{n+1} - \theta_n}{t_{n+1} - t_n}\} + \{F_n\} = 0 \qquad (4.3)$$

and by using the backward difference approach at time-node $t_{n+1}$, over the same time-step, equation (4.1) becomes:

$$[K_{n+1}] \cdot \{\theta_{n+1}\} + [C_{n+1}] \cdot \{\frac{\theta_{n+1} - \theta_n}{t_{n+1} - t_n}\} + \{F_{n+1}\} = 0 \qquad (4.4)$$

Since both of these equations (4.3) and (4.4) are satisfied over this time-step, we can choose to add any multiple of the second equation (4.4) to the first equation (4.3).

The Crank-Nicholson method is obtained when these two equations are added together equally, that is:

$$([K_{n+1}] + \frac{1}{\Delta t_n} ([C_{n+1}] + [C_n])) \cdot \{\theta_{n+1}\} +$$

$$([K_n] - \frac{1}{\Delta t_n} ([C_{n+1}] + [C_n])) \cdot \{\theta_n\} + (\{F_{n+1}\} + \{F_n\}) = 0 \qquad (4.5)$$

and the Galerkin method is obtained by adding twice equation (4.4) to equation (4.3), giving:

$$(2 \cdot [K_{n+1}] + \frac{1}{\Delta t_n} (2 \cdot [C_{n+1}] + [C_n])) \cdot \{\theta_{n+1}\} +$$

$$([K_n] - \frac{1}{\Delta t_n} (2 \cdot [C_{n+1}] + [C_n])) \cdot \{\theta_n\} + (2 \cdot \{F_{n+1}\} + \{F_n\}) = 0 \qquad (4.6)$$

More generally, by adding a parameter $\lambda$ times of equation

(4.4) to equation (4.3), we obtain:

$$(\lambda \cdot [K_{n+1}] + \frac{1}{\Delta t_n} \cdot (\lambda \cdot [C_{n+1}] + [C_n])) \cdot \{\theta_{n+1}\} +$$

$$([K_n] - \frac{1}{\Delta t_n} \cdot (\lambda \cdot [C_{n+1}] + [C_n])) \cdot \{\theta_n\} + (\lambda \cdot \{F_{n+1}\} + \{F_n\}) = 0 \qquad (4.7)$$

In this equation (4.7), $\lambda$ equal to unity yields the Crank-Nicholson method (4.5), and $\lambda$ equal to two yields the Galerkin method (4.6). Hence, the nodal temperatures, $\{\theta_{n+1}\}$, at the time-node $t_{n+1}$ can be expressed in terms of $K_n$, $K_{n+1}$, $C_n$, $C_{n+1}$, $F_n$ and $F_{n+1}$ and the nodal temperatures, $\{\theta_n\}$, at the time-node $t_n$ (the initial values). These are all assumed to be known. Therefore, if the temperature distribution is prescribed at any time-node, then it can be evaluated at the next time-node. Thus, at every subsequent time-node, namely, relation (4.7), is to be applied successively for all the time-steps; hence, it is then a recurrence relation.

Since the problem can be solved only if the initial values are prescribed, these problems are therefore called the "initial value" problems.

### 4.2.2 Special Cases

If the thermal properties remain constant over the time-step, then we can write:

$$K_{n+1} = K_n = K \qquad \text{and} \qquad C_{n+1} = C_n = C$$

Hence, for such idealised cases, equation (4.7) can be written as:

$$(\lambda.[K] + \frac{\lambda+1}{\Delta t_n} \cdot [C]) \cdot \{\theta_{n+1}\} +$$

$$([K] - \frac{\lambda+1}{\Delta t_n} \cdot [C]) \cdot \{\theta_n\} + (\lambda.\{F_{n+1}\} + \{F_n\}) = 0 \qquad (4.8)$$

For $\lambda$ equal to unity, we obtain the Crank-Nicholson formulation in the form shown by Donea [16], and for $\lambda$ equal to two we obtain the Galerkin formulation in the form as that used by the same author [16]. In this paper, Donea showed that when short time-steps are used, the Galerkin formula gives better accuracy than the Crank-Nicholson formula. Thus, for example, the Galerkin method ($\lambda$ = 2) would be more suitable than the Crank-Nicholson method around the time regions when a change of phase takes place. At other times, however, reasonable results can be obtained by the Crank-Nicholson method ($\lambda$ = 1) using coarser time-steps, with a consequent saving in computation cost. Ideally, one would like to change the value of $\lambda$ as a particular solution progresses and as various phase changes take place. This is in itself a major subject of investigation, which will divert us from the objectives of the present study. However, preliminary investigations for the test case of Section 4.4 revealed that $\lambda$ = 1.5 gave better results. Therefore, the value of $\lambda$ = 1.5 is used for the present calculations.

## 4.3 EVALUATION OF THE THERMAL ENERGY CAPACITY MATRIX, $[C]^{e}$

All the aforementioned relations in this chapter hold for the entire domain throughout the time region and, in particular, for each element. Therefore, for a typical element ($e$), each relation may be written with superscript (or subscript) $e$ throughout. The definitions and descriptions of all the components of these relations as described earlier in Chapter 2 are still valid for the general case. In Chapter 3, the $K$ and $F$ matrices

were described in detail for a general two-dimensional case and those formulations still hold for the transient case. We now have an additional matrix $[C]^e$ to evaluate. This matrix is treated as follows.

Consider relation (2.60) which is rewritten here for convenience:

$$[C]^e = \iiint_{V^e} \{[N]^T . (\rho^e . C_p^e) . [N]\} . dV \qquad (4.9)$$

Each individual element may be assumed to be homogeneous and, consequently, the value of $(\rho^e . C_p^e)$ or $(\rho . C_p)^e$ will be uniform throughout the element. Hence, relation (4.9) can be written as:

$$[C]^e = (\rho . C_p)^e . \iiint_{V^e} \{[N]^T . [N]\} . dV \qquad (4.10)$$

For a two-dimensional case, as explained in Section 3.1, $dV$ may be replaced by $\ell^e . dS$, as described for relation (3.1), where $\ell^e$ is the length of the element in question. Also, the volume integral becomes a surface integral on the mid-cross section of the element. Hence, relation (4.10) can be written as:

$$[C]^e = (\rho . C_p)^e . \ell^e . \iint_{S^e} \{[N]^T . [N]\} . dS \qquad (4.11)$$

A general term of this relation (4.11) can be written as:

$$C_{i,j}^e = (\rho . C_p)^e . \ell^e . \iint_{S^e} N_i . N_j . dx \, dy \qquad (4.12)$$

which is the thermal energy capacity, due to the material, between the two nodes $i$ and $j$ within the element $e$ only.

When the two-dimensional solution-domain is discretised solely into triangular elements, relations (4.11) and (4.12) can be easily calculated

and the final results will be the same as those found by Zienkiewicz [4]
and by Wilson and Nickell [14], that is:

$$
\iint_{S^e} N_i \cdot N_j \cdot dx \, dy = \begin{cases} \dfrac{1}{12} \cdot \Delta_e & \text{if } i \neq j \\[2em] \dfrac{1}{6} \cdot \Delta_e & \text{if } i = j \end{cases}
$$

where $\Delta_e$ is the area of the element $e$.  Hence, the thermal energy capacity

matrix (relation (4.11)) of a two-dimensional element with triangular

cross-section with a uniformly distributed value of $(\rho.C_p)$ is:

$$
[C]^e = (\rho.C_p)^e \cdot \ell^e \cdot \frac{\Delta_e}{3} \cdot \begin{bmatrix} \frac{1}{2} & \frac{1}{4} & \frac{1}{4} \\[0.5em] \frac{1}{4} & \frac{1}{2} & \frac{1}{4} \\[0.5em] \frac{1}{4} & \frac{1}{4} & \frac{1}{2} \end{bmatrix} \tag{4.13}
$$

Sometimes, the uniform distributive values can be equally lumped

at the vertices (or nodes) of the element, in which case the matrix on the

right hand side of relation (4.13) may be approximated by a unit matrix

simply for reasons of economy.  Of course, this would not be correct for

any general type of temperature field.

For any two-dimensional element where $\ell^e$ and $\Delta_e$ are constant, relation

(4.13) (or a similar one, depending on the shape of the element) depends

only on the value of $(\rho.C_p)^e$.  Therefore, the matrices $[C_n]$ and $[C_{n+1}]$ in

equation (4.7) will depend simply on the values of $(\rho.C_p)^e$ at the time-

nodes $t_n$ and $t_{n+1}$, respectively, which also vary with temperature.  Thus,

the value of $(\rho.C_p)^e$ must be calculated by simultaneous iterations with

temperature and other variables, as has been done for the value of thermal

conductivity $(k)$.  This introduces further oscillations (although of a

smaller order) and therefore uses more computer time.  One method of

reducing such oscillations is to approximate the value of $(\rho.C_p)^e$ by a

0th order approximation. Hence, the value of $(\rho.C_p)^e$ would then be

assumed to be constant over each time-step and equal to its value at the

initial time-node $t_n$, or its mid-interval value. This method has been

used by Wilson and Nickell [14], and also by Zienkiewicz and Parekh [15].

Although this technique is widely used, it is sometimes assumed by the

authors to be standard and is therefore totally omitted from their

descriptions. As a result of this, a great deal of time and computation

effort was necessary in order to duplicate some of their results.

There are other approximations, but certainly the safest and the most

accurate one is simply to iterate as was described earlier.


## 4.4  TRANSIENT PROBLEMS APPROCHING A STEADY-STATE CASE

The proposed method is an iterative procedure, by which a problem can

be solved over each time-step, using the values which are prescribed at

the beginning of that time-step. Upon the convergence of the solution

at the end of a time-step, the temperature distribution  thus obtained is

used as initial values for the following time-step.

The field is usually judged on its mean temperature value (the

average of the nodal temperatures), which can be denoted by $MT_1$ and $MT_2$ at

the beginning and the end of a time-step, respectively. Furthermore, the

relative change in the mean temperature value of the field over each time-

step, $T_{ch}$, can be found by:

$$T_{ch} = \frac{MT_2 - MT_1}{MT_1} \tag{4.14}$$

A positive value of $T_{ch}$ represents a "heating-up system", whereas a

negative value of $T_{ch}$ represents a "cooling-down system". In both cases,

the system is said to be in a transient state. However, the system is

said to be in steady-state when the value of $T_{ch}$ is zero.

The computer program, written for the proposed method, terminates execution when the absolute value of $T_{ch}$ tends to zero. A criterion sufficiently close to zero can be specified for a given problem so that computer time can be saved. When $T_{ch}$ approaches this criterion, a message, "Steady-state case approached", is issued and the results thus obtained can be printed out.

Of course, a system will approach steady-state if all activities of the internal sources within the solution-domain (for example, thermal energy generation) and also all the boundary conditions of the system remain steady.

## 4.5 VALIDATION STUDY

In the previous chapter, it was shown that the proposed method was stable and resulted in excellent agreement with exact solutions for steady-state (temperature) field problems. In this chapter, the method, proposed in the previous chapters, is developed so that it can be used to solve the transient field problems, which finally approaches a steady-state case if the thermal load and the boundary conditions did so. The method is shown here to be stable, accurate and capable of handling both the steady-state and the transient cases.

In order to validate this method, namely, to check its authenticity and its accuracy, a test case has been chosen for which an analytical and a numerical solution have already been given by Lewis [19] and Samiei [20], respectively. The problem is to solve the transient temperature field inside an LWR fuel pin subjected to axi-symmetric conditions and using the information given in Table 4.2 (as was used in [19] and [20]). In this case, the properties were taken to be constant and, also, the gap between the fuel and the cladding was regarded as negligible.

## TABLE 4.2

Data of the Fuel Pin Used in Section 4.4, Given in [20]

| The geometrical dimensions of: | | Used in [19] and [20] | Used Here |
|---|---|---|---|
| The fuel { inner radius | | 0.0 m | 0.0 m |
| outer radius | | 0.0062484 m | 0.0062250 m |
| The clad { inner radius | | 0.0062484 m | 0.0062750 m |
| outer radius | | 0.0070104 m | 0.0070104 m |

| The thermal conductivity of: | $W.m^{-1}.°K^{-1}$ |
|---|---|
| The fuel | 2.0 |
| The clad | 1000.0 |

| The specific heat of: | $J.kg^{-1}.°K^{-1}$ |
|---|---|
| The fuel | 330.0 |
| The clad | 340.0 |

| The density of: | $kg.m^{-3}$ |
|---|---|
| The fuel | 10,000.0 |
| The clad | 6,500.0 |

| The thermal expansion coefficient of: | $°K^{-1}$ |
|---|---|
| The fuel | 0.0 |
| The clad | 0.0 |

| | $W.m^{-2}.°K^{-1}$ |
|---|---|
| The coolant heat transfer coefficient | 13627.8 |

| | $°K$ |
|---|---|
| The coolant bulk temperature | 273.0 |

This idealised test case was first chosen by Lewis because of the nature of his solution method which was one-dimensional with non-variable properties. Samiei chose this test case because his numerical method was one-dimensional. Samiei's method, which is based on the finite differencing scheme, could tackle variable properties and showed good agreement with Lewis's results, whereas the proposed method, which is based on the finite element method, is two-dimensional (also extendable to three dimensions) and can handle variable physical properties and non-axisymmetrical problems. The fact that the new method is applicable to almost any general two-dimensional transient heat conduction problem, in real life the test case adopted cannot, of course, be a rigid test for its validation. Nevertheless, this method is applied to the test case in its general manner (as a general case) and the results obtained have shown very good agreement with those given by Samiei [20].

To apply the proposed method to the test case, the same data as those used in [19] and [20] (given in Table 4.2) were obviously used. Besides, for numerical reasons, a very narrow gap (of $50 \times 10^{-6}$ m) was, necessarily, assumed between the fuel and the cladding. This entailed some small alterations on the fuel outer radius and the clad inner radius (see Table 4.2), namely, they were both taken to be 0.0062484 m in [19] and [20], but the values taken here are 0.0062250 m for the fuel outer radius and 0.0062750 m for the clad inner radius. The fuel inner radius and the clad outer radius are, of course, unchanged (0.0 and 0.0070104 m, respectively). The gap thermal conductivity was calculated (using the temperature drop across the assumed gap) and was taken to be 0.281 $W.m^{-1}.°K^{-1}$ to match the same gap conductance as used by Samiei [20]. Also, the gap thermal energy capacity $(\rho . C_p)$ was taken to be 150.0 $J.m^{-3}.°K^{-1}$. Boundary conditions on the outer surface were also chosen to be the same as those of Samiei's on match his results.

As the problem is axi-symmetric, a small sector of the fuel pin cross-section can be considered to reduce the computation time (see Section 3.4.2). The mesh used here is as shown in Figure 4.2. As explained in Section 4.2.2, this particular problem can be easily solved by equation (4.8); nevertheless, it is solved here using the more general equation (4.7).

The fuel pin is assumed to be initially at equilibrium conditions such that the radial temperature distribution can be shown by the curve labelled $t = 0$ in Figure 4.3. At time zero ($t = 0$), the reactor suddenly scrams (the heat source term suddenly becomes zero), while the coolant (outside the fuel pin) remains at a constant temperature of 273.0°K. This idealised situation was solved here using $\lambda = 1.0$, 1.5 and 2.0. The three sets of results obtained were found to be always considerably close to each other. Also, the results obtained for $\lambda = 1.5$ were found to be always lying between those obtained for $\lambda = 1.0$ and 2.0, as expected. Although the results obtained were all in perfect agreement with those given in [20], in this case $\lambda = 1.5$ yielded the best solution. The radial temperature profiles are then plotted for $\lambda = 1.5$ at some selected time nodes in Figure 4.3. The results given in [20] are also plotted in the same figure; the extreme closeness between the results obtained from the proposed method and those given in [20] can be seen.

In this test case, the number of radial divisions across the clad, gap and fuel are as few as two, one and nineteen, respectively (see Figure 4.2). Despite the very high aspect-ratio (about 15) in the elements within the gap region (very sharp elements), the proposed method still showed stability and produced excellent results.

As explained in Sections 4.2.1 and 4.2.2, two apparently different forms of equation (4.7) are found in the literature, which appear to be quite distinct. These two forms are known as:
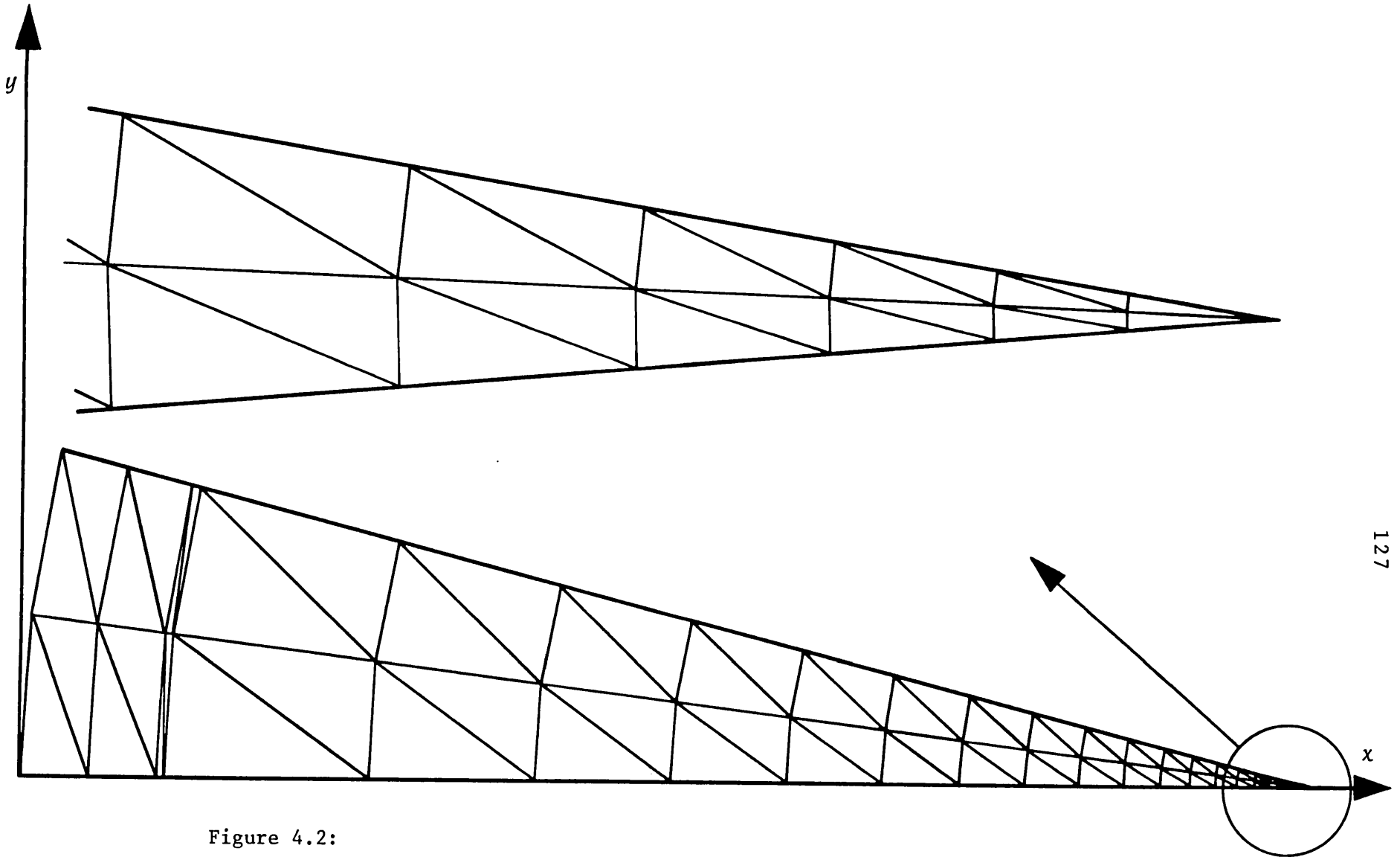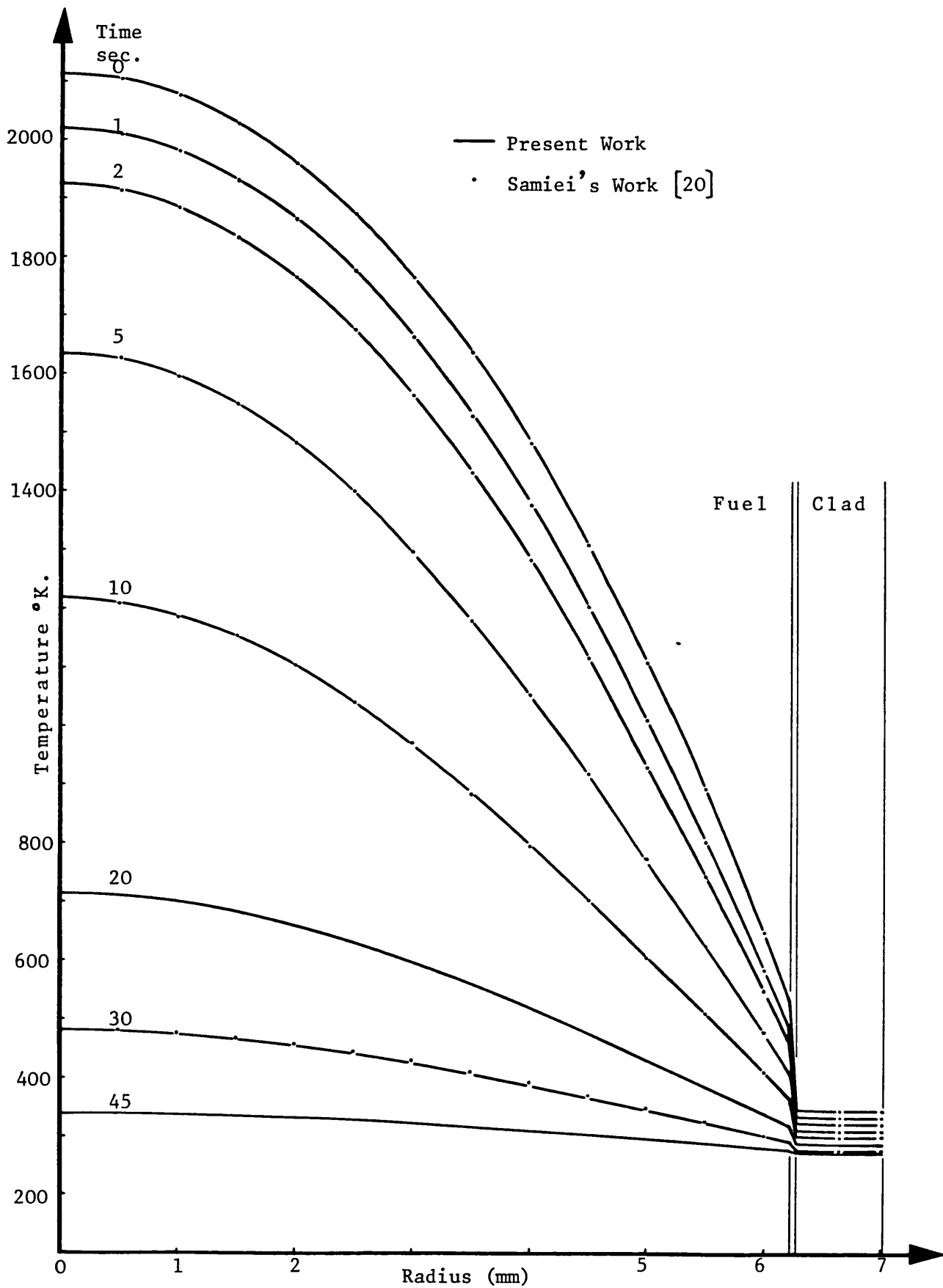
Figure 4.2:

128



Figure 4.3:

(i) The Crank-Nicholson formula (which can be obtained from equation (4.7) by letting $\lambda = 1.0$ {see equation (4.5)})

(ii) The Galerkin formula (which can be obtained from equation (4.7) by setting $\lambda = 2.0$ {see equation (4.6)})

Furthermore, this approach opens up a wide range of new formulations for different values of $\lambda$. This generalisation now replaces the choice between the two aforementioned methods by the choice of the best value of the parameter $\lambda$. This latter choice would inevitably depend on the particular problem being considered and also on the requirements. In view of this, no attempt has been made to give a universal recommendation.

## 4.6 APPLICATION OF THE METHOD TO SOME MORE GENERAL EXAMPLES

### 4.6.1 Application of the Method to a Heating-Up System

A general transient heat conduction problem has been chosen here to investigate the numerical behaviour and the performance of the proposed method using the more general equation (4.7). The geometry of the solution-domain, the distribution of the initial values, the variation of the field variables, and the boundary conditions can also be of a very general nature.

The problem which is considered here is to solve transient temperature fields within an LMFBR fuel pellet as defined in Section 3.4.1 and in Figure 3.6. The properties of the pellet (which were used in the steady-state calculations) were partially given in Section 3.4.2; the remaining properties (which were used in the transient calculations) are given in Table 4.3. These values are temperature-dependent and can be found in [11].

Figure 4.4 shows the values of $(\rho.C_p)$ versus temperature. The initial temperature distribution is assumed to be uniform and equal to

TABLE 4.3

Temperature-Dependent Properties of an

LMFBR Fuel Pellet [11] in Solid State

---

Density:

$$\rho = \frac{10{,}970.0}{(1.0 + 9.0 \times 10^{-6} \times t + 6.0 \times 10^{-9} \times t^2 + 3.0 \times 10^{-12} \times t^3)}$$

$t$ = temperature (°C)

$\rho$ = density (kg.m$^{-3}$)

---

Specific heat:

$$C_p = 47.445 + 0.1985 \times T + \frac{1.1532 \times 10^7}{T^2}$$

$T$ = temperature (°K)
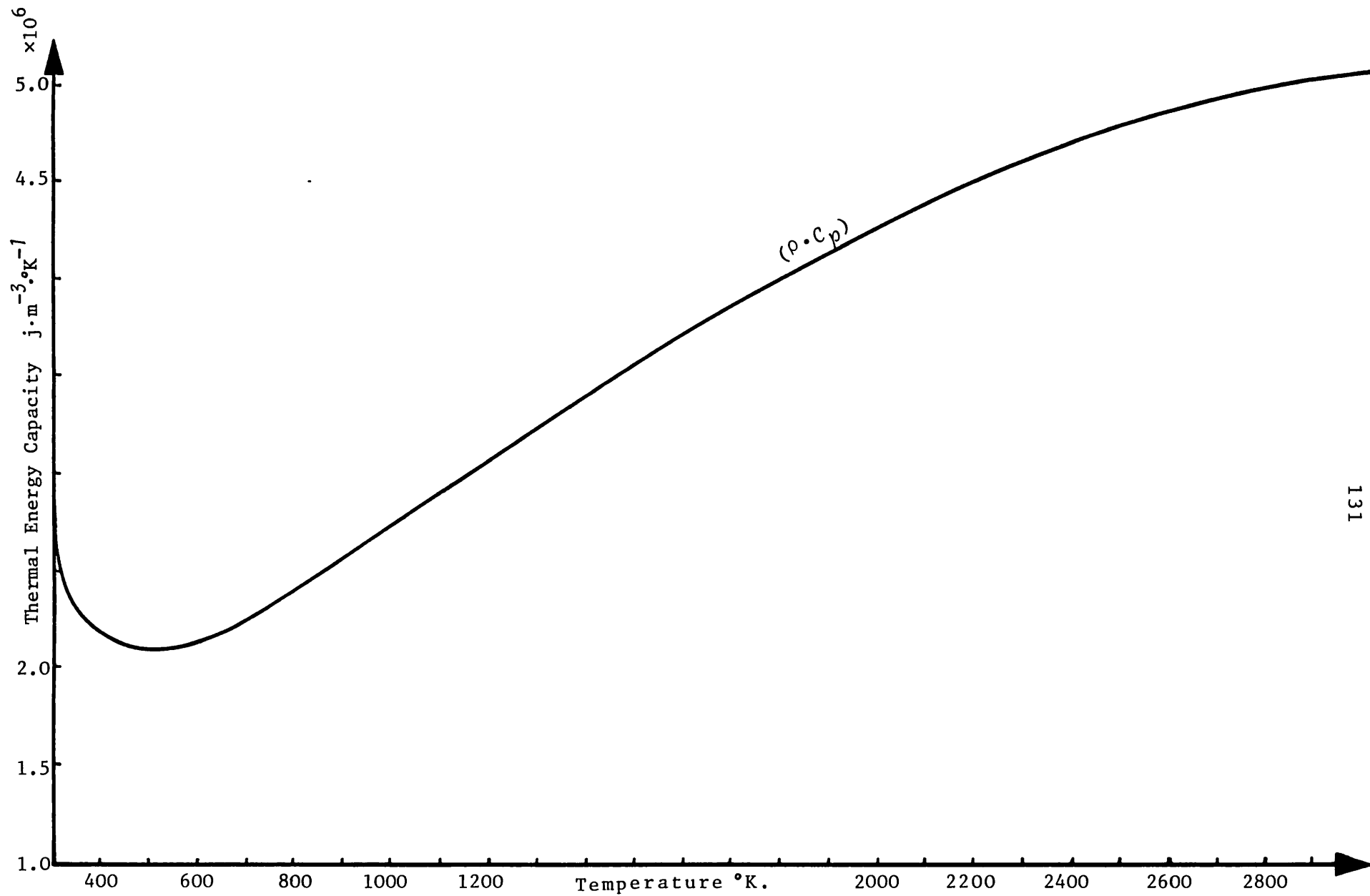
$C_p$ = specific heat (J.kg$^{-1}$.°K$^{-1}$)

Figure 4.4:  Thermal Energy Capacity of Solid $UO_2$ versus Temperature.

131

1000.0°K.   The boundary conditions are prescribed as:


(i) The outer surface is always kept at a constant temperature of

1000.0°K (for $t_i \leqslant t \leqslant t_\delta$).

(ii) The inner surface is assumed to be adiabatic at all times.


The rate of thermal energy generation of the pellet is assumed
to vary linearly with respect to time (from an initial value of $Q_0$ to a
certain value of RATE, for example) over a certain period of time (TIMSTD)
and remains constant thereafter.

Although the method is applicable to unequal time-steps,
nevertheless, for reasons of economy, the time-steps are chosen to be
equal in each individual example (this policy is pursued throughout this
chapter).

A problem of this kind is solved here using the following
settings:

$$\lambda = 1.5$$

$$Q_0 = 0.0 \ \text{W}\cdot\text{m}^{-3}$$

$$\text{RATE} = 0.27 \times 10^{10} \ \text{W}\cdot\text{m}^{-3}$$

$$\text{TIMSTD} = 10 \ \text{seconds}$$

$$\text{Time-step} = 0.25 \ \text{seconds}$$


For economical reasons, and due to the nature of the problem, which is

axi-symmetrical, a small sector (9.6°) of the solution-domain is

considered (Figure 4.5).   A finite element triangular mesh is adopted for

this sector, in which only 15 nodes are considered in the radial direction

(see Figure 4.5).

The variations of the pellet's internal rate of thermal energy

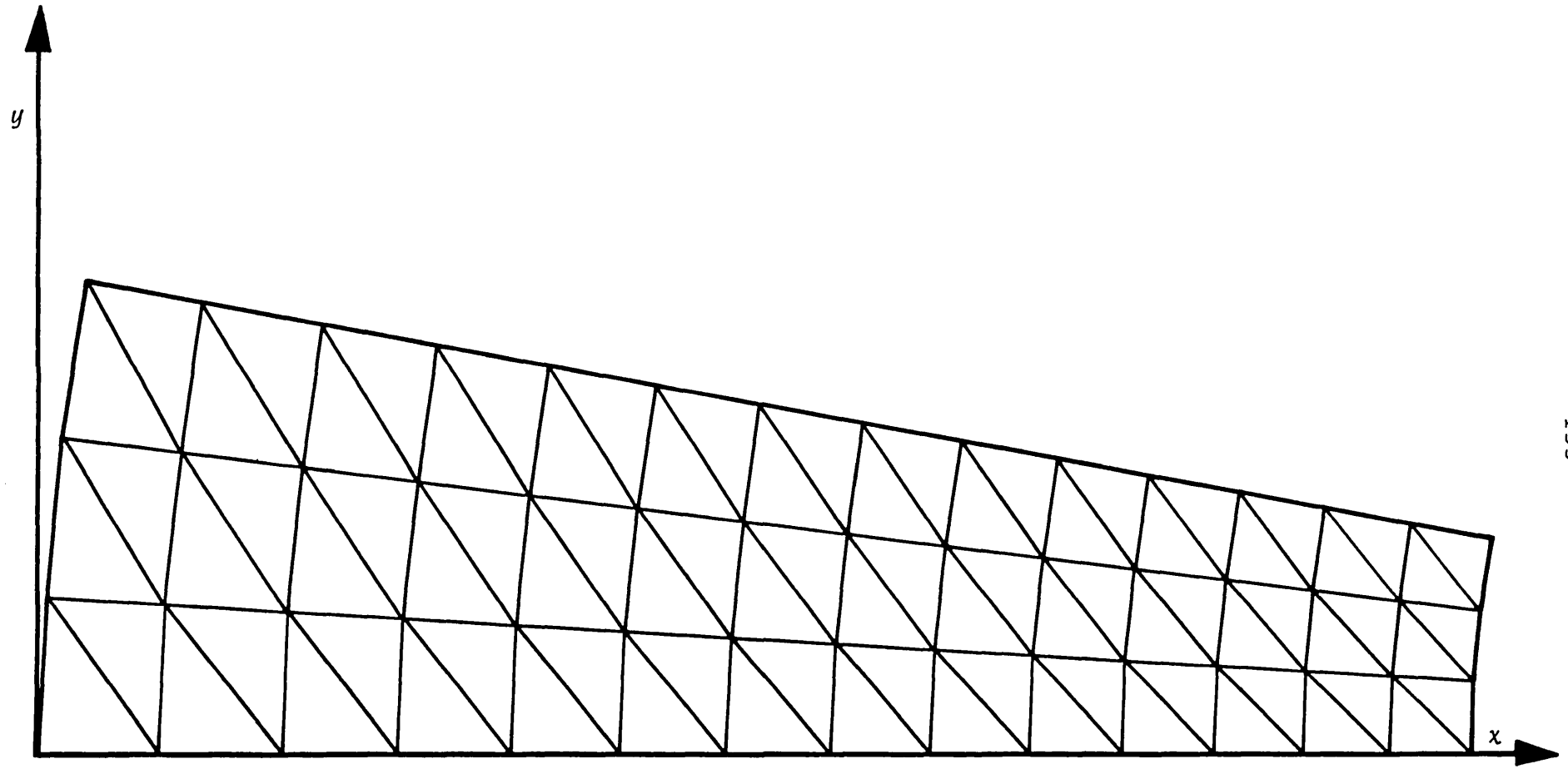generation (rate-history or load-history) are shown by curve 2 in Figure
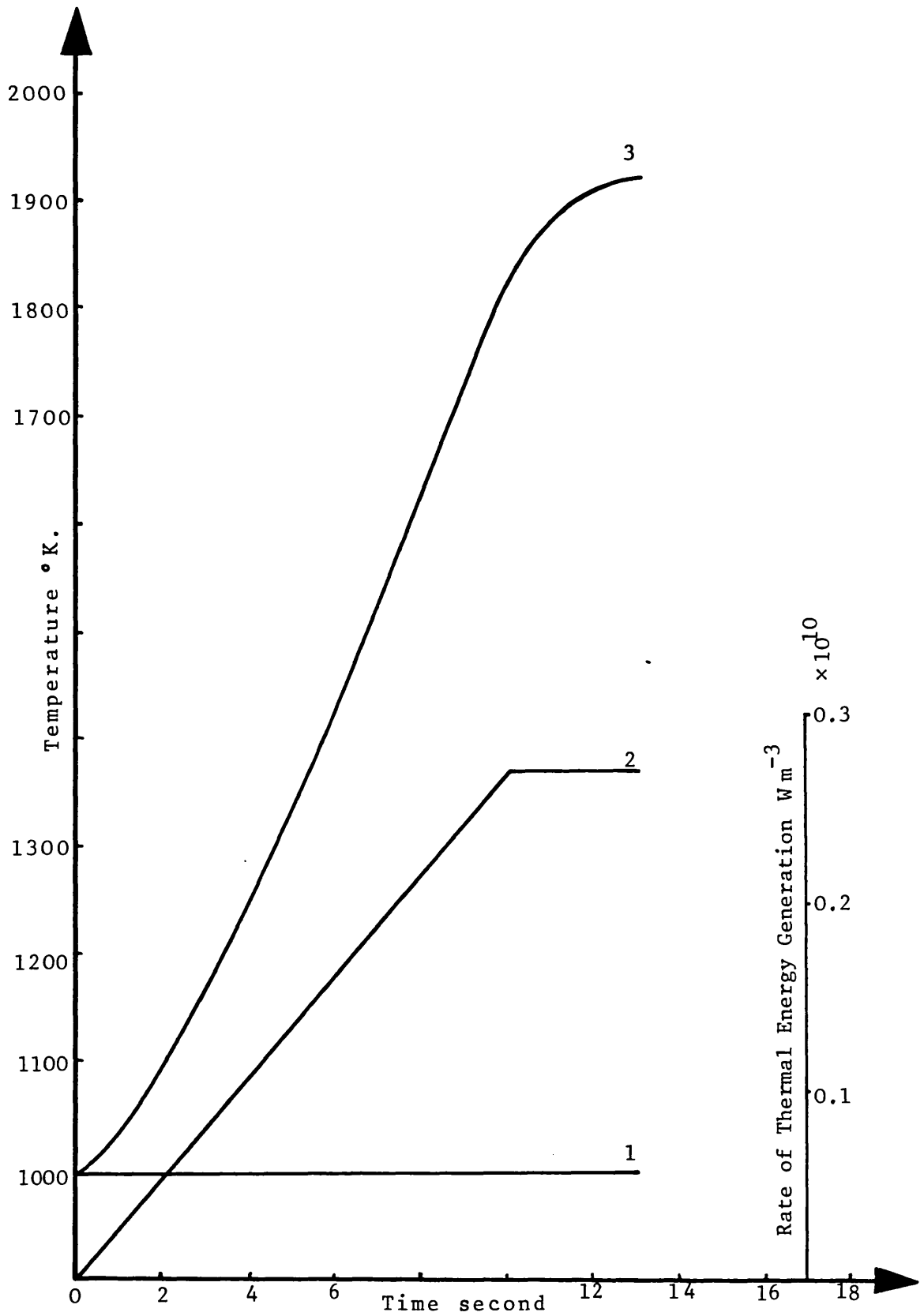
Figure 4.5:

Figure 4.6:

Key to curve numbers:

1. Outer Surface Temperature history
2. Rate of Thermal Energy Generation
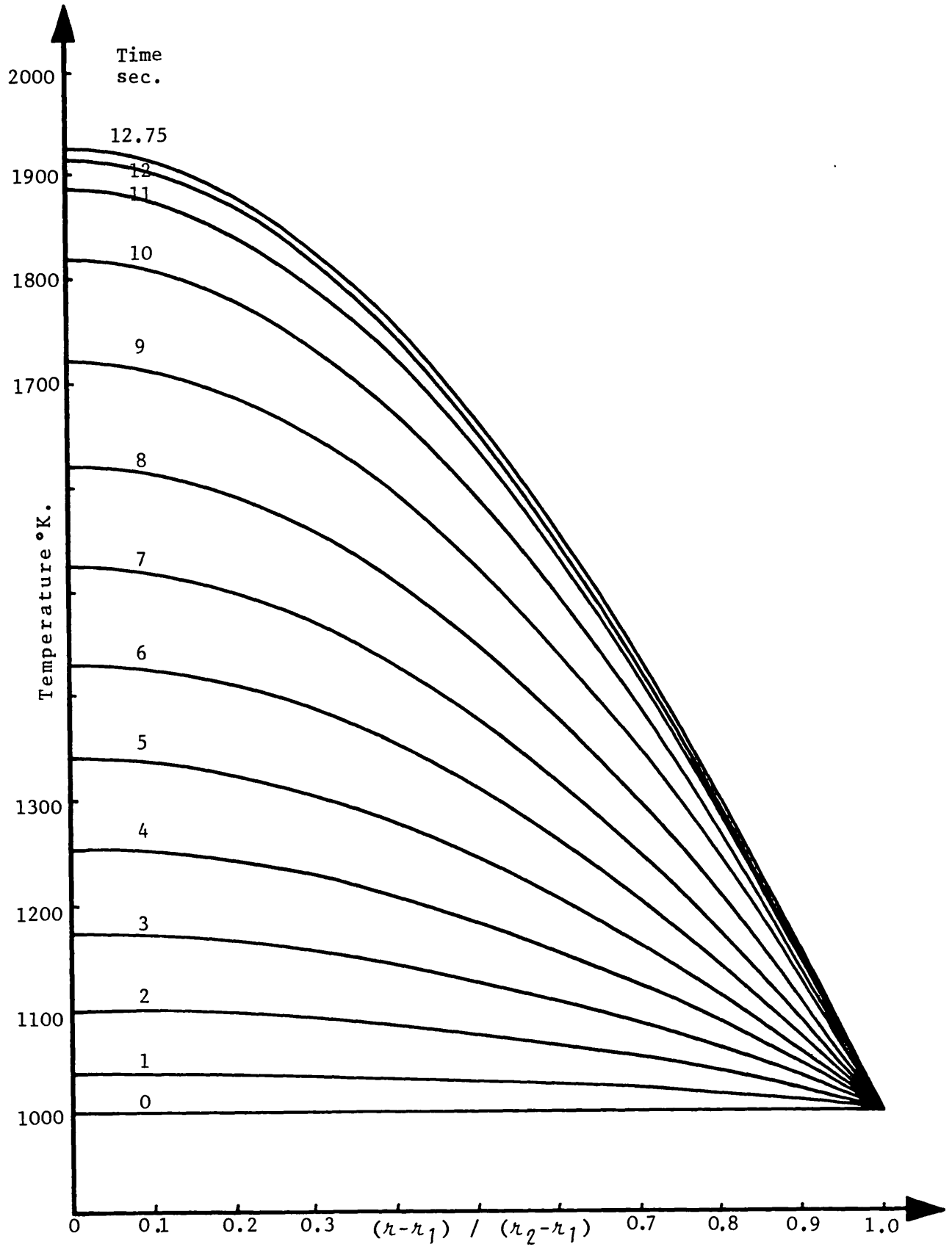3. Inner Surface Temperature history

Figure 4.7:

4.6. In the same figure, the temperature histories of the inner and outer

surfaces of the pellet are shown by curves 3 and 1, respectively. The

steady-state case was approached after 12.75 seconds. The radial

temperature distributions inside the fuel pellet, at some selected time-

nodes, as labelled, are plotted in Figure 4.7. The CPU time used on the

Imperial College CDC 6500 computer to solve this problem was reported to

be 2.126 seconds. The inner surface temperature finally approached

1924.23°K.


### 4.6.2  Application of the Method to a Cooling-down System

The same fuel pellet as that described in Section 4.6.1 is

again considered here. All the conditions are assumed to be axi-symmetric

for all times, therefore, a small sector of the cross-section of the

pellet can be considered for economical reasons (Figure 4.5). The

boundary conditions are prescribed as:


(i) The outer surface is always (for $t_i \leqslant t \leqslant t_\delta$) kept uniformly at

a constant temperature of 1600.0°K.

(ii) The inner surface is always adiabatic.


The pellet is assumed to be initially at equilibrium conditions with the

internal temperature distributions (radial profile), as shown by the curve

labelled $t = 0$ in Figure 4.8. Suddenly, the reactor scrams (the heat

source term suddenly becomes zero), while the boundary conditions remain

unchanged. Time-steps were chosen to be 0.025 seconds and the steady-

state case was approached, in this case, after 4.0 seconds. The radial

temperature profiles at some selected time-nodes, as labelled, are also

plotted in Figure 4.8. The temperature histories of the inner and outer

surfaces are presented in Figure 4.9 by curves labelled 3 and 1,

respectively. In Figure 4.9, the curve labelled 2 represents the volumetric bulk temperature history of the pellet. The volumetric bulk temperature is defined as:

$$BT = (\sum_{e=1,NEL} T_c^e \cdot V^e) / (\sum_{e=1,NEL} V^e) \qquad (4.15)$$

where $NEL$ is the number of elements, $T_c^e$ is the centroid temperature of the element $e$, and $V^e$ is the volume of the element $e$.
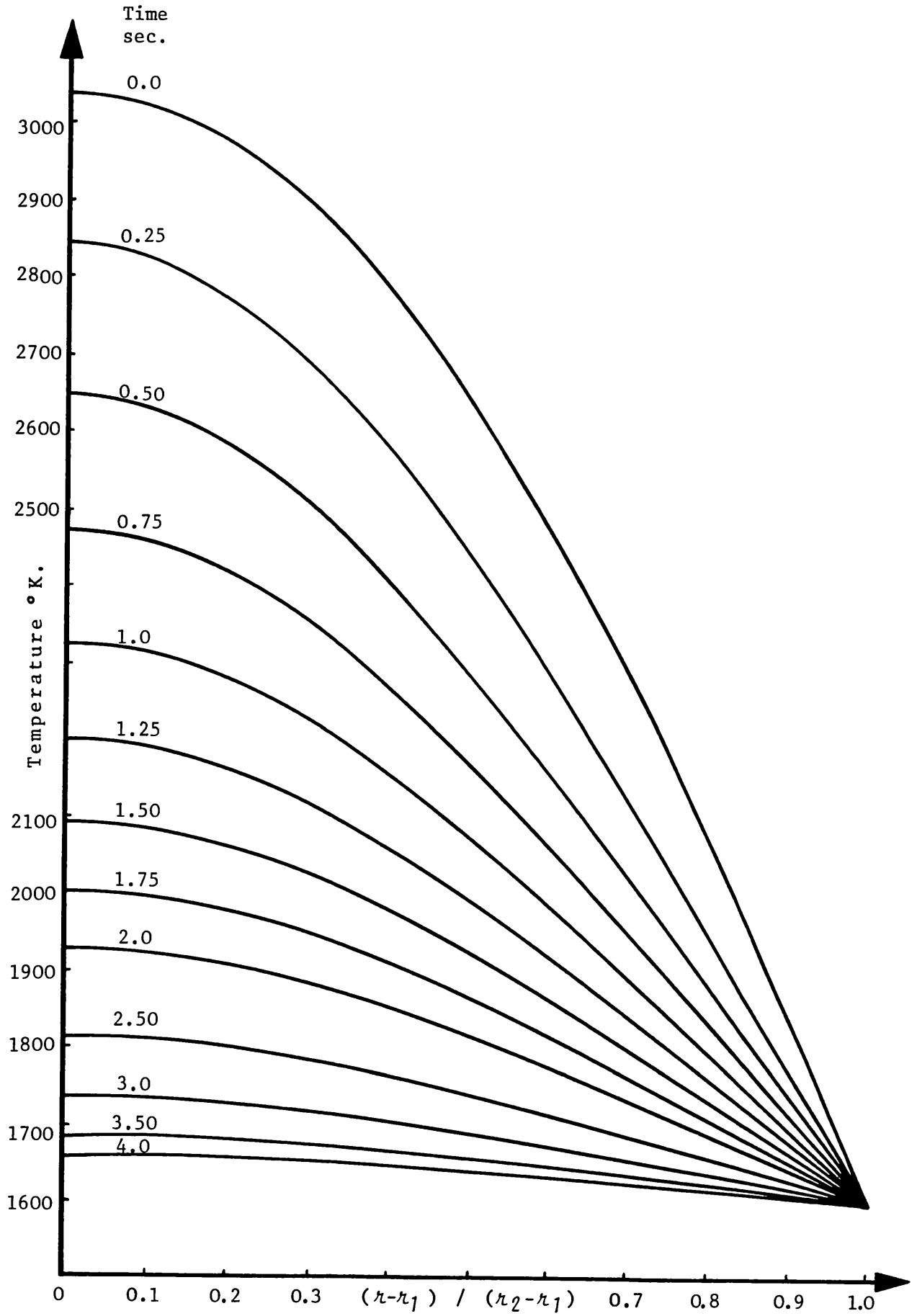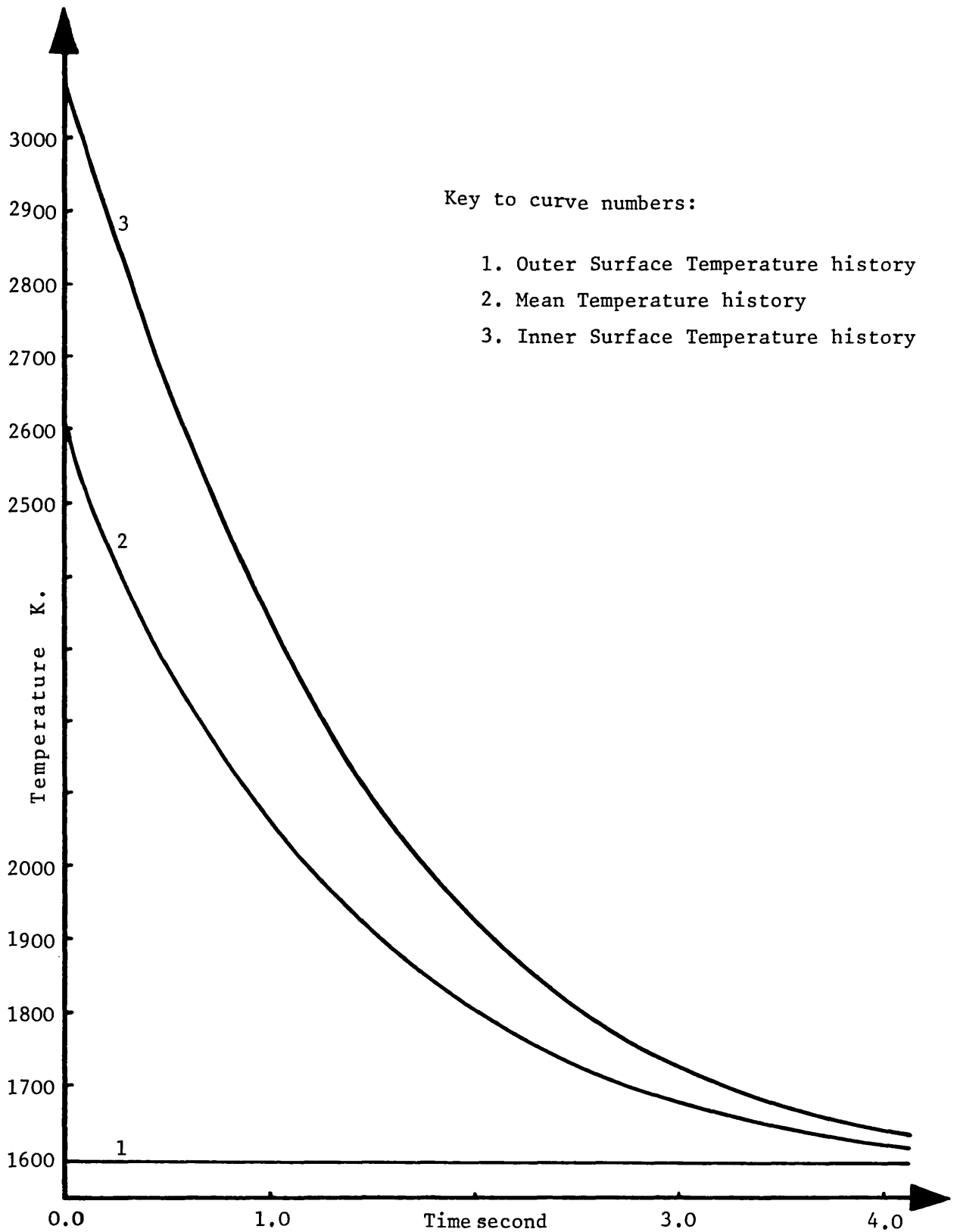
Figure 4.8:

Figure 4.9: Temperature histories just after sudden loss of Thermal
Energy Supplies.

CHAPTER 5

THE STEADY-STATE AND THE TRANSIENT (PHASE-CHANGING) HEAT

CONDUCTION IN A MULTI-PHASE MEDIUM

ABSTRACT

In this chapter, steady-state and transient multi-phase problems
(change of phase) are considered. The problem is generally formulated
such that the latent heat effect is also included. The original mesh is
retained intact and the free boundaries are located using linear
approximation. The original mesh is then refined using the free
boundaries. Due to the lack of reliable data, the method is applied to
some examples for which well-established theoretical ideas are known.
These out-coming are finally compared to show how they are interlinked for
a single case, as must be the case.

5.1 INTRODUCTION

### 5.1.1 The Steady-state and Transient Multi-phase Problems

A multi-phase medium is defined here as a given confined region
in which the material is in two or more phases (with different physical
and thermal properties) and may co-exist in such a way that any two
neighbouring phases meet at an interface. The conduction of heat in such
regions is considered as in the coupled problems (as defined in [4] and
[5]), where:

(i) The material at any point does not change phase in steady-
state problems, hence all the boundaries (interfaces) are
fixed.

(ii) The material, at some points, may change phase in transient
problems, hence the shape and the position of the boundaries

(interfaces) may change with respect to time.

The heat transfer problem is evident in many of today's practical problems in which a change of phase occurs. For example, in the freezing of foodstuffs, in the ablation of missle skins under aerodynamic heating, in welding, and in studies of Nuclear Reactor Accidents.

The serious scientific study of phase-change problems was undertaken as early as 1891 by Stefan, from which the title "Stefan's problem" originated [21]. He started with the investigation of water, but his method has gradually been extended to most other industrial materials. Despite the importance of the topic, very few solutions which may be extended to practical problems have so far been established due to the difficulties.

### 5.1.2  A Brief Review of Previous Studies in Phase-Change Problems

Several disciplines (engineering, physics and metallurgy) are concerned with heat conduction in materials and substances, especially during a change of phase. The prime concern is to evaluate the transient temperature distribution and modes of deforming or transforming the material, while the transformation is taking place. To achieve these objectives, many attempts have been made.

Analytical solutions to the melting of a one-dimensional semi-infinite solid body have been introduced by different investigators; for example, Sadd and Didlake [21] introduced a method which was successfully tested for aluminium. In the same paper, they also made a comparison between various Fourier and non-Fourier type methods in this field. Another analytical solution to the same problem was given by Murray and Huang [22] for the case when the body was initially at its melting point

and the physical and thermal properties in both the solid and liquid states were constant. Muehlbauer and Sunderland [23] also give an analytical solution to the same problem. An important observation they make is that alloys solidify with two jagged phase fronts, which do not necessarily move at the same speed. In this paper, some of the previous work in this field has been reviewed and a useful list of references relevant to this subject was given.

Further analytical solutions to one-dimensional problems concerning fuel plates and rods of reactors have been studied by Lahoud and Boley [24] and some others.

Most of the analytical solutions deal only with the one-dimensional geometry and very special boundary and initial conditions, and also with constant physical properties. Unfortunately, these solutions cannot easily be extended to the more realistic conditions usually applicable to practical problems. Numerical methods have therefore been tried in order to solve some specific problems of this kind. For example, Wellford and Ayer [25] used a numerical method to solve a one-space-dimensional problem with fixed mesh. Another one-space-dimensional variation to the above numerical approach has been studied by Murray [26], in which some of the existing relative solutions have been briefly reviewed, followed by two alternatives to the fixed mesh: "variable space network" and "fixed space network". In both versions, the physical and geometrical changes, and also the change of properties due to the change in temperatures, are ignored while the fusion front progresses. Also, the internal thermal energy sources are not considered.

Hence, a lot of numerical investigation has still to be done, especially with more space-dimensions, with more general initial and boundary conditions, with temperature-dependent properties, and with internal thermal energy sources.

In this chapter, such a general problem in two space-dimensions with any shape of geometry, with any type of initial and boundary conditions, with internal thermal energy sources, and with temperature-dependent properties are formulated. Thermal expansions are assumed to be small, although it must be accounted for in the formulations. The method is applicable to a change of phase in any multi-phase problem and is extendable to a three-space-dimensional method. Finally, a particular application to reactor materials has been chosen as a test case.

### 5.1.3 The Present Work

Heat may be conducted between any two neighbouring phases across their interface. All the points on such an interface have the same temperature (or in the general case, the same potential). Hence, in temperature field problems, each of these interfaces is considered as an "isothermal surface". These problems are, therefore, considered as coupled problems (as mentioned in Section 5.1.1), in which each interface between any two neighbouring phases is an isothermal surface (or a contour).

In transient problems, the temperature may change with respect to time at any point with fixed position, whereas the temperature at any point on an interface (between any two phases) is fixed but its position may then change with respect to time. Thus, the shape and the position of the interface will change with respect to time; in other words, the interface can be considered as a boundary which is free to move. Hence, these types of problems have traditionally been called "free boundary problems" or "moving boundary problems". Accordingly, the interface will be called the "free boundary".

In the proposed method, all free boundaries are located at any time-node and only the elements which are crossed by at least a free boundary are refined (subdivided) such that each element throughout the

mesh is in a single state.

In a pure substance, a phase-change takes place at a precise temperature (for example, solid changes to liquid at a specific temperature which is termed the melting point), whereas in most substances, such as metal alloys, foodstuffs, compositions or impure materials, the transformation takes place over a finite range of temperature. The highest temperature at which a stubstance can be termed solid (the solidus temperature) and the lowest temperature at which a substance can be termed liquid (the liquidus temperature) are usually different. If the temperature of a substance at any point lies between (and including) its solidus and liquidus temperatures, then the substance is said to be in the transition state at that point. Therefore, there are, in general, two free boundaries separating the distinct solid phase and the distinct liquid phase with the transition state in between. The same analysis also applies to liquid to vapour phase-changes, or the reverse transformation.

## 5.2 FORMULATIONS AND TREATMENT OF FIELD VARIABLES OF A MULTI-PHASE PROBLEM

### 5.2.1 A Steady-State Multi-Phase Problem

In general, multi-phase problems would involve a region which, at any time, can be divided into distinct phases. For a medium in the steady-state with solid, transition and liquid states, the system of equations developed in Chapter 3 can be applied using the appropriate physical properties for each element, provided that each element is in a unique state.

In order to solve such a system, the field variables have to be carefully studied. The physical and mechanical properties (for example, the thermal conductivity, $k$) of the substance in different phases vary depending on many parameters, especially on temperature. Each of

these properties is uniformly continuous throughout each phase;

nevertheless, they are, in general, not uniformly continuous at each free

boundary where their derivatives are usually discontinuous. Furthermore,

the temperature distribution is continuous throughout the region of

interest, because any of the two neighbouring phases are assumed to be in

perfect contact with each other. Although the temperature gradient (or

heat flux) is continuous throughout each phase, but is discontinuous at

each free boundary. Therefore, to solve the problem for temperature,

each free boundary has to be located carefully and the values of the field

variables ($k$, $Q$, etc.) have to be specified everywhere within each phase.

Much research has been done on the properties of materials in

both the solid and liquid states, but experimental work regarding these

properties in the transition state has lagged behind. Whilst these

properties are not well-established, in order to keep the continuity a

simple continuity hypothesis may be applied to a linear approximation in

the transition region as follows.

Let $\phi$ be a scalar property of a material. Then, in the

transition state, it may be approximated by $\phi_T$ at temperature $T$ (between

the solidus and the liquidus temperatures), which can be expressed as:

$$\phi_T = \phi_s + \left(\frac{\phi_\ell - \phi_s}{T_\ell - T_s}\right) \cdot (T - T_s) \tag{5.1}$$

where subscripts $s$ and $\ell$ refer to the values at the solidus and the liquidus

temperatures, respectively.

For example, the thermal conductivity of a material may obey

such an approximation, over the transition state, which can be shown

schematically as the curve labelled $k$ in Figure 5.1. Therefore, the

thermal conductivity of a material can be shown as a continuous function

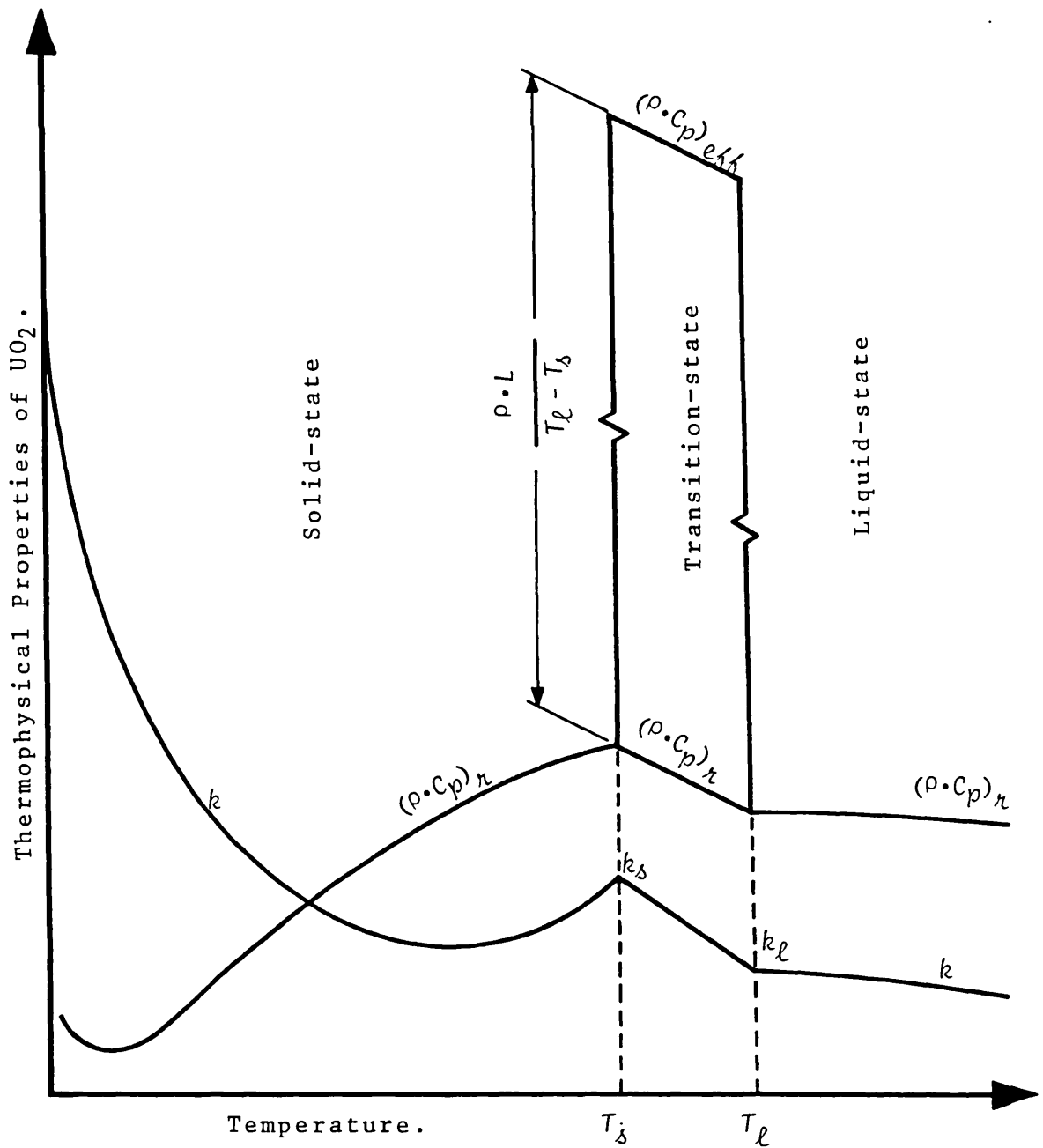of temperature throughout the solid, transition and liquid states, as

Figure 5.1: Schematical Variations of Thermal Conductivity ($k$) and Thermal Energy Capacity ($\rho \cdot C_p$) of $UO_2$, over Solid, Transition and Liquid states versus Temperature. See also Table 5.1.

shown in the same figure.   If, of course, convection within the liquid region is not negligible, then an effective thermal conductivity in the liquid region may be defined, which accounts for both convection and conduction of heat.


### 5.2.2  A Transient Multi-Phase Problem

In a transient multi-phase problem, the free boundaries would move with respect to time, but at any instant the whole region of interest can be divided into distinct zones of unique states.   Thus, for example, for a medium with solid, transition and liquid states, all the governing equations would be similar to those developed in Chapter 4, except for the regions (elements) which are in the transition state, where the equations would have an additional term representing the latent heat effect.   This can be denoted by a generalised matrix functional $[L]$ whose actual form will be discussed later (see Section 5.2.3).   Therefore, the governing equation can be written as:

$$[K] \cdot \{\theta\} + ([C] + [L]) \cdot \{\frac{\partial \theta}{\partial t}\} + \{F\} = 0 \qquad (5.2)$$

This equation can be shown as:

$$[K] \cdot \{\theta\} + [C_{eff}] \cdot \{\frac{\partial \theta}{\partial t}\} + \{F\} = 0 \qquad (5.3)$$

where $[C_{eff}]$ is defined as the "effective heat capacity matrix", such that:

$$[C_{eff}] = [C] + [L]$$

Now, all the analysis developed in Chapter 4 can be applied using the new effective heat capacity matrix.   Hence, the final system of

equations will look like equation (4.7), in which the matrix $[C]^e$ is replaced by $[C_{eff}]^e$ (see equation (4.10)). This can be shown as:

$$[C_{eff}]^e = (\rho.C_p)^e_{eff} . \iiint_{V^e} [N]^T . [N] . dV \tag{5.4}$$

where the effective heat capacity of an element $e$ can be written as:

$$(\rho.C_p)^e_{eff} = (\rho.C_p)^e + (\rho.L_f)^e \tag{5.5}$$

where $L_f$ is a scalar elemental functional which is explained later (see Section 5.2.3).

For the field variables, all the analysis of Section 5.2.1 for the steady-state case can still be applied here. For instance, the real heat capacity $(\rho.C_p)_h$ also obeys the same approximation as equation (5.1) over the region of the transition state, as can be shown schematically by the curve labelled $(\rho.C_p)_h$ in Figure 5.1. Thus, the real heat capacity will vary continuously with respect to temperature throughout the solid, transition and liquid states. In order to obtain a similar formulation using the effective heat capacity, the latent heat effect needs to be studied first.

### 5.2.3   The Study of the Latent Heat Effect

In a phase-change process, any transformation is accompanied by either absorption or liberation of latent heat (for example, melting or solidification, respectively). For a given amount of heat (liberated or absorbed), when the temperature reaches a phase-change temperature, a transformation begins and some of the exchanged heat will effectively change the internal thermal energy (the enthalpy) of the system, while the transformation is in progress. In a pure substance at a specified

temperature, a transformation takes place when all the exchanged heat is used up for the latent heat and there is no change in temperature. In an impure substance (alloys, for example) over a range of temperature $(T_1$ to $T_2)$, a transformation takes place when part of the exchanged heat is used up for the change of temperature and the rest is for the latent heat. The latter can be approximated by spreading the latent heat effect uniformly over the range of temperature (transition temperature interval). Hence, the elemental functional $L_\delta$ in equation (5.5) may be written as:

$$L_\delta = \begin{cases} 0 & \text{for} \quad T \leqslant T_1 \\ \dfrac{L}{T_2 - T_1} & \text{for} \quad T_1 \leqslant T \leqslant T_2 \\ 0 & \text{for} \quad T_2 \leqslant T \end{cases} \tag{5.6}$$

where $L$ is the latent heat.

In the problems which involve pure substances, $T_2$ is almost equal to $T_1$ which makes this functional very large. For numerical purposes, a very small range of temperature can be introduced. This approach has already been successfully employed by Comini and Del Guidice [7], and Bonacina and Comini [27].

Therefore, using equations (5.5) and (5.6), the effective heat capacity can be written as:

$$(\rho \cdot C_p)_{eff} = (\rho \cdot C_p)_r + 0 \qquad \text{out of the transition state} \tag{5.7a}$$

and

$$(\rho \cdot C_p)_{eff} = (\rho \cdot C_p)_r + \frac{\rho \cdot L}{T_2 - T_1} \qquad \text{over the transition state} \tag{5.7b}$$

where the real heat capacity $(\rho.C_p)_{\hbar}$ varies continuously with respect to temperature throughout the subsequent states. Of course, in general, if the real heat capacity is not well-established over the transition state, it can be approximated by a relation like (5.1), for example (see Figure 5.1). Whereas the effective heat capacity varies in a discontinuous manner such that the effective heat capacity over the transition state only becomes as a combination of the real heat capacity (equation (5.1)) and a component which represents the latent heat effect. Hence, equation (5.7b) can be written as:

$$(\rho.C_p)_{eff} = (\rho.C_p)_s + (\frac{(\rho.C_p)_\ell - (\rho.C_p)_s}{T_\ell - T_s}) \cdot (T - T_s) + \frac{\rho.L}{T_\ell - T_s} \qquad (5.8)$$

where $L$ is the latent heat for melting or solidification.

## 5.3 LOCATION AND APPLICATION OF FREE BOUNDARIES

### 5.3.1 The Mesh and its Refinement

A normal finite element mesh used for a one-phase problem is termed here as an original mesh. The conditions which a given mesh must obey were discussed in Sections 1.7, 2.3.2 and 4.1. Those conditions were very general and are applicable to most problems solved by the finite element method. Thus, for convenience and uniformity, the original mesh is retained intact throughout the analysis and is used effectively for multi-phase problems within the same framework of the finite element method as used for the one-phase problems. Hence, the same formulations can be generalised for all kinds of heat conduction problems (including transient multi-phase (phase-change) problems).

Previously, some different methods were proposed to deal with the multi-phase elements, although those methods were mostly restricted and too difficult to implement in practice. However, a one-dimensional

numerical method was proposed in which a free boundary was located and then the whole mesh was regenerated effectively as two separate solution domains (like coupled problems) on either side of the free boundary with a previously prescribed number of nodes on each side [26]. This method has an advantage that no new mathematical modelling is needed since each element is in a unique phase, whose properties can be clearly defined. However, if the free boundary is too close to any outer boundary, one could have too many points close together on one side of the free boundary, thus storing some unnecessary details, while having few points on the other side of the free boundary, hence possibly losing some essential details.

In this work, this problem with any number of free boundaries has been tackled very effectively by using the original mesh, which is refined only over the elements that are crossed by the free boundaries, such that each portion of a free boundary is then replaced by a boundary of an element (a party boundary common between two elements) and, therefore, each element is now entirely in a single phase. The physical properties of each element can thus be clearly defined or approximated as explained in Section 5.2. Therefore, the whole formulation developed here so far is applicable hereinafter just as before.

### 5.3.2 A General Numerical Method for Location of Free Boundaries

Here, a general method is proposed to locate the positions of each free boundary. The method can be applied to most numerical algorithms. This is done simply by identifying the state of each point of the solution-domain by its temperature. Then each point (B) is examined in turn within a small neighbourhood of a given point (A). If the neighbourhood point B is in the same phase as point A, then, since we are considering a small neighbourhood, it can safely be assumed that all the points on the line joining A and B are also in the same phase. Hence,

no free boundary crosses this line AB. Further, if all such B points in the neighbourhood are in the same phase as point A, then it may be said that the whole neighbourhood is also in that phase.

Whereas, if any two such points (A and B) lie in any two different but neighbouring phases, then there is only one free boundary passing between these two points. Thus, the free boundary crosses the line joining points A and B at a point I, which is termed here as the "interface point" or the "interface-node". This point has to be located by some interpolation.

Let us consider two such points (A and B) that are in two neighbouring phases. Let them be distance $\ell$ apart (see Figure 5.2) and their temperatures be some known values, $T_A$ and $T_B$, respectively. For this pair of points, the interface point (I) may be located by a linear interpolation as:

$$x = \ell \cdot \frac{T_I - T_A}{T_B - T_A} \tag{5.9}$$

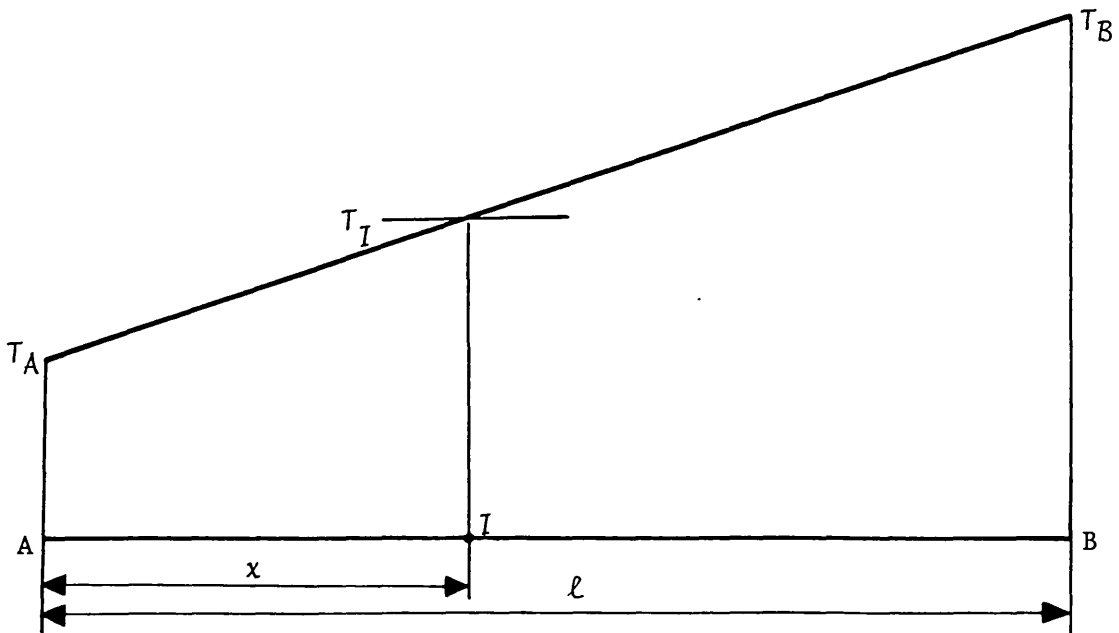where $T_I$ is the temperature of the free boundary passing point I, and $x$ is measured from point A.



Figure 5.2

This is repeated for all points B in the neighbourhood of point A. The free boundary in the neighbourhood of A is then the locus of all such interface points (I). This is therefore applied to all the neighbourhoods of points A in the solution domain. Then, since the union of these finite number of neighbourhoods should be the whole solution-domain, each free boundary is obtained by the union of all the corresponding free boundaries of each neighbourhood. Depending on the method used, one can select convenient points on each free boundary that are most useful in the calculations. A more accurate free boundary is, of course, obtained for smaller neighbourhoods.

If the problem is solved over a large region using relatively few points (nodes), then the neighbourhoods also have to be correspondingly larger. Therefore, there is also a possibility that more than one free boundary may pass through a neighbourhood. If any pair of such points (A and B) lie in any two different but not neighbouring phases, then there are two or more free boundaries passing between these two points. Hence, the line joining them (AB) is crossed by more than one interface. To locate these interfaces (free boundaries) between these two points (A and B), a similar procedure to that explained for equation (5.9) may be used again. This is formulated as follows.

Let us consider such a pair of points (A and B), a distance $\ell$ apart. Let A and B be $n$ phases apart on an ascending temperature scale. Then there will be $n$ distinct free boundaries passing in between these two points. The line joining A and B is then crossed at $n$ distinct interface points $I_K$ ($K = 1, \ldots, n$) by these free boundaries. The distance $x_K$ from A on line AB of the interface point $I_K$ can be calculated by a linear interpolation formula as:

$$x_K = \ell \cdot \frac{T_K - T_A}{T_B - T_A} \qquad (5.10)$$

where $T_K$ is the prescribed temperature of the particular $K$th free boundary (see Figure 5.3). As before, the $K$th free boundary passes through the locus of all the interface points $I_K$.
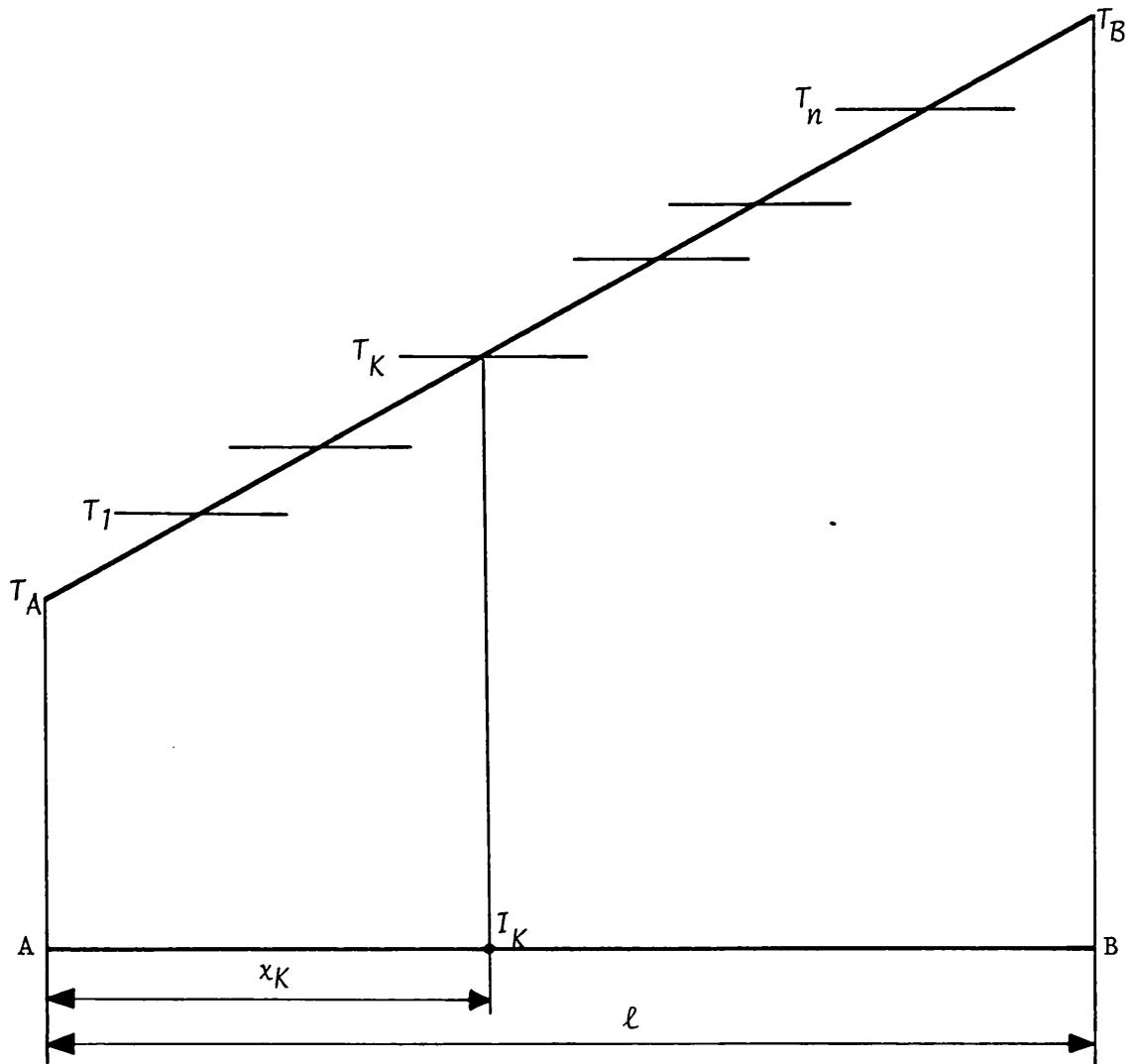


Figure 5.3

For example, let point A be in the solid state and point B be in the liquid state of a material, where a transition state exists in between. The line joining A and B will be crossed by the solidus interface at the solidus interface point, $I_s$, and by the liquidus

interface at the liquidus interface point, $I_\ell$. These points ($I_\delta$ and $I_\ell$) can be located by using equation (5.10) as:

$$x_\delta = A\,I_\delta = \ell \cdot \frac{T_\delta - T_A}{T_B - T_A} \tag{5.11a}$$

and:

$$x_\ell = A\,I_\ell = \ell \cdot \frac{T_\ell - T_A}{T_B - T_A} \tag{5.11b}$$
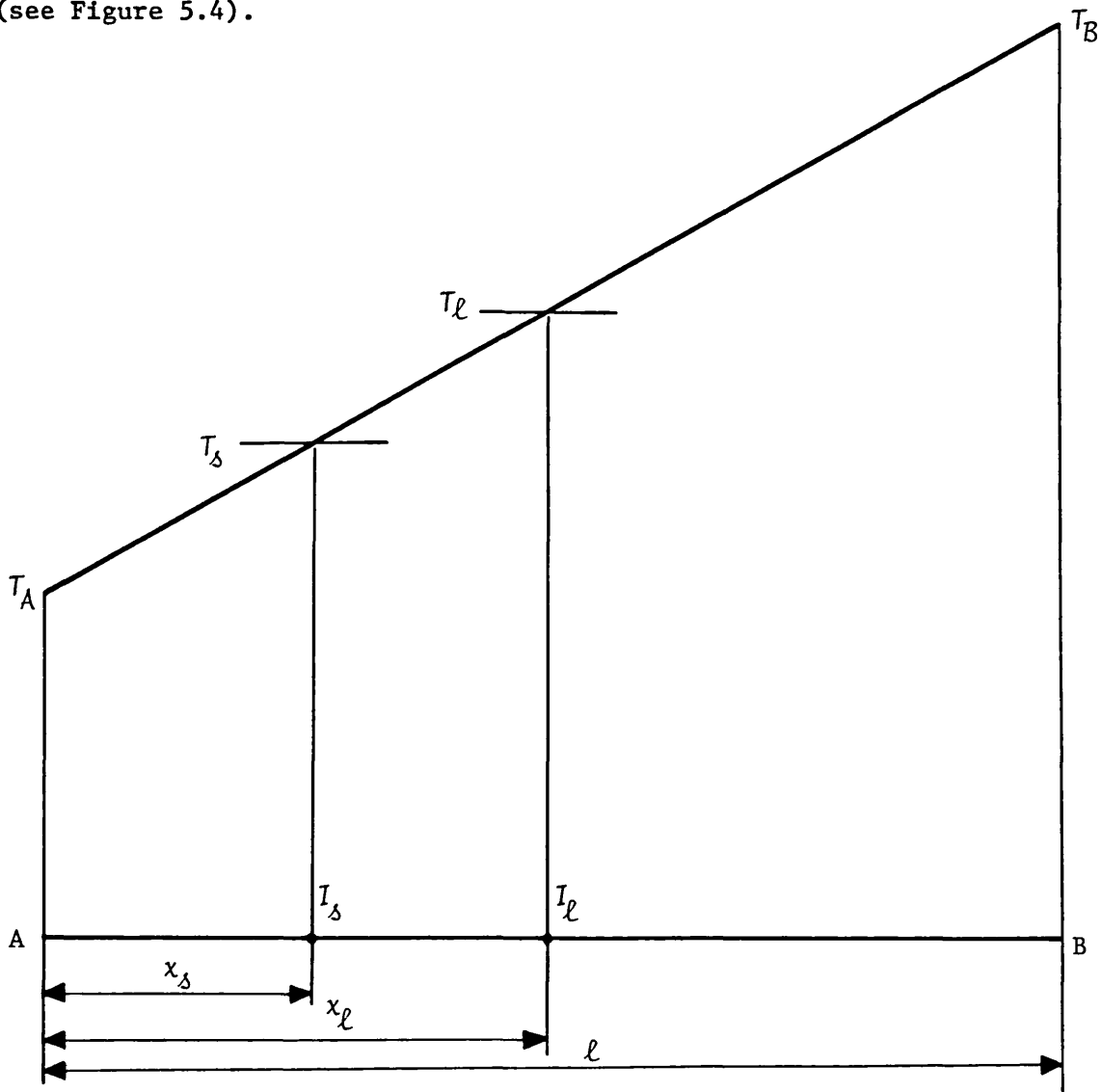
(see Figure 5.4).



Figure 5.4

### 5.3.3 Location of Free Boundaries in the Finite Element Framework

In the finite element framework, the solution domain is replaced by a number of finite elements. For the nodes that are entirely in any particular element, the neighbourhood is taken to be the element itself. For the nodes that are at the vertices, the neighbourhood is subdivided by the boundaries of the elements. Each portion is taken to overlap the entire element, for which the node is a vertex. Hence, each element can be considered as whole or part of a neighbourhood for the nodes and vertices of itself. All the neighbourhoods will therefore be accounted for as the nodes and vertices of each element are examined. Thus, the ideas discussed in Section 5.3.2 can now be applied here. We can look at all the possible different pairs of nodes (vertices) for each element and obtain the interface-nodes wherever applicable for each pair. However, realistically, we do not need all these interface-nodes because of the modelling used to formulate the governing equations and the information will not improve the accuracy. The interface-nodes inside the element are not very useful (unless an individual problem requires otherwise). We only need to consider the intersections of a free boundary with the boundaries (sides) of the element in question. This yields only the interface-nodes on the boundaries of the element which are later used to subdivide the element (refinement).

Therefore, in brief, we simply need to examine the boundaries of each element of the original mesh and locate the position of the interface-nodes on the element boundaries. The analysis described in Section 5.3.2 can now be applied easily to each boundary of each element. Each element boundary links two vertices whose states are examined by their temperatures. If they are both in the same phase, then no free boundary crosses this element boundary. This is not detected only in an exceptional case when a U-shaped interface crosses one element boundary at

two points, in which case either finer elements or longer time-steps are advised. If one vertex (node) is in one phase and the other (at the other end of an element boundary) is in a neighbouring phase, then there is only one free boundary which crosses this element boundary. Hence, there is only one interface-node on the element boundary which may be located using equation (5.9). If one vertex (node) is in one phase and the other is in another phase, but not the neighbouring phase, then there is more than one free boundary crossing the element boundary. In such cases, of course, there is more than one interface-node on the element boundary which may be located using equation (5.10). In the case of just two interfaces, equations (5.11) can be used.

An element may be classified according to the number of free boundaries (interfaces) that cross it, or by the number of phases that occupy it. Single-phase, two-phase or multi-phase elements are said to be the elements occupied by one, two or several phases, respectively.

### 5.3.4 Application of the Free Boundaries to Refine the Original Mesh

A refined mesh is obtained using the original mesh (as a base) and all the interface-nodes obtained by using the method explained in Section 5.3.3. Any set of interface-nodes (free boundary) from the previous iteration can be discarded (except in the first iteration) and can be replaced by the new set. The new interface-nodes of equal temperature may be joined by straight lines (linear approximation) to represent a new set of approximate free boundaries. These are used to generate a new refined mesh.

A one-phase element, which is entirely in a single-phase, is obviously not refined at all. The finite element formulations for such an element are applicable as before. A two-phase element, which is crossed by one interface, has two interface-nodes at the same temperature

on the element boundaries. These are joined to subdivide the element into two parts (Figure 5.5). Each sub-element is now in a single phase and the same finite element formulations are applicable in principle as before.



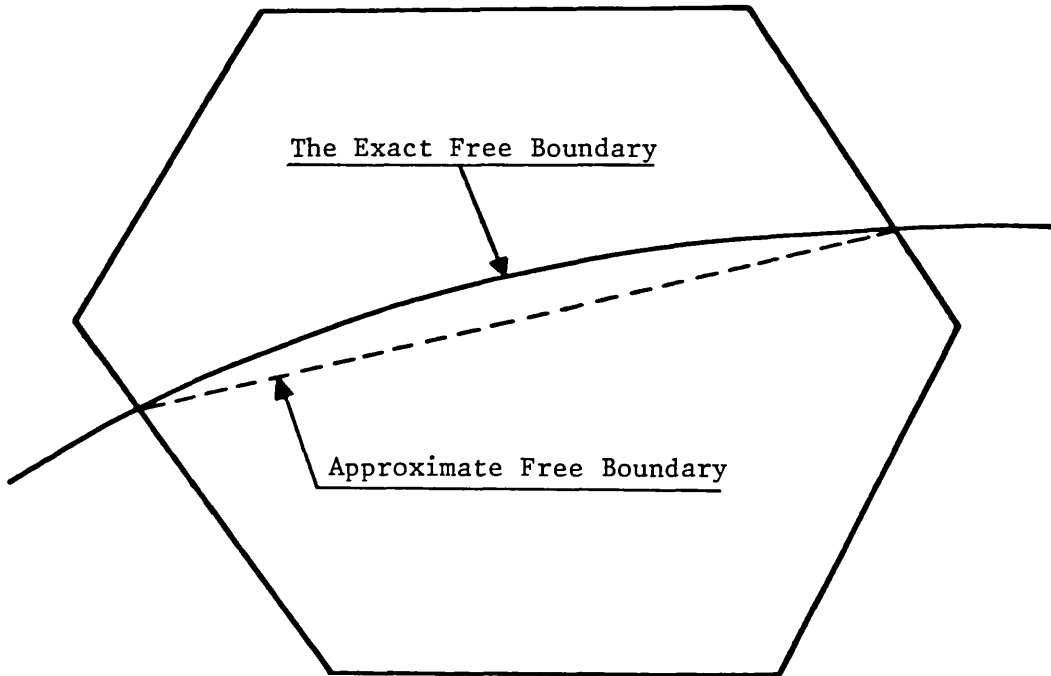The Exact Free Boundary

Approximate Free Boundary

Figure 5.5: Refinement of a Two-phase Element

A multi-phase element, which is crossed by more than one interface, has a number of equal temperature pairs of interface-nodes. These are jointed to subdivide the element into a number of sub-elements, each of which is now in a single phase, to which the same finite element formulations are applicable as before (Figure 5.6). If, in an element, there were more than one pair of equal temperature interface-nodes, then these points have to be joined carefully, such that none of the free boundaries cross each other. Each sub-element is now, again, in a single phase and, as before, the finite element formulations are applicable in principle.

In practice, however, there may be some additional restrictions due to the computer code. For example, the code may restrict the mesh to
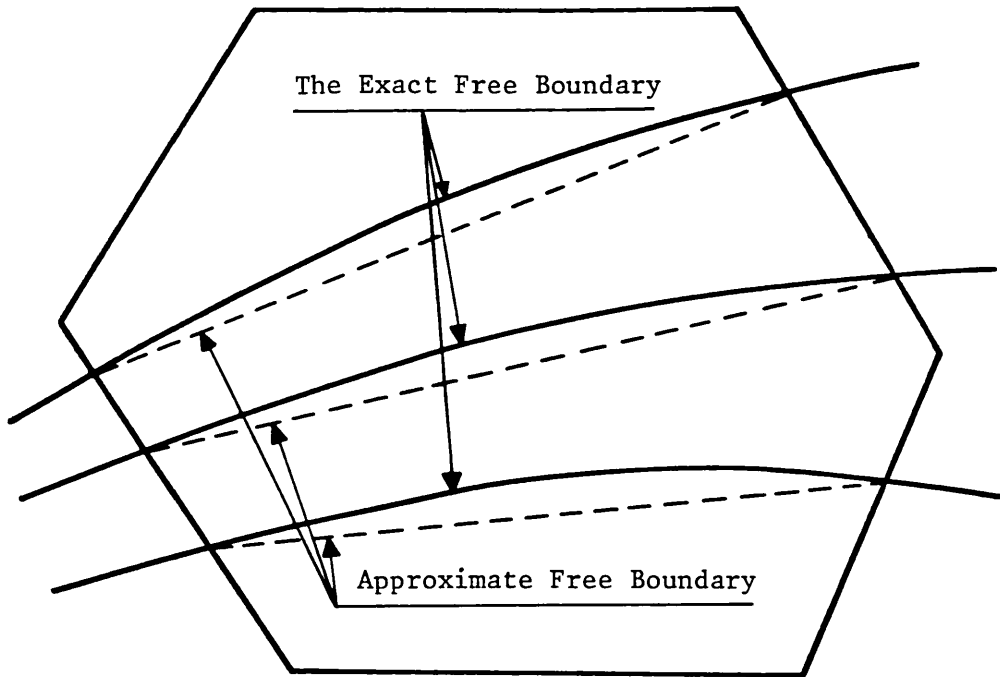
Figure 5.6: Refinement of a multi-phase element

triangular elements only, as was the case in this work.

For a two-phase triangular element, the above description yields a triangular sub-element and a quadrilateral sub-element. The latter has to be further subdivided into two triangular sub-elements to satisfy the computer code, namely, the element is finally subdivided into three triangular sub-elements. Similarly, for a three-phase triangular element, the method yields:

(i) A triangular sub-element and two quadrilateral sub-elements if only two sides of the element are crossed by the two free boundaries.

(ii) Two triangular sub-elements and one pentagonal (five-sided) sub-element if all the three sides of the element are crossed by the two free boundaries.

Generally, the element is finally, in both cases, subdivided into five

triangular sub-elements.  This further subdivision is easier to include

into well-tested codes (for triangular elements) than to write correct or

alternative codes to incorporate a multi-sided element.

The problem can now be solved over the new refined mesh and

new temperatures are obtained at all the nodes of the original mesh and

also at the interface-nodes.  If the temperatures thus obtained at the

interface-nodes do not coincide with the corresponding free boundary

temperature(s), the process is repeated (from Section 5.3.3 onwards) until

they coincide (correspondingly).  Then this is the required solution for

a steady-state problem.  In order to reduce the computing time, a

criterion (tolerance) may be introduced to check the proximity of the

calculated temperatures at the interface-nodes and the corresponding

interface temperature(s).  If the absolute differences are less than the

tolerance, the solution is acceptable and the execution is terminated.

For a transient problem, this is a solution to the problem at a particular

instant, usually at a time-node, and then we move on to the next time-node

in the usual manner.  The whole process is repeated at all the time-nodes.

In this way, no extraordinary or new models are needed.  The

storage is also used very economically and the overall accuracy is kept

nearly uniform by the use of the same formulations.  Moreover, by this

method, the same computer code is used for the transient multi-phase

problems just as efficiently as for the steady-state single-phase problems.

In the solutions to the transient problems, particularly when a

change of phase takes place, large gradients in the properties of the

material may emerge.  Therefore, large steps (intervals) both in time and

space dimensions can lead to oscillatory solutions.

## 5.4 APPLICATION OF THE PROPOSED METHOD TO SOME MULTI-PHASE EXAMPLES

### 5.4.1 Application of the Method to a Transient Two-Phase Example

The method described in this chapter is, in general, applicable to a wide range of both steady-state and transient multi-phase problems (Sections 5.2.1 and 5.2.2, respectively). In order to validate this method, much effort had been made but without success because reliable data (experimental or otherwise) were not available. Nevertheless, the method is applied here to a selected example and its performance is thus examined over three different viewpoints for which well-established theoretical ideas exist. These are:

(i) The variation of temperature with respect to time (temperature history) at any fixed point within the solution-domain.

(ii) The variation of the shape and position of each free boundary with respect to time (position history).

(iii) The temperature distribution at any time within the solution-domain.

The curves representative to these aspects are then plotted. Finally, a comparison is made among these curves to show how they are interlinked.

Let us assume that the same fuel pellet of an LMFBR as the one chosen in Chapters 3 and 4 is so overheated that its cross-section (the solution-domain) has attained two different phases (solid and transition, in this case). The geometry of the pellet is still tubular (axi-symmetric) with internal and external radii being 0.00114 and 0.00254 m, respectively, as before. All the physical, geometrical and thermal properties in the solid state are as used in Chapters 3 and 4; these are given in Table 5.1. In the same table, these properties are given in the liquid state as well as the ways of their approximation used here.

## TABLE 5.1

### The Physical Properties of UO$_2$ Used in This Section ([11], [28], [29], [30] and [31]) (see also Figure 5.1)

| Property \ State | Units | Solid | Transition | Liquid |
|---|---|---|---|---|
| Density, $\rho$ = | kg/m$^3$ | $$\frac{10970.0}{(1 + 9 \times 10^{-6} \times T_c + 6 \times 10^{-9} \times T_c^2 + 3 \times 10^{-12} \times T_c^3)}$$ | Approximated by equation (5.1) | $$\frac{8740.0}{[1.0 + 1.045 \times 10^{-4} \times (T_K - T_\ell)]}$$ |
| Specific Heat, $C_p$ = | J/kg°K | $$47.445 + 0.1985 \times T_K + \frac{1.1532 \times 10^7}{T_K^2}$$ | Approximated by equation (5.7b) | 520.0 * |
| Thermal Conductivity, $k$ = | W/m°K | $$6.9 \times 10^{11} \times T_K^3 + \frac{1}{(0.042 + 2.71 \times 10^{-4} \times T_K)}$$ | Approximated by equation (5.1) | $$\frac{0.625 + 1.38 \times 10^{11} \times T_K^3 + 0.2}{(0.042 + 2.71 \times 10^{-4} \times T_K)}$$ ** |

Solidus temperature = 3060.0°K *  
Liquidus temperature = 3065.0°K *

Latent heat, $L$ = 2.75 × 10$^5$ J/kg *  
Expansion coefficient = 0.0 *

* Different values are given in the literature, but these values are used here.
** The value adopted here is due to lack of data.

The pellet is assumed to be initially at equilibrium conditions, such that the rate of thermal energy generation is $0.27 \times 10^{10}$ W/m$^3$. The outer surface is always kept at a uniform temperature ($T_2$ = 1600°K), while the inner surface is assumed to be always adiabatic, as before. The initial radial temperature distribution within the pellet is shown by curves labelled $t_i'$ in Figures 5.7 and 5.8, where the inner surface temperature (3058.85°K) is just under the melting point (3060°K).

Suddenly, due to misoperation of course, the rate of thermal energy generation is assumed to increase to $0.594 \times 10^{10}$ W/m$^3$, while the boundary conditions are assumed to be unchanged.

The problem is now entirely axi-symmetric and just a sector of the cross-section is enough to be considered, thus saving in the computation time. A mesh with 10 nodes in the radial direction, as shown in Figure 5.9, is used. Although this particular (axi-symmetric) example can be solved as a one-dimensional problem, but more general problems are not always axi-symmetric. Therefore, the proposed two-dimensional method has been used here just to demonstrate its behaviour and performance, but it must be noted that this method is very general and is capable of dealing with many problems of this nature.

The problem is solved here using the general equation (4.7) for $\lambda$ = 1.5. Figure 5.10 shows the temperature history of (a fixed point on) the inner surface of the pellet; there is shown that the inner surface temperature rises while the whole pellet remains in the solid state. As the temperature of the point in question exceeds the material solidus temperature (just after time $t_a$ in the same figure), the rate of temperature rise drops sharply but without any oscillation (see Figure 5.10 about point (A) of discontinuity). This is expected because, for the point which is going to melt, the governing equation now changes to
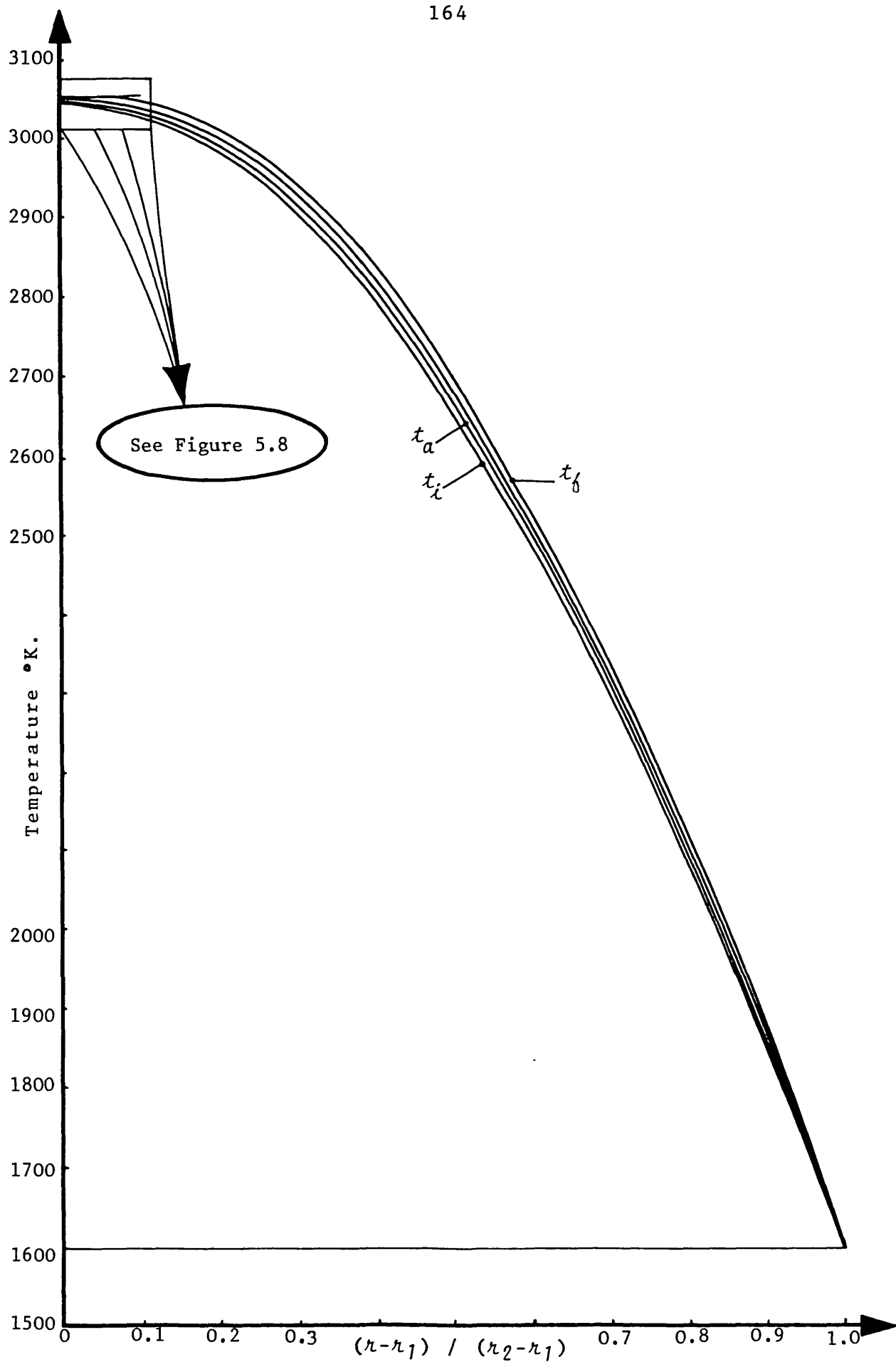
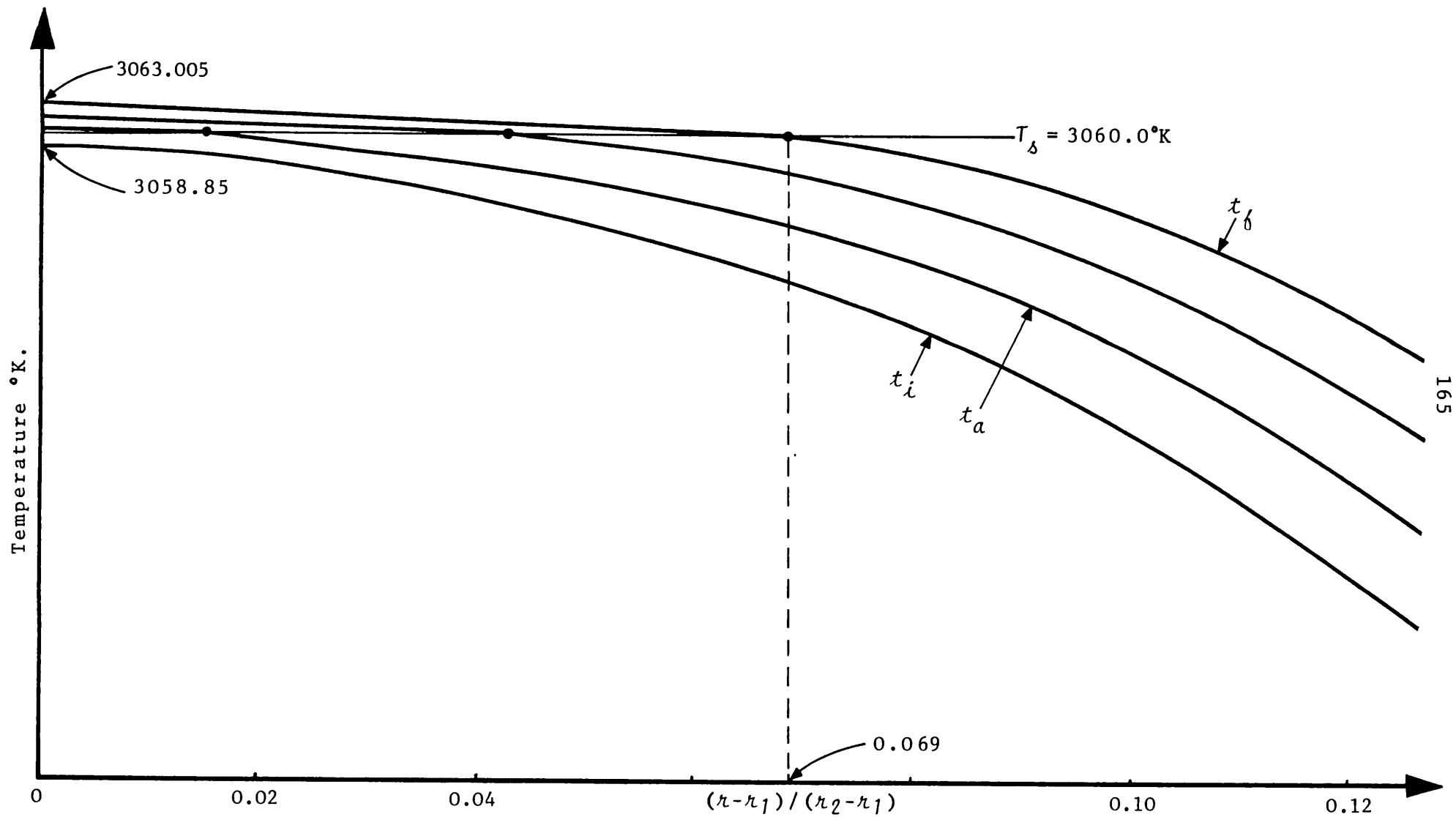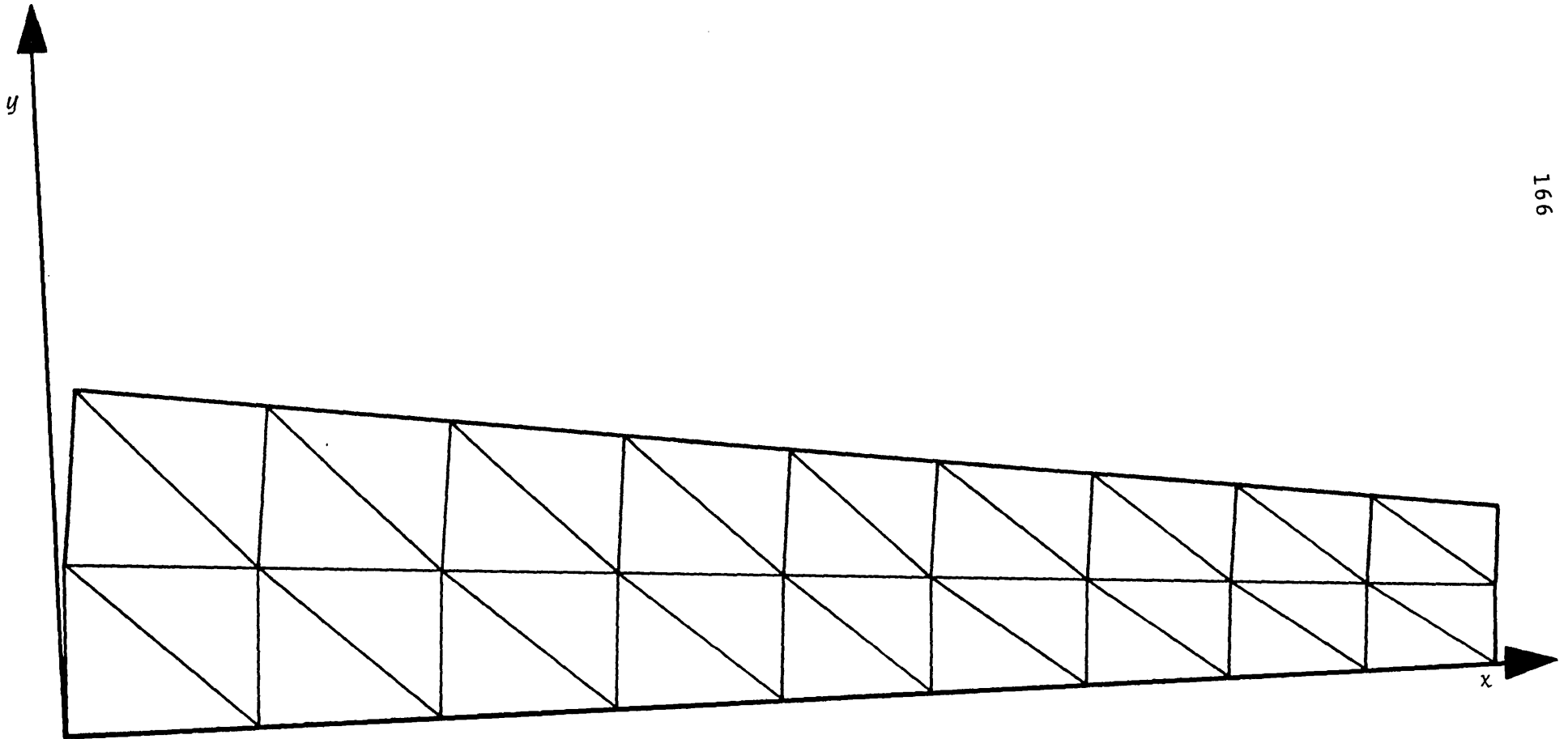Figure 5.7: Radial Temperature Profiles
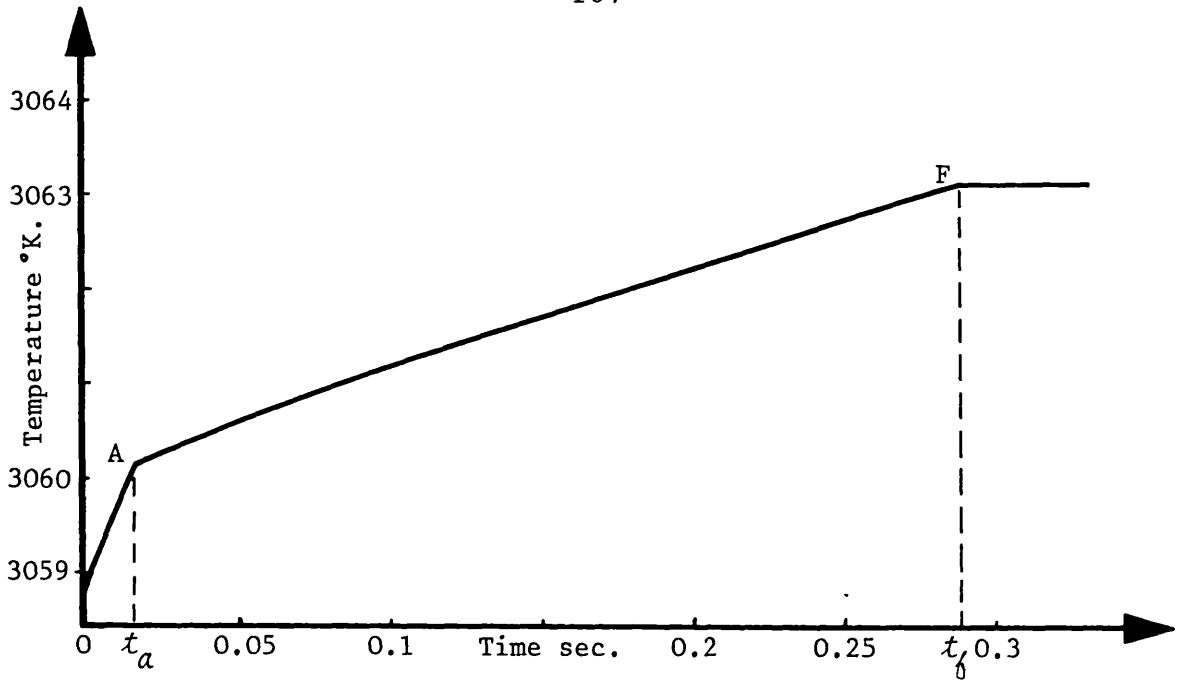
Figure 5.8:

Figure 5.9:

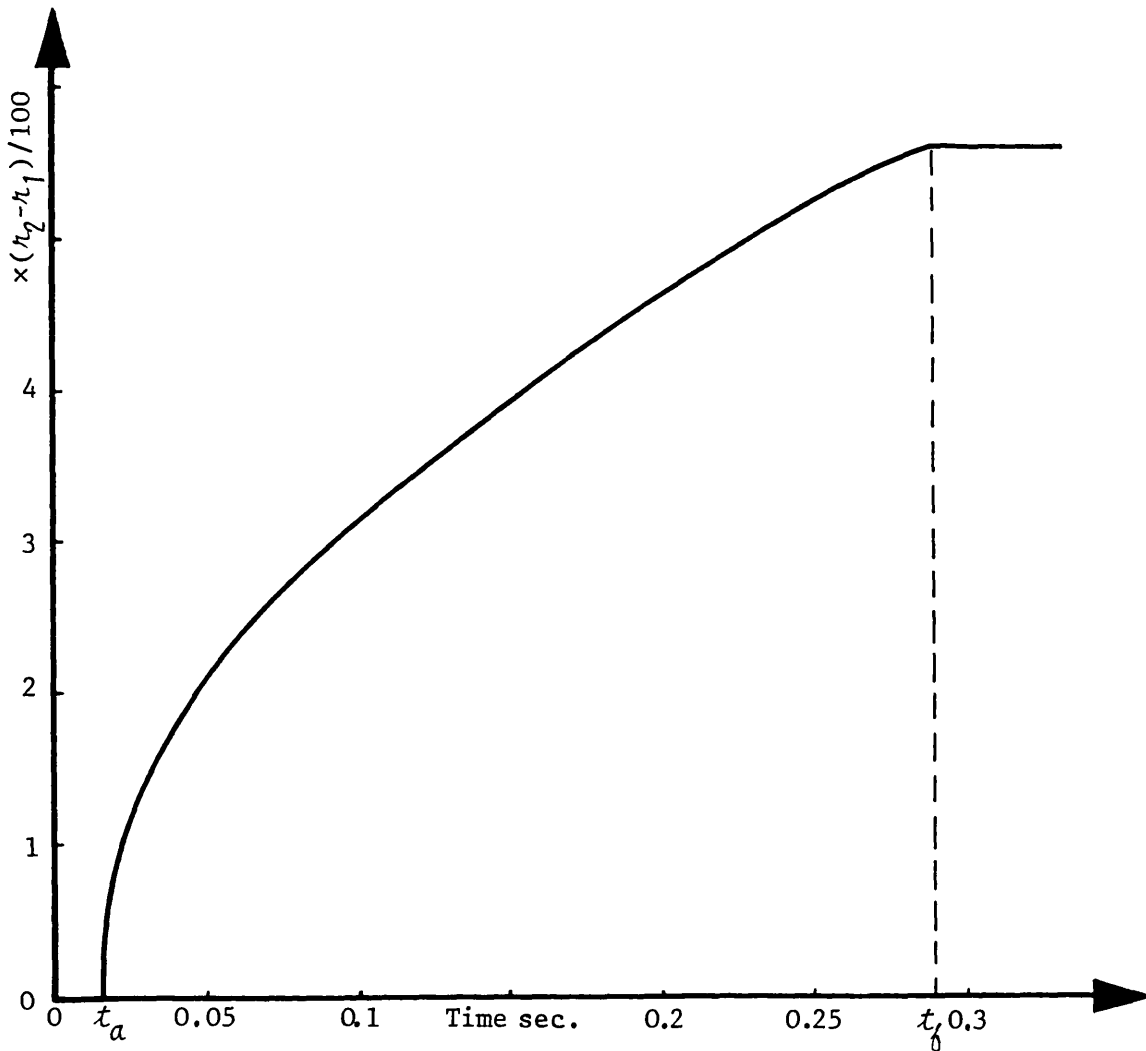Figure 5.10: Inner surface Temperature history.



Figure 5.11: Solidus Interface Position history.

equation (5.3) using relations (5.4) and (5.7b). This equation is incorporated with the latent heat effect included in the specific heat, which causes damping in the temperature variations with respect to time. Further, there are also sharp changes in the material properties (see Figure 5.1) which must be taken into account.

The position history of the free boundary (the solidus interface) along the radius (radial movement with respect to time) is plotted in Figure 5.11. A comparison between Figures 5.10 and 5.11 can be made such that, from times $t_i$ to $t_a$, the whole body is in the solid state and there is, of course, no free boundary. At time $t_a$, the temperature of the inner surface approaches the solidus temperature (see Figure 5.10). At the same time, the free boundary (solidus interface) begins to develop and moves gradually towards the outer surface of the pellet (see Figure 5.11), although it never reaches that surface because the outer surface is assumed to be always kept at a fixed temperature (1600°K) which is lower than the solidus temperature.

The radial temperature profiles at some selected time-nodes are plotted in Figure 5.7, in which the curve labelled $t_0$ represents the initial radial temperature distribution (at time $t_0$) when the whole solution domain is in the solid state. Other curves in the same figure each show a discontinuity at the solidus temperature where the position of the free boundary at the respective time is accordingly located. The curve labelled $t_b$ represents the steady-state solution.

The steady-state case is approached (after time $t_b$) when the free boundary becomes stationary and also the temperatures intend to be steady, including the inner surface temperature (3063.005°K). This temperature is lower than the liquidus temperature of the material. Therefore, the solution-domain remains in two phases (solid and transition) which are separated by a free boundary (solidus interface).

Figures 5.8 and 5.10 show that there is not any oscillation at the discontinuity points (both in the temperature profiles and temperature history). Also, Figure 5.11 shows that the free boundary develops and moves very smoothly, and without any oscillation. However, since the method is numerical, short time-steps are advised to obtain better solution at the discontinuities. In order to verify the stability of the method, it was applied to seven different examples of this type. The method performed very well, in each case, and it never introduced any oscillation throughout.

Correlation among Figures 5.7, 5.10 and 5.11 is always guaranteed because they are solution representatives of a single problem. Figure 5.12 shows schematically how they are interlinked, where there are three parameters ($t$, $T$ and $X$ for time, temperature and the free boundary position, respectively), given that any one of them should lead to the determination of the other two.

### 5.4.2  Application of the Method to a Transient Three-Phase Example

In order to verify the behaviour and to check the stability of the proposed method in the cases involving three-phases, it must be validated at least for some aspects. However, due to the lack of reliable data, the same viewpoints as those explained in Section 5.4.1 are again studied here. Therefore, the same example as considered in that section is assumed to be extended to a three-phase case. The same fuel pellet as that chosen in Section 5.4.1 is assumed to be so overheated that its cross-section (the solution-domain) has simultaneously attained three distinct phases (solid, transition and liquid states).

The physical, geometrical and thermal properties, as well as all boundary conditions, are assumed to be the same as those used for the example studied in Section 5.4.1. Since the example which is going to be
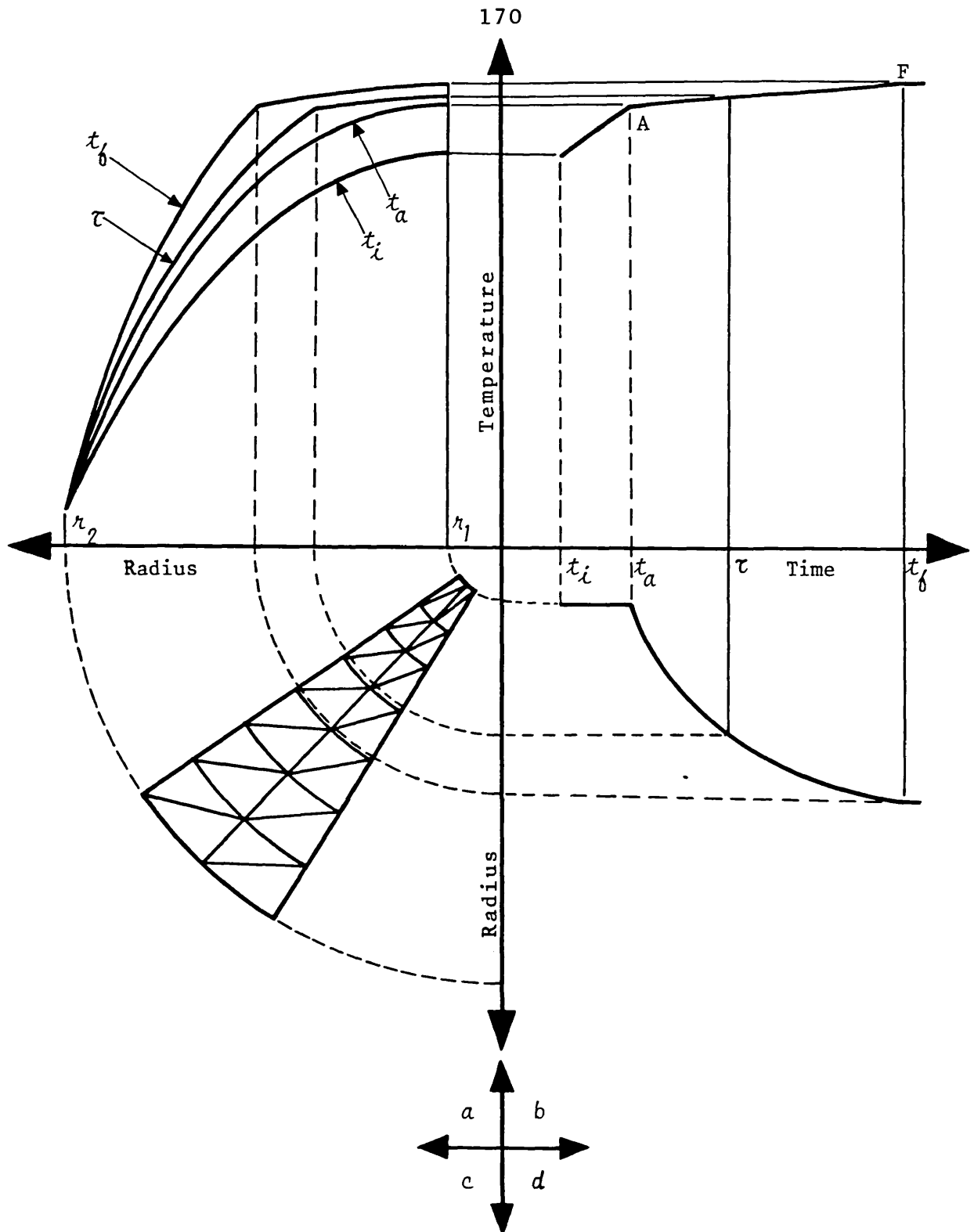
Key:

a = Radial Temperature Profiles, see Figure 5.7

b = Inner Surface Temperature history, see Figure 5.10

c = Geometry of the Solution-domain, see Figure 5.9

d = Solidus Interface Position history, see Figure 5.11

Figure 5.12:   Correlations among Solution Curves of a Two-phase Problem.

considered here is an extension of the same example studied in Section

5.4.1, the final conditions in that example will be the initial conditions

for the example considered here. Hence, the initial radial temperature

distribution within the pellet is the same as shown by the curve labelled

$t_{\delta}$ in Figure 5.7. This is represented by the curve labelled $t_0$ in Figure

5.13.

The rate of thermal energy generation is assumed to suddenly

increase up to $0.725 \times 10^{10}$ W/m$^3$. Then the radial temperature profiles at

some selected time-nodes, the position history of both interfaces and,

finally, the temperature history of the pellet inner surface are discussed

here.

The problem is solved here using the same mesh as shown in

Figure 5.9. This mesh is always refined, using the free boundary(ies),

such that each element lies in a single phase. The governing equation

for the elements in the solid and liquid states is, in general, equation

(4.7) using $\lambda = 1.5$, whereas for the elements in the transition state due

to the latent heat effect, the solution is based on equation (5.3) using

equations (5.4) and (5.7b).

The radial temperature profiles at some selected time-nodes,

as labelled, are shown in Figure 5.13, in which the curve labelled $t_0$

represents the initial radial temperature profile in the example

considered here (these temperatures are exactly the same as shown by the

curve labelled $t_{\delta}$ in Figure 5.7). The curve labelled $t_b$ in Figure 5.13

implies that at time $t_b$, the inner surface temperature has reached the

liquidus temperature and, thereafter, the solution domain will be in three

phases. In the same figure, the curve labelled $t_g$ represents the steady-

state solution, which means from time $t_g$ the whole solution domain will

steadily remain in three phases (solid, transition and liquid) separated
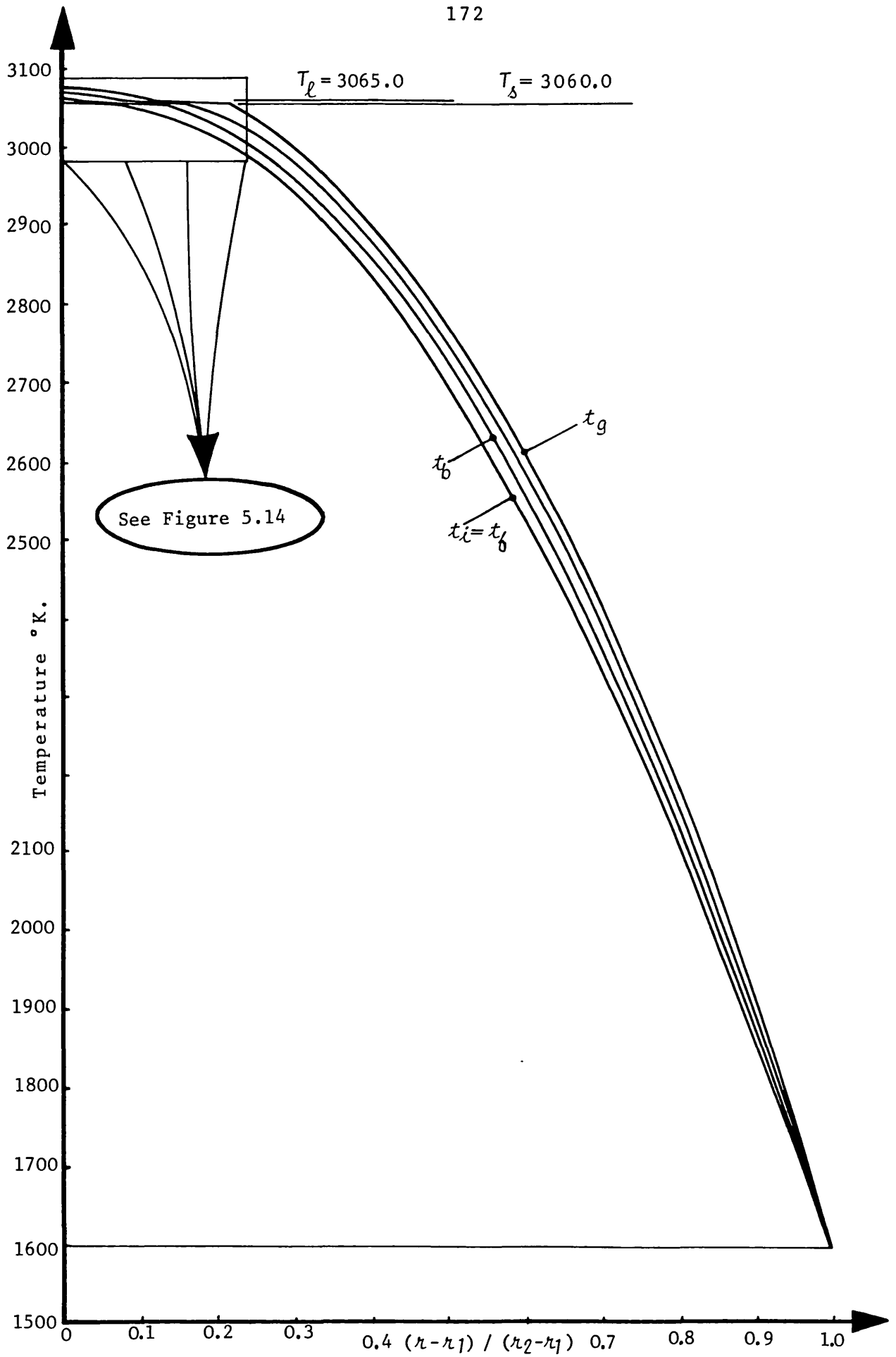
by two motionless interfaces.
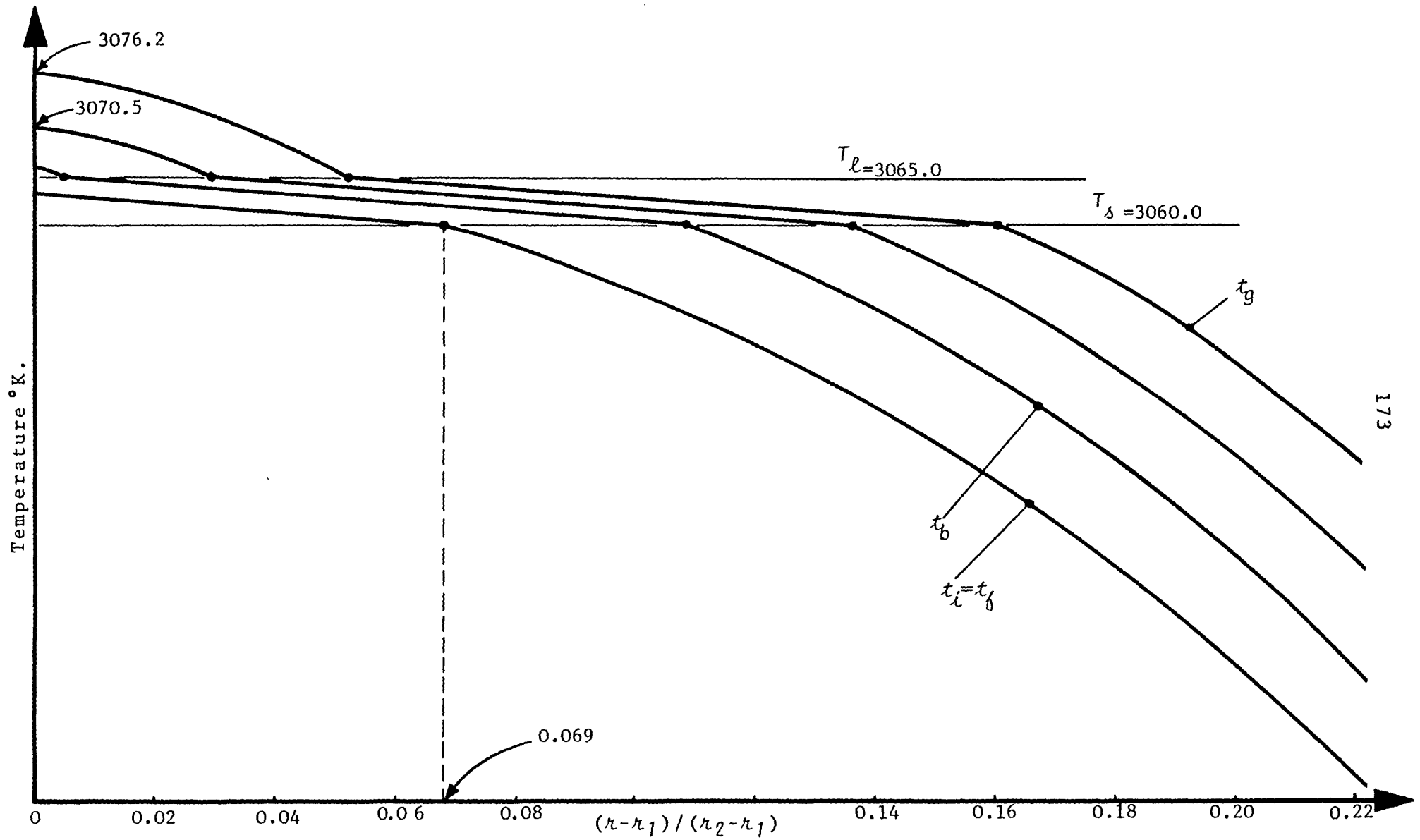
Figure 5.13: Radial Temperature Profiles.
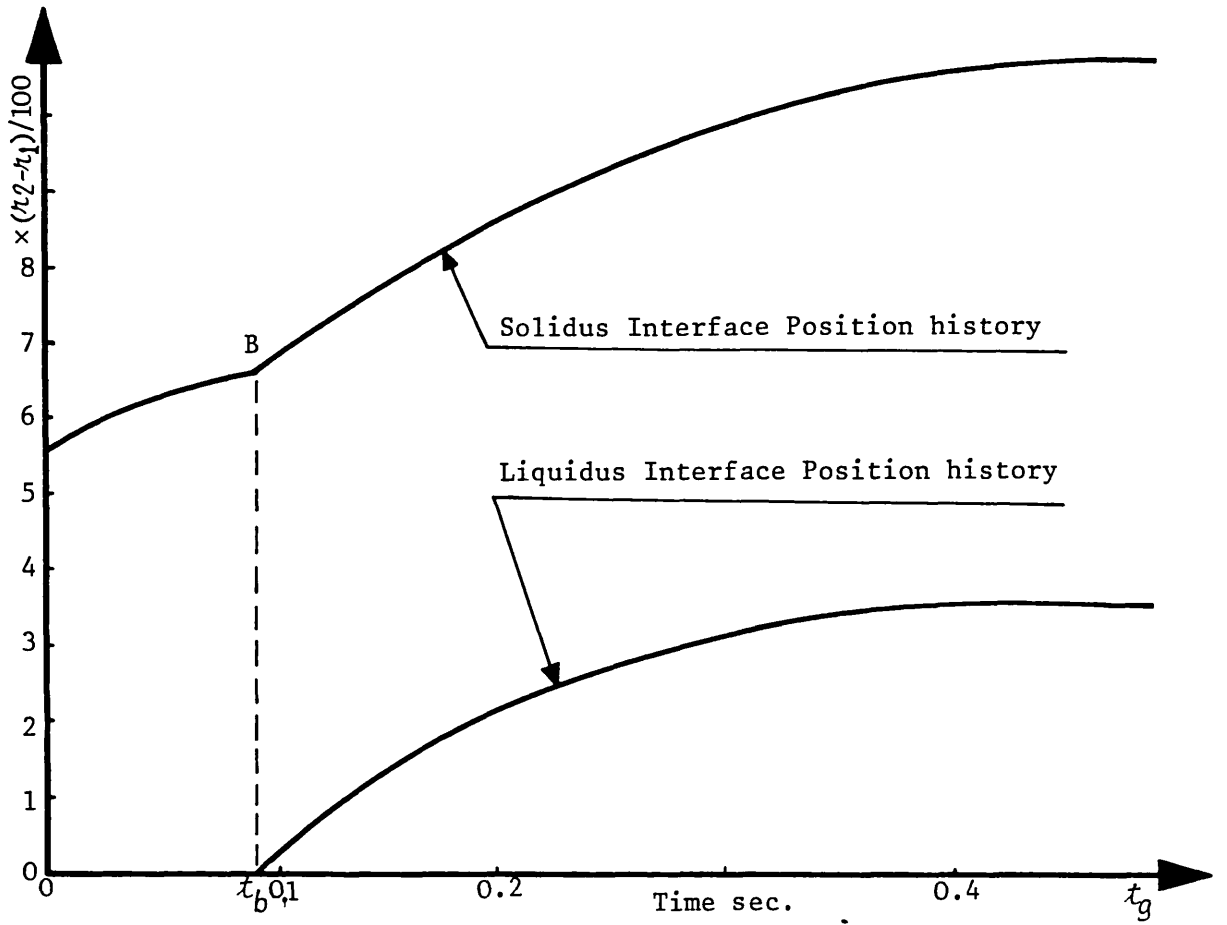
Figure 5.14:   See Figure 5.13.

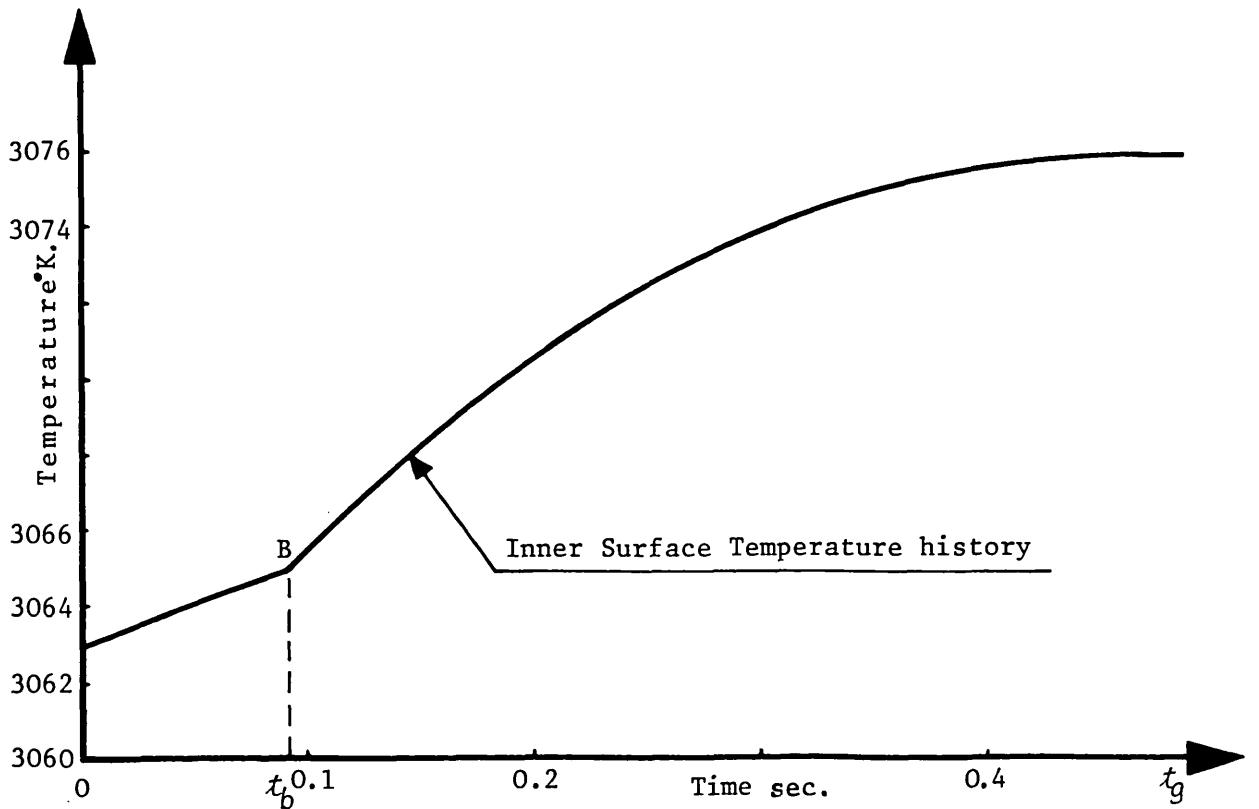Figure 5.15: See also Figure 5.11.



Figure 5.16: See also Figure 5.10.

At any time after $t_b$, the radial temperature profile has two discontinuities, one at the solidus temperature and one at the liquidus temperature (see Figure 5.13); each locates the position of the respective interface along that radius at that particular time. Therefore, the radial position history of the two free boundaries may be as shown in Figure 5.15. In this figure, the steady-state case is approached after time $t_g$, from when both interfaces become motionless.

The temperature history of the pellet inner surface can be shown as in Figure 5.16. As the temperature (of the inner surface) passes the liquidus temperature $(T_\ell)$, just after time $t_b$, the state of the material at the inner surface changes from transition to liquid. At the same time, the rate of temperature-rise increases sharply (see Figure 5.16).

The discontinuities (in Figures 5.13 and 5.16) are all expected due to the latent heat effect, as explained earlier. Within the transition state, the latent heat effect causes very slow temperature changes with respect to time, whereas in the solid and liquid states, the latent heat is not effective at all. Hence, at the interfaces, sharp changes will appear in the temperature gradients both with respect to time and to radius. Moreover, the physical and thermal properties of the material will also change sharply at these (discontinuity) points (see Figure 5.1). The proposed method never introduced any oscillation at these critical points (see Figures 5.14, 5.15 and 5.16).

A comparison between the time dimensions in Figures 5.15 and 5.16 can be made such that, from time $t_\ell' = t_\delta$ to time $t_b$, the body is in two phases (solid and transition), with only one interface. At time $t_b$, the temperature of the pellet inner surface approaches the liquidus temperature (see Figure 5.16). At the same time, another free boundary (the liquidus interface) begins to develop and moves towards the pellet outer surface. This interface, of course, can never reach the solidus

interface or the pellet outer surface, as explained in Section 5.4.1.

The steady-state case, in general, is approached after time $t_g$ when both free boundaries become motionless and also all the temperatures tend to remain steady. The temperature of the pellet inner surface (3076.2°K) is now higher than the liquidus temperature of the material. Therefore, the solution domain will steadily remain in three phases (solid, transition and liquid).

The proposed method performed very well throughout this application and never introduced any oscillation, particularly at the interfaces, where discontinuities occur for all the field variables (see Figures 5.1, 5.14 and 5.16). The free boundaries develop and move very smoothly and without any oscillation (see Figure 5.15) as must be the case. The method showed to be stable throughout these applications. Its behaviour conformed with the theoretical ideas in all aspects.

Correlation among Figures 5.13, 5.15 and 5.16 is always guaranteed, as explained for Figure 5.12, because they are solution curves representative to a single problem.

## CHAPTER 6

## CONCLUSIONS AND RECOMMENDATIONS

### 6.1 CONCLUSIONS

In recent years, the numerical methods have been improved tremendously from some very simple idealised cases to highly sophisticated and generalised systems. Nowadays, because of the increasing need for safety in industries (particularly in the nuclear industry), reliable and economical predictive numerical methods have clearly become indispensable tools for design engineers. In many cases, one of the most important factors in a new design is, of course, the conduction of heat through the materials. This has been the prime consideration of this work.

The technology of harvesting nuclear energy has now been well-established. The most crucial hurdle a design engineer faces today is the safety aspects of each component he proposes to use, particularly inside a reactor core where the operating temperatures are very high. In the event of an accident, these temperatures may rise even further and may even exceed the material melting point and have to be considered by the designer. Some of these possible events can be simulated with the help of numerical techniques.

On the other hand, in addition to the safety of a nuclear reactor, its efficiency must also be as high as possible. The best performance of a set-up would ideally be when the fuel zone temperature is uniformly just under its melting point. In practice, however, peak fuel temperatures are, for various reasons, well below the melting point. Therefore, the highest efficiency of a reactor is obtained when the temperatures are at the highest possible level. Moreover, the most critical conditions inside a reactor, whilst being operated, are usually around the core centre, where a minor accident or over-heat might introduce phase-change. This

is considered in Chapter 5.

In the present work, three-dimensional numerical formulations for a very general potential field problem have initially been derived (in Chapter 2) for any shape of geometry using all possible kinds of boundary conditions (see Table 1.2). In the same chapter, a procedure for replacing all kinds of loads acting on the solution-domain by a set of distinct loads acting only at the nodes is proposed (see Section 2.4.3). This technique is established both physically and mathematically. This is explained well for any shape of element including two- and one-dimensional (see also Section 3.3.3).

The method has particularly been applied to a general heat conduction problem (see Section 2.4) with all four different kinds of boundary conditions (as given in Table 1.3). The first three kinds of boundary conditions are used throughout this work. Although some work was done on the radiative boundary conditions, the modelling was not satisfactory enough and it has not been reported here.

This work was primarily concerned with the conductive heat transfer through nuclear reactor components, which can be regarded as a two-dimensional problem. We have, therefore, re-derived the method for this type of problem for steady-state situations in Chapter 3.

Throughout this work, in the derivation of the formulations, all the thermophysical properties are considered to be variable (temperature-dependent, for example). Moreover, the proposed method is also very general and can deal with a heat conduction problem (including coupled-problems) in any geometrical shape of the solution-domain, involving any kind of boundary conditions. This can prove to be of an enormous advantage.

In Chapter 3, the formulations are re-derived for a two-dimensional steady-state problem. These can be applied either in a cartesian system

or in an axisymmetric system using the same computer code with minimal changes (see Section 3.1). In the same chapter, a linear temperature model has been proposed, for which the temperature has to be prescribed at at least three nodes. Therefore, for a triangular element, it is very simple and suitable, but for any other shaped elements, three well-distributed nodes are most suitable. Further, the construction of the thermal conductivity matrix and the load matrix for a typical element is also discussed here (in Sections 3.3.2 and 3.3.3, respectively).

Finally, the method (so far for steady-state problems) is compared with an analytical solution (in Section 3.4) and the method showed very good accuracy and stability. Furthermore, to demonstrate some of the features of the method, it is applied to more axisymmetric and non-axisymmetric geometrical configurations with various boundary conditions (see Section 3.5) that can exist in a typical real life LMFBR fuel element. For example, an LMFBR fuel element with the pellet eccentrically mounted in the cladding, namely, with a non-uniform gap in between.

Next, the time derivative term is formulated and added to the existing formulations in order to solve transient problems in a single-phase medium. A generalised formulation is derived using a parameter $\lambda$. The well-known Crank-Nicholson and Galerkin methods are regenerated when $\lambda$ takes values of one and two, respectively. The variations of the thermophysical properties are also considered here (in Section 4.2).

The status of the solution-domain (the system), whether it is cooling down, heating up or being steady, is verified by comparing the (nodal) temperatures at the beginning and end of each time-step (equation (4.14)). For a sufficient time lag, some transient solutions can approach steady-state solutions.

The proposed formulations are tested against the only available one-dimensional exact solutions (Section 4.5). The solutions were in very

good agreement and were stable. Some of the examples used in Chapter 3 were re-calculated to include the transient stage. Some of these examples were solved for an extended time period to achieve steady-state conditions. These compared very well with the solutions given in Chapter 3.

As the temperatures rise and there is persistent over-heat loading, the temperatures of some components (or some parts) may exceed their melting points. This would change the conductive problems studied so far to phase-change (or multi-phase) problems. These are studied in Chapter 5. A typical interface (free boundary) is well-defined and a very general method has been proposed to locate each interface (see Section 5.3.2) for a wide range of possibilities. Then this method has been applied here in the frame of the finite element method (see Section 5.3.3). These located interfaces are then used for refining the mesh to produce elements, each in a single phase (see Section 5.3.4). Only the elements crossed by interface(s) need be refined. In steady-state multi-phase problems, each interface remains steady, but in transient problems (of this type), the shape and the position of each interface changes with respect to time. Hence, the problem has to be solved more cautiously.

Unless the components are made up of pure materials, there is always a finite difference between the solidus and liquidus temperatures. If the temperature of any node lies between these two temperatures, the node is then in a transition state. This state is treated here as an independent state. In this state, the field variables, obviously, have to keep continuity and thus, if a variable is not known, a continuity hypothesis may be applied to approximate it over the transition temperature range (for instance, see equation (5.1)).

Change of phase takes place only in transient multi-phase problems and latent heat will affect only in the transition state. This is well explained and is formulated in Section 5.2.3. For these problems, no

analytical solutions, against which the method and the code could be validated, were found in the literature. Nevertheless, the solutions are found to be stable and are seen in all respects to be very reasonable.

This formulation is first applied to an LMFBR fuel pellet in two phases, namely, solid and transition. The qualitative agreement is very good. Next, it is applied to the same pellet with heat loading such that the pellet attains three phases simultaneously. Again, qualitative agreement is very good.

The method is very general and flexible, and it can deal with an geometrical shape and with any type of boundary condition (except radiative). It can be applied to a wide range of multi-phase problems as well as single-phase problems in both steady-state and transient cases. In this method, there is not any restriction either on geometrical or on thermophysical properties. Each of the thermophysical properties of each element is entirely independent of neighbouring elements, which means that they may vary from element to element. These degrees of freedom can prove the method to be of enormous advantage. A two-dimensional computer code has been developed, based on this method, such that it can be applied to either cartesian systems or axisymmetric systems.

In conclusion, briefly, the finite element formulations of the conductive heat transfer process have been fully discussed here in three dimensions with all possible boundary conditions. The two-dimensional computer coding can deal with any geometrical system. None of the thermophysical properties of each element is restricted by neighbouring elements. The code can be applied to problems both in steady-state and transient cases. The system can be in the single-phase or multi-phase, and also to systems which are in the transient state approaching a steady-state case. The method and the solutions have always been stable for the problems and applications considered here. The computer coding has been

arranged such that any new application can easily be incorporated. It can handle problem with the following properties:

(1) Any two-dimensional geometrical shape.

(2) All possible boundary conditions (except radiative).

(3) Variable thermophysical properties.

(4) Steady-state cases in single-phase and multi-phase problems.

(5) Transient cases in single-phase and multi-phase problems.

(6) Each free boundary in transient multi-phase problems can carefully be located at any time.

(7) The code is simple to adapt to new applications and has been stable for all the problems considered throughout this work.

It is worth noting that the formulations presented here for the temperature field analysis are compatible with the finite element solution for the stress distribution analysis, and hence both problems can be solved simultaneously and jointly, even by the same code. A lot of effort has already been made to make it as economical as possible. This code can be employed to calculate the temperature distribution in the reactor components at any conditions needed as input to the thermal and irradiation stress analysis computer code developed by the Nuclear Power Section at Imperial College.

6.2  FUTURE WORK AND RECOMMENDATIONS

The two-dimensional computer code has reached a stage of development where it can be of real benefit to industry. For many applications and restrictions of finance and computer facilities, the two-dimensional code is very adequate. The next step in its development, which a typical industry may require , is to be able to solve three-dimensional problems.

The formulations have been presented in Chapter 2. The treatment of each of the matrices (heat load matrix, thermal conductivity matrix and thermal energy capacity matrix) for any type of problem (steady-state or transient in single-phase or multi-phase medium) would remain virtually the same. No doubt these classes of problem would require an enormous amount of computational effort.

As regards the two-dimensional problems, the expansion of the elements has still to be taken into account, even though it may be a very small fraction of its dimensions. This would, of course, be useful only in transient problems. The other major area of development is to include thermal radiation. This is not a very simple task and requires further modelling to tackle it successfully.

The most important thing is to be able to obtain more experimental data for both phase-change problems and problems involving the radiative boundary so that this method can systematically be validated.

APPENDIX A

To replace a distributed load by a point load, we consider a typical (three-dimensional) element ($e$) which is under a continuously distributed load with a local density of $\vec{Q}^e$ per unit volume. All this distributed load is equivalent to a point-load ($\vec{F}_Q^e$) which is:

$$\vec{F}_Q^e = \iiint_{V^e} \vec{Q}^e \cdot dV \qquad (A.1a)$$

acting at a load-centre ($G$) whose coordinate vector ($\vec{r}_G$) is given by:

$$\vec{r}_G = \left( \iiint_{V^e} \vec{Q}^e \cdot \vec{r} \cdot dV \right) / \left( \iiint_{V^e} \vec{Q}^e \cdot dV \right) \qquad (A.2)$$

where the net moment due to the distributed load ($\dot{\vec{Q}}^e$) over the entire element is zero. For a uniform load distribution, the load-centre ($G$) coincides with the gravity centre of the element, and:

$$\vec{F}_Q^e = \vec{Q}^e \cdot V^e \qquad (A.1b)$$

where $V^e$ is the volume of the element.

Similarly, the distributive loads acting on a surface (boundary loads), or the loads due to the potential flow passing through a finite surface (boundary face), can be replaced by a point-load. For a typical boundary face ($S^e$) of a typical boundary element ($e$), which is under a continuously distributed load with a local density of $\vec{q}_{S^e}$ per unit area, all this distributed load is equivalent to a point-load ($\vec{F}_q^e$) as:

$$\vec{F}_q^e = \iint_{S^e} \vec{q}_{S^e} \cdot dS \qquad (A.3a)$$

acting at a load-centre ($c$) whose coordinate vector ($\vec{\hbar}_c$) is given by:

$$\vec{\hbar}_c = \left( \iint_{S^e} \vec{q}_{S^e} \cdot \vec{\hbar} \cdot dS \right) / \left( \iint_{S^e} \vec{q}_{S^e} \cdot dS \right) \tag{A.4}$$

where the net moment due to the distributed load ($\vec{q}_{S^e}$) on the face $S^e$ is

zero. For a uniform load distribution, the load-centre ($c$) coincides

with the centroid of the face $S^e$, if the face $S^e$ is flat, and:

$$\vec{F}_q^e = \vec{q}_{S^e} \cdot \Delta e \tag{A.3b}$$

where $\Delta e$ is the area of the boundary face, $S^e$.

Finally, the loads distributed over a line can also be replaced by a

point-load. For a typical side (edge) ($ij$, for example) under a

continuous distributed load with a local density of $\vec{q}_{ij}$ per unit length,

all this distributed load is equivalent to a point-load ($\vec{F}_{ij}$) which is:

$$\vec{F}_{ij}^e = \int_{ij} \vec{q}_{ij} \cdot dc \tag{A.5a}$$

acting at a load-centre ($m$) whose coordinate vector ($\vec{\hbar}_m$) is given by:

$$\vec{\hbar}_m = \left( \int_{ij} \vec{q}_{ij} \cdot \vec{\hbar} \cdot dc \right) / \left( \int_{ij} \vec{q}_{ij} \cdot dc \right) \tag{A.6}$$

where the net moment due to the distributed load $\vec{q}_{ij}$ on the side $ij$ is

zero. For a uniform load distribution, the load-centre ($m$) coincides

with the mid-point of the side $ij$, if the side $ij$ is not curved, and:

$$\vec{F}_{ij}^e = \vec{q}_{ij} \cdot L_{ij} \tag{A.5b}$$

where $L_{ij}$ is the length of the side $ij$.

To replace a point-load ($\vec{F}^e_p$) acting on an element ($e$) at a point $p$ by an equivalent system of distinct loads acting at some distinct points (for example, some selected nodes of that element), we need to obey both the conservation law and the moment law. The conservation law states that the total load (resultant) at any instant must be equal to the point-load, namely, for the typical element:

$$\vec{F}^e_p = \sum_i \vec{F}^e_i \qquad\qquad (A.7)$$

where $i$ is the summation over all the selected nodes of the element ($e$), and $\vec{F}^e_i$ is the load acting at a typical node $i$ of the element due to the point-load ($\vec{F}^e_p$). Moreover, the moment law states that the sum of the moments of all the loads (again due to $\vec{F}^e_p$ or $\vec{F}^e_i$) acting on the element at any instant about any point must remain unchanged. Hence, since the net moment about the point of action of $\vec{F}^e_p$ (point $p$) is zero, we can write:

$$\sum_i \vec{m}_i = 0 \qquad\qquad (A.8)$$

where $\vec{m}_i$ is the moment of the nodal load $\vec{F}^e_i$ about point $p$. The typical nodal load $\vec{F}^e_i$ is then the component of $\vec{F}^e_p$ at the respective node ($i$). Such systems ($\vec{F}^e_p$ and $\vec{F}^e_i$) are then said to be equivalent.

On the other hand, the formulations derived in equations (2.58), (2.62) and (2.63) using the finite element method can also be used for replacing any distribution of loads acting on a typical element by another system of distinct loads acting only at the nodes of that element. Obviously, the resultant load must always be the same. In order to evaluate those integrals, firstly, we need to introduce some special mathematical functions to ease their understanding and then relate them to the relations (A.1) to (A.8).

A point-load can be considered as a continuous distributive load such that its local density is zero everywhere, except at its point of action where it is infinite. We can construct a mathematical function which behaves in this fashion by introducing here a special generalised function usually used in electromagnetic problems [32].

For a point $P$ at $x_p$, let us define a function (a Dirac delta function), denoted by the symbol $\delta(x-x_p)$, such that it is everywhere zero except at the point $P$ where it is infinite, namely:

$$
\begin{aligned}
\delta(x - x_p) &= 0 \qquad \text{if} \qquad x \neq x_p \\
\delta(x - x_p) &= \infty \qquad \text{if} \qquad x = x_p
\end{aligned}
\tag{A.9}
$$

and for $P$ outside the interval $ab$, we can write:

$$
\int_a^b \delta(x - x_p) \, . \, dx = 0 \qquad \text{if} \qquad x_p \notin [a,b]
\tag{A.10a}
$$

but for $P$ inside the interval $ab$, we can write:

$$
\int_a^b \delta(x - x_p) \, . \, dx = 1 \qquad \text{if} \qquad x_p \in [a,b]
\tag{A.10b}
$$

It can then be proved that for a point $P$ at $\hbar_p$ for any constant $A$ and the interval of integration containing the point $P$, we can write:

$$
\int_a^b A \, . \, \delta(\hbar - \hbar_p) \, . \, dV = A
\tag{A.11}
$$

This can be written in the cartesian system as:

$$
\iiint_V A \, . \, \delta(x - x_p) \, . \, \delta(y - y_p) \, . \, \delta(z - z_p) \, . \, dx \, dy \, dz = A
\tag{A.12}
$$

Also, for any function of $N(\hbar)$ depending on $\hbar$ (for example, $x$, $y$ and $z$) and the interval of integration containing $\hbar_p$ (for example, $x_p$, $y_p$ and $z_p$), it can be proved that:

$$\iiint\limits_{V} A \cdot N(\hbar) \cdot \delta(\hbar - \hbar_p) \cdot dV = A \cdot N(\hbar_p) \qquad \text{(A.13)}$$

where $N(\hbar_p)$ is the value of the function $N$ at point $P$ ($x_p$, $y_p$ and $z_p$) ([32] and [33]).

Hence, for a point-load of strength $\vec{F}_Q^e$ acting at a point $P$ inside an element $(e)$, we can define a local load density function as:

$$\vec{F}_Q^e \cdot \delta(\hbar - \hbar_p) \qquad \text{(A.14)}$$

such that this is zero everywhere but infinite at $P$, and by the relation (A.11) we can write:

$$\iiint\limits_{V^e} \vec{F}_Q^e \cdot \delta(\hbar - \hbar_p) \cdot dV = \vec{F}_Q^e \qquad \text{(A.15)}$$

Using the relation (A.14) as a special local load density function instead of the local load density $\underset{\sim}{Q}^e$ in equation (2.58) and using relations (A.13) and (A.15), we finally obtain:

$$\{F_Q\}^e = \iiint\limits_{V^e} \vec{F}_Q^e \cdot [N(\hbar)]^T \cdot \delta(\hbar - \hbar_p) \cdot dV = \vec{F}_Q^e \cdot [N(\hbar_p)]^T \qquad \text{(A.16)}$$

where $\vec{F}_Q^e$ is the point-load equivalent to the total of the distributed load over the element, given by relations (A.1a) and (A.1b), and the $N(\hbar_p)$'s are the values of the position functions ($N$'s) evaluated at the point $P$ (the point of action of $\vec{F}_Q^e$ or the load-centre of the distributed load $\underset{\sim}{Q}^e$), located by the relation (A.2).

Similarly, the relation (2.62) can be written as:

$$\{F_q\}^e = \iint_{S^e} \vec{F}_q^e \cdot [N(\hbar)]^T \cdot \delta(\hbar - \hbar_p) \cdot dS = \vec{F}_q^e \cdot [N(\hbar_p)]^T \qquad (A.17)$$

where $\vec{F}_q^e$ is the point–load equivalent to the total of the distributed load on the face $S^e$ (the boundary face of the element $e$ associated with the approximated surface of $S_2$), $\vec{F}_q$ can be calculated from relations (A.3a) and (A.3b), and the $N(\hbar_p)$'s are the values of the position functions ($N$'s) evaluated at the point $P$ (the point of action of $\vec{F}_q^e$ or the load–centre of the distributed load $\vec{q}_{S^e}$), located by the relation (A.4).

Also, the relation (2.63) can be written as:

$$\{F_h\}^e = \iint_{S^e} \vec{F}_h^e \cdot [N(\hbar)]^T \cdot \delta(\hbar - \hbar_p) \cdot dS = \vec{F}_h^e \cdot [N(\hbar_p)]^T \qquad (A.18)$$

where $\vec{F}_h^e$ is the point–load equivalent to the total of the distributed load on the face $S^e$ (the boundary face of the element $e$ associated with the approximated surface of $S_3$), $\vec{F}_h^e$ can be calculated from relations (A.3a) and (A.3b) using $\vec{q}_{S^e} = h_{S^e}^e \cdot \theta_\infty$, and the $N(\hbar_p)$'s are the values of the position functions ($N$'s) evaluated at the point $P$ (the point of action of $\vec{F}_h^e$ or the load–centre of the distributed load due to $h_{S^e}^e \cdot \theta_\infty$), located by the relation (A.4).

Finally, for a distributed load acting on a one–dimensional element $ij$, we can write:

$$\{F_{ij}\}^e = \int_{ij} \vec{F}_{ij}^e \cdot [N(\hbar)]^T \cdot \delta(\hbar - \hbar_p) \cdot dc = \vec{F}_{ij}^e \cdot [N(\hbar_p)]^T \qquad (A.19)$$

where $\vec{F}_{ij}^e$ is the point–load equivalent to the total of the distributed load on the line $ij$, given by relations (A.5a) and (A.5b), and the $N(\hbar_p)$'s are the values of the position functions ($N$'s) evaluated at the point $P$

(the point of action of $\vec{F}^e_{ij}$ or the load-centre of the distributed load $\vec{q}_{ij}$), located by the relation (A.6).

Hence, any distributed load acting on a typical element can be first replaced by a point-load. Next, this point-load can be broken up into some distinct loads, acting only at the nodes of the element, in such a way that the total load is divided proportionally to the values of the position functions ($N$'s) at the respective load-centre (or at the point of action of the point-load).

Let us verify the result (A.16) for a point-load acting on a three-dimensional tetrahedral element. Consider a typical tetrahedral element as described in Section 2.4.1, and as shown in Figure A.1. If a point
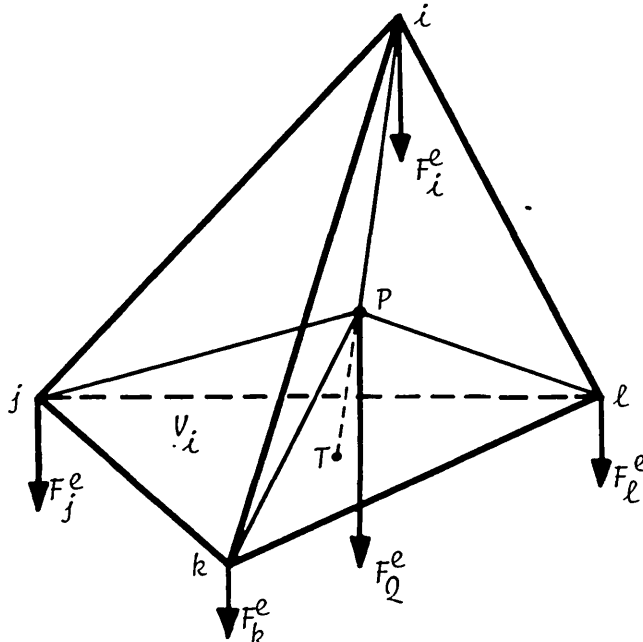


Figure A.1:  A tetrahedral element

load ($\vec{F}^e_Q$) acts at a point $P(x,y,z)$ inside the element, it can be replaced by a system of four distinct loads ($\vec{F}^e_i$, $\vec{F}^e_j$, $\vec{F}^e_k$ and $\vec{F}^e_\ell$) acting at the vertices of the element ($i$, $j$, $k$ and $\ell$, respectively), all parallel to $\vec{F}^e_Q$. Let $ip$ intersect the face $jk\ell$ at the point $T$. Now, $\vec{F}^e_Q$ can be replaced by two loads acting at points $i$ and $T$, so that both are parallel to $\vec{F}^e_Q$, and the load acting at $i$ ($\vec{F}^e_i$) can be written as:

$$\vec{F_i^e} = \vec{F_Q^e} \cdot \frac{\overline{PT}}{\overline{iT}} \qquad (A.20)$$

such that: $\qquad \dfrac{\overline{PT}}{\overline{iT}} = \dfrac{V_i}{V_e}$

where $V_i$ is the volume of the tetrahedron (sub-element) $pjk\ell$, and $V_e$ is the volume of the tetrahedron (main element) $ijk\ell$. Therefore, by using relations (2.20), we can write:

$$\vec{F_i^e} = \vec{F_Q^e} \cdot \frac{V_i}{V_e} = \vec{F_Q^e} \cdot N_i \qquad (A.21)$$

Similarly: $\qquad \vec{F_j^e} = \vec{F_Q^e} \cdot \dfrac{V_j}{V_e} = \vec{F_Q^e} \cdot N_j$ , etc.

This can be expressed in matrix form as:

$$\{F_Q\}^e = \vec{F_Q^e} \cdot [N(P)]^T \qquad (A.22)$$

where the $N(P)$'s are the values of the $N$'s given by relations (2.20) evaluated at the point $P$. Hence, the relation (A.22) confirms the result (A.16).

For a uniform load distribution, the load-centre $(P)$ coincides with the gravity centre $(G)$ of the element, where:

$$\sum_i V_i = V_i + V_j + V_k + V_\ell = V_e$$

and: $\qquad \sum_i N_i = N_i + N_j + N_k + N_\ell = 1$

Also: $\qquad V_i = V_j = V_k = V_\ell = \frac{1}{4} . V_e \qquad\qquad$ (A.23)

Hence: $\qquad N_i = N_j = N_k = N_\ell = \frac{1}{4}$

Then: $\qquad \vec{F}_i^e = \vec{F}_j^e = \vec{F}_k^e = \vec{F}_\ell^e = \frac{1}{4} . \vec{F}_Q^e$

where the total uniform load distributed over the element is equivalent to a point-load $(\vec{F}_Q^e)$ acting at $G$, which is given by relation (A.1b) as:

$$\vec{F}_Q^e = \iiint\limits_{V^e} \vec{Q}^e . dV = \vec{Q}^e . V^e$$

Therefore, relations (2.58) or (A.16) for such an element can finally be written in the matrix notation as:

$$\{F_Q\}^e = \frac{\vec{F}_Q^e}{4} . \begin{Bmatrix} 1 \\ 1 \\ 1 \\ 1 \end{Bmatrix} = \frac{\vec{Q}^e . V^e}{4} . \begin{Bmatrix} 1 \\ 1 \\ 1 \\ 1 \end{Bmatrix} \qquad\qquad \text{(A.24)}$$

where $\vec{Q}^e$ is the density of the uniform load (volumetric).

In order to verify the results (A.17) and (A.18) for a two-dimensional case, we consider a typical triangular element as described in Section 2.4.1 and shown in Figure A.2. If a point-load $(\vec{F}_q^e)$ acts at a point $P(x,y)$ inside the element, it can be replaced by a system of three distinct loads $(\vec{F}_i^e, \vec{F}_j^e$ and $\vec{F}_k^e)$ acting at its vertices $(i, j$ and $k)$, all parallel to
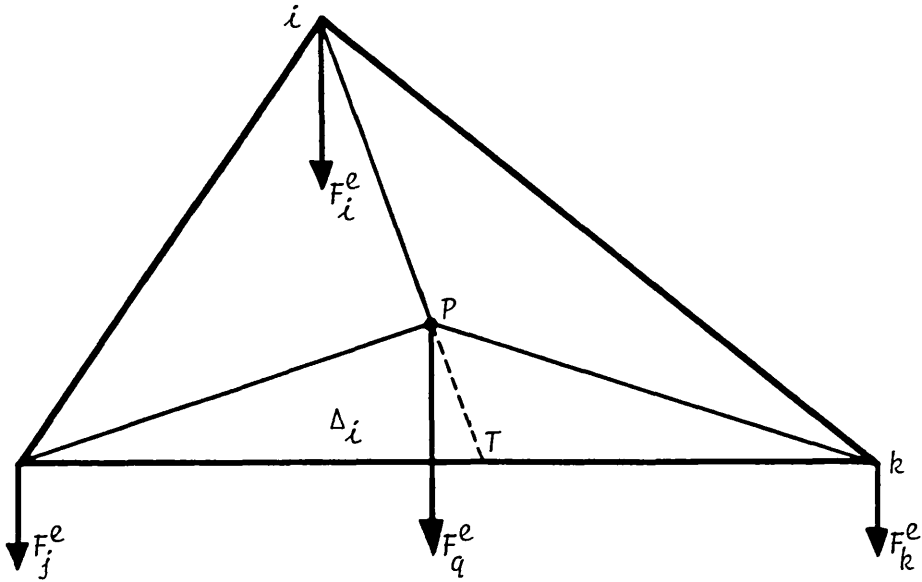
Figure A.2: A triangular element

$\vec{F}^e_q$. Let $ip$ intersect the side $jk$ at a point $T$. Now, $\vec{F}^e_q$ can be replaced by two loads acting at points $i$ and $T$, and that both are parallel to $\vec{F}^e_q$, such that the load $\vec{F}^e_i$ acting at point $i$ can be expressed as:

$$\vec{F}^e_i = \vec{F}^e_q \cdot \frac{\overline{PT}}{\overline{iT}} \qquad (A.25)$$

where:

$$\frac{\overline{PT}}{\overline{iT}} = \frac{\Delta_i}{\Delta_e}$$

in which $\Delta_i$ is the area of the triangle (sub-element) $pjk$, and $\Delta_e$ is the area of the triangle (main element) $ijk$. Therefore, by using relations (2.22), we obtain:

$$\vec{F}^e_i = \vec{F}^e_q \cdot \frac{\Delta_i}{\Delta_e} = \vec{F}^e_q \cdot N_i \qquad (A.26)$$

Similarly:

$$\vec{F}^e_j = \vec{F}^e_q \cdot \frac{\Delta_j}{\Delta_e} = \vec{F}^e_q \cdot N_j \quad , \quad \text{etc.}$$

This can be written in matrix form as:

$$\{F_q\}^e = \vec{F}^e_q \cdot [N(P)]^T \qquad (A.27)$$

where the $N(P)$'s are the values of the $N$'s given by the relations (2.22) evaluated at the point $P$. Hence, the relation (A.27) confirms the result (A.17).

For a uniform load distribution, the load-centre $(p)$ coincides with the centroid of the element $(c)$, where:

$$\sum_i \Delta_i = \Delta_i + \Delta_j + \Delta_k = \Delta_e$$

and:
$$\sum_i N_i = N_i + N_j + N_k = 1$$

Also:
$$\Delta_i = \Delta_j = \Delta_k = \frac{1}{3} \cdot \Delta_e \qquad \text{(A.28)}$$

Hence:
$$N_i = N_j = N_k = \frac{1}{3}$$

Then:
$$\vec{F}_i^e = \vec{F}_j^e = \vec{F}_k^e = \frac{1}{3} \cdot \vec{F}_q^e$$

By using relations (A.3b), (2.62), (2.63), (A.17) and (A.18) for such an element, it can finally be expressed in matrix notation as:

$$\{F_q\}^e = \frac{\vec{F}_q^e}{3} \cdot \begin{Bmatrix} 1 \\ 1 \\ 1 \end{Bmatrix} = \frac{\vec{q}_{s^e} \cdot \Delta_e}{3} \cdot \begin{Bmatrix} 1 \\ 1 \\ 1 \end{Bmatrix} \qquad \text{(A.29)}$$

where $\vec{q}_{s^e}$ is the density of the uniform load.

In order to verify the result (A.19) for a one-dimensional case, we consider a straight line joining two typical nodes $i$ and $j$, as described in Section 2.4.1 and shown in Figure A.3. If a point-load $(\vec{F}_{ij}^e)$ acts at a point $P(x)$ on the element, it can be replaced by a system of two distinct loads $(\vec{F}_i^e$ and $\vec{F}_j^e)$ acting at its ends $(i$ and $j)$, both parallel to $\vec{F}_{ij}^e$, such that:

$$\vec{F}_i^e = \vec{F}_{ij}^e \cdot \frac{\overline{Pj}}{\overline{ij}} \qquad \text{and} \qquad \vec{F}_j^e = \vec{F}_{ij}^e \cdot \frac{\overline{iP}}{\overline{ij}}$$
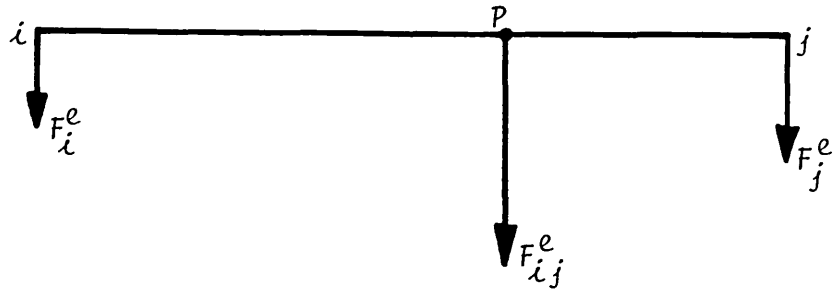
Figure A.3:  A one-dimensional element

Using the relation (2.24), we can obtain:

$$\vec{F_i^e} = \vec{F_{ij}^e} \cdot \frac{\ell_i}{\ell_e} = \vec{F_{ij}^e} \cdot N_i$$

and:

$$\vec{F_j^e} = \vec{F_{ij}^e} \cdot \frac{\ell_j}{\ell_e} = \vec{F_{ij}^e} \cdot N_j$$

This can be expressed in matrix form as:

$$\{F_{ij}\}^e = \vec{F_{ij}^e} \cdot [N(P)]^T \tag{A.30}$$

in which the $N(P)$'s are the values of the $N$'s given by relations (2.24) evaluated at the point $P$.   Hence, the relation (A.30) confirms the results (A.19).

For a uniform load distribution, the load-centre $(p)$ coincides with the mid-point of the element $(m)$, where:

$$\sum_i \ell_i = \ell_i + \ell_j = \ell_e$$

and:

$$\sum_i N_i = N_i + N_j = 1$$

Also:

$$\ell_i = \ell_j = \frac{1}{2} \cdot \ell_e \tag{A.31}$$

Hence:

$$N_i = N_j = \frac{1}{2}$$

Then:

$$\vec{F_i^e} = \vec{F_j^e} = \frac{1}{2} \cdot \vec{F_{ij}^e}$$

By using the relation (A.5b), the relation (A.19) for such an element can finally be written in matrix form as:

$$\{F_{ij}\}^{e} = \frac{\vec{F}_{ij}^{e}}{2} \cdot \begin{Bmatrix} 1 \\ 1 \end{Bmatrix} = \frac{\vec{q}_{ij} \cdot L_{ij}}{2} \cdot \begin{Bmatrix} 1 \\ 1 \end{Bmatrix} \tag{A.32}$$

where $\vec{q}_{ij}$ is the density of the uniform load.

Since the sum of the $N$'s is always equal to one, the conservation laws are always satisfied, but it is difficult to prove for general $N$'s that the moment is conserved. However, for all the examples considered above, the moment was conserved. Further, another method is also described in Section 3.3.3, where the same results are derived using a different method for a general two-dimensional element, and the moment is also conserved. Very often, the standard text books only deal with the discretisation of uniform load distributions and then divide the total load equally among the nodes, often the only reason being intuition. Here, we have now managed to prove rigorously how to discretise any general load (point—load or distributed load) to the nodes. During the literature survey on the subject, it was found that none of the authors had proved these results, although the usage had been almost universal.

APPENDIX B

## THEOREM

A uniformly distributed load over a flat $n$ sided polygonal element is equivalent to a system of $n$ distinct loads acting at its vertices, such that the load at each vertex is equal to all the loads on the quadrilateral whose vertices are the vertex itself, the polygon centroid and the mid-points of the two sides adjacent to that vertex.

## PROOF

Consider a plane (two-dimensional) $n$ sided polygonal element $(e)$ of height $\ell^e$ and with a uniform load distribution $\vec{Q}^e$ per unit volume (Figure B.1, for example). Let the element be sub-divided into $n$ triangles by joining its centroid $(c)$ to its vertices $(i, j, \text{etc.})$.
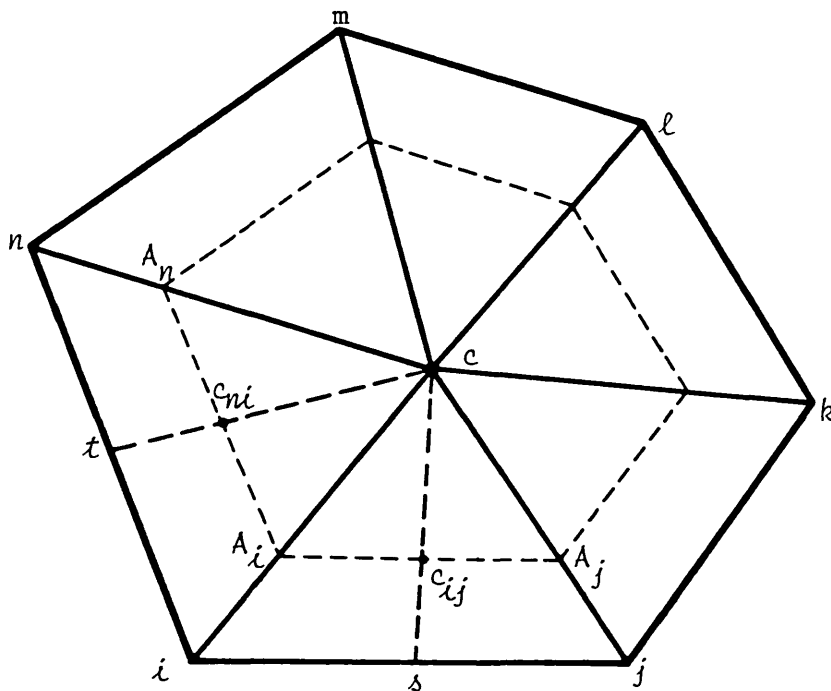


Figure B.1: A polygonal element with a uniform load

The uniform load over each triangle $(ijc, \text{for example})$ is equivalent

to a point-load $F_{ij}$, as given by the relation (3.31), and will be:

$$\vec{F}_{ij} = \vec{Q^e} \cdot \ell^e \cdot \Delta_{ijc}$$

where $\Delta_{ijc}$ is the area of the triangle $ijc$. This load acts at its centroid ($c_{ij}$) situated on the median labelled $cs$. Hence, the total load acting on the polygonal element is then equivalent to the system of $n$ distinct loads ($\vec{F}_{ij}$, for example), acting at the centroid of each triangle ($c_{ij}$, for example).

Next, draw a line parallel to the side $ij$ passing through $c_{ij}$. Let it intersect the lines $ci$ and $cj$ at the points $A_i$ and $A_j$, respectively. It can be shown that:

$$A_i \, c_{ij} = c_{ij} \, A_j$$

and:

$$\Delta_{isc} = \Delta_{jsc} = \frac{1}{2} \cdot \Delta_{ijc}$$

where $\Delta_{\ell mn}$ is the area of a triangle $\ell mn$. Therefore, by using these two results, $\vec{F}_{ij}$ can be replaced by a system of two equal loads, $\vec{F}_{A_i}$ and $\vec{F}_{A_j}$, acting at $A_i$ and $A_j$, respectively, such that:

$$\vec{F}_{A_i} = \vec{Q^e} \cdot \ell^e \cdot \Delta_{isc} = \vec{F}_{A_j} = \vec{Q^e} \cdot \ell^e \cdot \Delta_{jcs} = \frac{1}{2} \cdot \vec{F}_{ij} \qquad (B.1)$$

Applying the same procedure to the adjacent triangle ($icn$, for example), we obtain another load acting at $A_i$ of the magnitude:

$$\vec{F}_{A_i} = \vec{Q^e} \cdot \ell^e \cdot \Delta_{ict}$$

Hence, the net load acting at point $A_i$ is equal to:

$$\vec{F}_{A_i} = \vec{Q^e} \cdot \ell^e \cdot (\Delta_{isc} + \Delta_{ict})$$ (B.2)

This is repeated for all the triangles of the polygon to yield a system of $n$ distinct loads of the form (B.2), acting at the points $A_i$ (Figure B.1), which is equivalent to the point-load of the form (3.31) acting at $c$. Therefore, we can write:

$$\sum_n \vec{F}_{A_i} = \vec{F^e_Q}$$ (B.3a)

and:

$$\sum_n (\vec{F}_{A_i} \wedge c\vec{A}_i) = 0$$ (B.3b)

where $n$ is the summation over all the points $A_i$.

By the properties of a triangle ($ijc$, for example), it can be easily shown that:

$$\frac{\overline{cA_i}}{\overline{ci}} = \frac{\overline{cA_j}}{\overline{cj}} = \frac{\overline{c\,c_{ij}}}{\overline{c\,s}} = \frac{2}{3} \quad \ldots\ldots, \text{ etc.}$$ (B.4)

Multiplying the moment balance equation (B.3b) by a factor of 3/2 and using equations (B.4), we obtain:

$$\sum_n (\vec{F}_{A_i} \wedge c\vec{A}_i \cdot \frac{2}{3}) = \sum_n (\vec{F}_{A_i} \wedge \vec{ci}) = 0$$

Hence, if all the loads $\vec{F}_{A_i}$ were now acting at the corresponding vertex ($i$, for example), we will have the same resultant as given by the relation (B.3a). Hence, we finally obtain a system of $n$ distinct loads ($\vec{F}_i$, for example), acting at the vertices ($i$, for example), and each equal to, for example:

$$\vec{F_i} = \vec{F_{A_i}} = \vec{Q^e} . \ell^e . (\Delta_{isc} + \Delta_{ict}) = \vec{Q^e} . \ell^e . \Delta_{isct} \qquad (B.5)$$

which is equal to the load over the quadrilateral $isct$, acting at the vertex $i$ (Figure B.1).

This load (B.5) corresponds with the component of the load given by the relation (3.31) at vertex $i$ represented by the relation (3.32); thus:

$$\vec{F_i} = \vec{Q^e} . \ell^e . \Delta_{isct} = (\vec{Q^e} . \ell^e . \Delta_e) . N_i(c) \qquad (B.6)$$

Therefore: $\qquad N_i(c) = \dfrac{\Delta_{isct}}{\Delta_e} \qquad \ldots\ldots, \text{ etc.} \qquad (B.7)$

## COROLLARY

In particular, when the polygonal element is a triangle ($ijk$, for example), all the quadrilaterals constructed as before have the same area (because the medians pass through the centroid $c$) (Figure B.2). Hence,
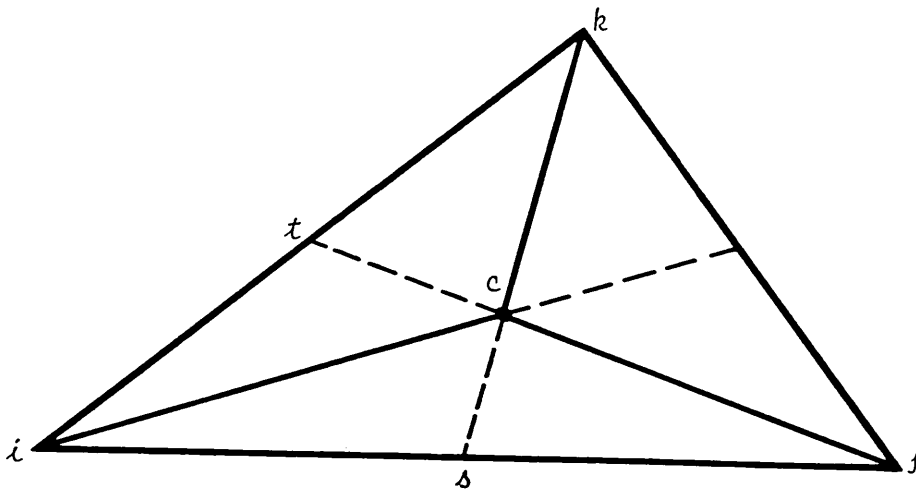


Figure B.2: Replacement of a uniform load on a triangle by three loads at its vertices

the load at each vertex is simply:

$$\vec{F}_i = \vec{F}_j = \vec{F}_k = \frac{\vec{Q}^e \cdot \ell^e \cdot \Delta_e}{3}$$

This can be written in matrix notation as:

$$\{F_Q\}^e = \begin{Bmatrix} F_i \\ F_j \\ F_k \end{Bmatrix} = \frac{\vec{Q}^e \cdot \ell^e \cdot \Delta_e}{3} \cdot \begin{Bmatrix} 1 \\ 1 \\ 1 \end{Bmatrix}$$

which is the same result as that obtained by the relation (3.33).

REFERENCES

1 . Norrie,D.H. & Vries,G.De. "An introduction to Finite Element Analysis."

Text Book, A.P. New York, 1978.

2 . Fenner,R.T. "Finite Element Method for Engineers."

The McMilan Press Ltd. London, 1975.

3 . Stuart,J.T. "Lecture notes, Imperial College."

Professor at the Mathematical Department, 1974.

4 . Zienkiewicz,O.C. "The Finite Element Method in Engineering Science."

McGraw-Hill, London, 1971.

5 . Desai,C.S. & Abel,J.F. "Introduction to the Finite Element Method"

VNR, New York, 1972.

6 . Norrie,D.H. & Vries,G.De. "The Finite Element Method fundamentals and applications."

Text Book, A.P. New York, 1973.

7 . Comini,G. & Delguidice,S. "Finite Element Solution of Non-linear heat conduction problem with special refrence to Change of Phase."

Int.Jour. for Num. Meth. in Eng. Vol.8,1974, pp(613-624).

8 . Carre,B.A. "The Determination of the Optimum Accelerating Factor for Succesive Over-relaxatio."

Computer Journal, Vol.4,1961, pp(73-78).

9 . Eysink,B.J. "Two-dimensional Heat Conduction Analysis of Nuclear Reactor Components using the Finite Element Method."

M.Sc. Dissertation, Imperial College, London, 1973.

10 . Head,J.L. & Eysink,B.J. "Finite Element Heat Conduction in Reactor Solids".

Development of reference 9.

12 . Mazumdar,J. "A method for the study of Transient Heat Conduction in Plates of arbitrary Cross-section."

Nucl. Eng. & Design, Vol.31,1974, pp(383-390).

13 . Nijsing, R. & Eifler,W. "*The Hybrid Method, A new accurate computation method for Transient Temperature Distribution.*"

Nucl. Eng. & Design, Vol.32,1975, pp(208-220).

14 . Wilson,E.L. & Nickell,R.E. "*Application of the Finite Element Method to Heat Conduction Analysis.*"

Nucl. Eng. & Design, Vol.4,1966, pp(276-286).

15 . Zienkiewicz,O.C. & Parekh,C.J. "*Transient Field Problems Two-dimensional and Three-dimensional Analysis by Isoparametric Finite Element.*"

Inter. Jour. for Numer. Methods in Engg, Vol.2,1970, pp(61-71).

16 . Donea,J.R. "*On the Accuracy of Finite Element Solutions to the Transient Heat Conduction Equation.*"

Inter. Jour. for Numer. Methods in Engg. Vol.8,1974, pp(103-110).

17 . Keegstra,P.N.R. "*Computer studies of Dinamic Crack Propagation in Elastic Continua.*"

Ph.D.Thesis at Imperial College, 1977, London.

18 . Keegstra, .N.R. "*A Transient Finite Element Crack Propagation Model for Nuclear Pressure Vesel Steels.*"

Inter. Nucl. Eng. Vol.17, No.4-j, August 1976, pp(89-96).

19 . Lewis,E.E. "*A Transient Heat Conduction Model for Reactor Fuel Element.*"

Nucl. Eng. & Design, Vol.15,1971, pp(33-40).

20 . Samiei,M. "*A Computer Model for the study of Light Water Reactor Fuel pin behaviour.*"

Ph.D.Thesis at Imperial College, 1980, London.

21 . Sadd,M.H. & Didlake,J.E. "*Non-fourier Melting of a Semi-infinite Solid.*"

Jour. of Heat Transfer. Transactions of the ASME. Feb.1977, pp(25-28).

22 . Murray,I. & Huang,P.N.S. "*Phase-change in a Semi-infinite Solid with Temperature Dependent Thermal Properties.*"

Inter. Jour. Heat Mass Transfer, Vol.16,1973,pp(1951-1954).

23 . Muehlbauer,J.C. & Sundeland,J.E. *"Heat Conduction with Freezing or Melting."*

Applied Mechanics Review, Vol.18, No.12, Dec.1965, pp(951-959).

24 . Lahoud,A. & Boley,B.A. *"Some Considerations on the Melting of Reactor Fuel Plates and Rods."*

Nucl. Engg. & Design, Vol.32,1975, pp(1-19).

25 . Wellford,L.C. & Ayer,R.M. *"A Finite Element Free Boundary Formulation for the Problem of Multi-phase Heat Conduction."*

Inter. Jour. Numer. Methods in Engineering, Vol.11,1977, pp(933-943).

26 . Murray,W.D. & Landis,F. *"Numerical Machine Solutions of Transient Heat-conduction Problems involving Melting or Freezing."*

Jour. Heat Transfer. Transactions of the ASME. May 1959, pp(106-112).

27 . Bonacina,C.,Comini,G.,Fasano,A. & Primicerio,M. *"Numerical Solution of Phase-change Problems."*

Inter. Jour. Heat Mass Transfer, Vol.16,1973,pp(1825-1832).

28 . Stehle,H., Assmann,H. & Wunderlich,F. *"Uranium Dioxid Properties for LWR fuel rods."*

Nucl. Engg, & Design,Vol.33,1975, pp(230-260).

29 . Chasanov,M.G., Leibowitz,L. & Gabelnick,S.D. *"High Temperature Physical Properties of Fast Reactor Materials."*

Jour. Nucl. Materials, Vol.49,1973/74, pp(129-135).

30 . Leibowitz,L., Mishler,W. & Chasanov,M.G. *"Enthalpy of Solid Uranium Dioxid from 2500 K to its melting Temperature."*

Jour. Nucl. Materials, Vol.29,1969, pp(356-358).

31 . Christensen,J.A. *"Thermal Expansion and Change in Volume of Uranium Dioxid on Melting."*

Jour. American Ceramic Society, Vol.46,No.12, Discussions and notes, Dec.1963, pp(607-608).

32 . Jones,D.S. *"The Theory of Electromagnetism."*

Pergamon Press,Oxford, London, 1964.

33 . Shah,N. *"Private communications."*

Mechanical Engineering Department, Imperial College, London, 1981.